The effect of haptic feedback on operator control behaviour in telemanipulation

Wildenbeest, Jeroen

DOI
10.4233/uuid:3a1eca29-7eef-401e-8f77-45003536eb70

Publication date
2020

Document Version
Final published version

Citation (APA)
Wildenbeest, J. (2020). *The effect of haptic feedback on operator control behaviour in telemanipulation*. [Dissertation (TU Delft), Delft University of Technology]. https://doi.org/10.4233/uuid:3a1eca29-7eef-401e-8f77-45003536eb70

Important note
To cite this publication, please use the final published version (if applicable).
Please check the document version above.

THE EFFECT OF HAPTIC FEEDBACK ON OPERATOR CONTROL BEHAVIOUR IN TELEMANIPULATION

Jeroen WILDENBEEST

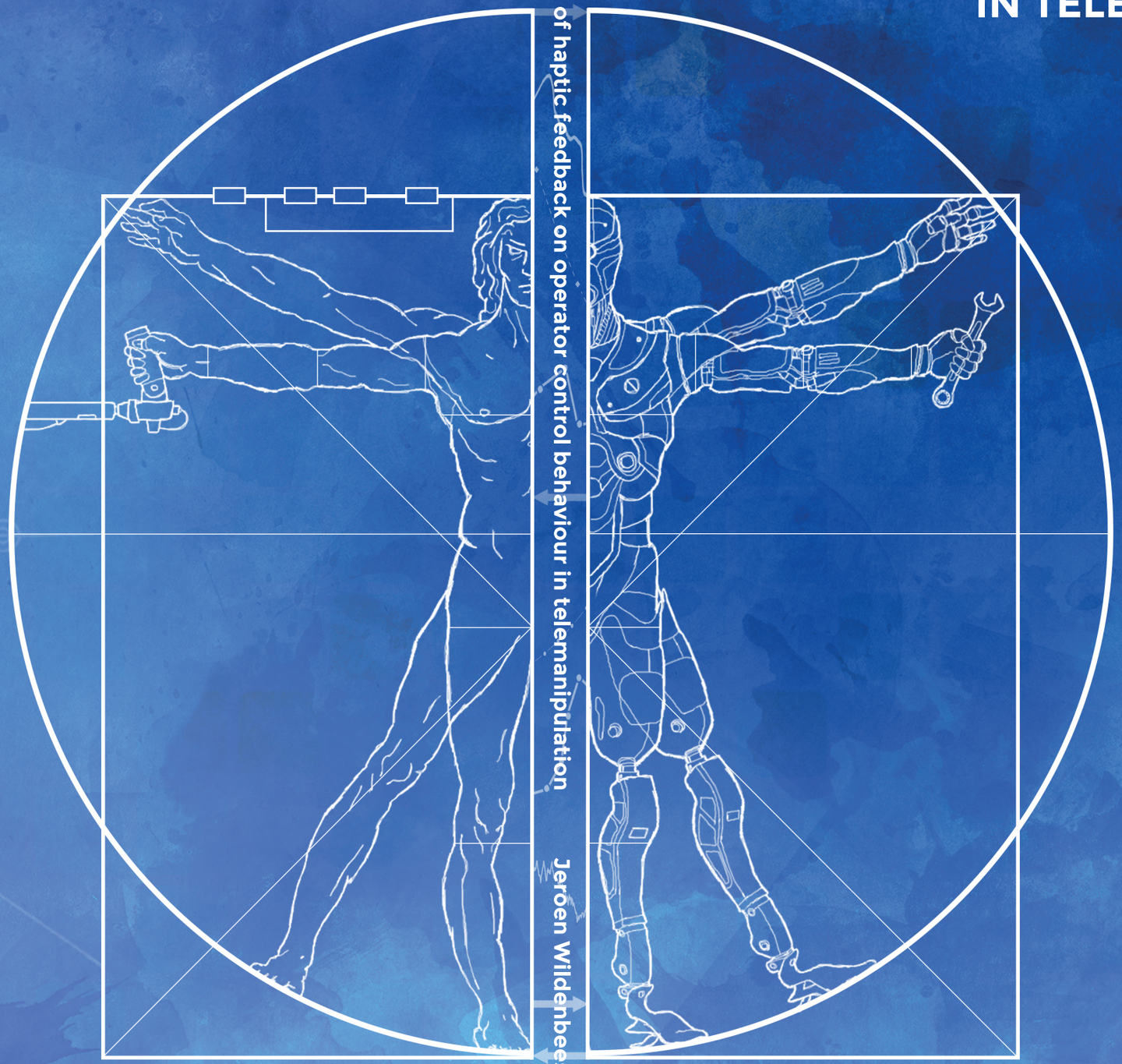

The effect of haptic feedback on operator control behaviour in telemanipulation

Jeroen Wildenbeest

TU Delft

THE EFFECT OF HAPTIC FEEDBACK ON OPERATOR CONTROL BEHAVIOUR IN TELEMANIPULATION

Jeroen Gerrit Willem WILDENBEEST

THE EFFECT OF HAPTIC FEEDBACK ON OPERATOR CONTROL BEHAVIOUR IN TELEMANIPULATION

Proefschrift

ter verkrijging van de graad van doctor
aan de Technische Universiteit Delft,
op gezag van de Rector Magnificus Prof. dr. ir. T.H.J.J. van der Hagen,
voorzitter van het College voor Promoties,
in het openbaar te verdedigen op maandag 8 juni 2020 om 10:00 uur

door

Jeroen Gerrit Willem WILDENBEEST

Master of Science in Mechanical Engineering,
Technische Universiteit Delft, Delft, Nederland,
geboren te Lisse, Nederland.

Dit proefschrift is goedgekeurd door de promotoren:

Prof. dr. ir. D.A. Abbink
Prof. dr. F.C.T. van der Helm
Prof. dr. ir. M. Steinbuch

Samenstelling promotiecommissie:

Rector Magnificus	voorzitter
Onafhankelijke leden:	
Prof. dr. R.B. Gillespie	University of Michigan, VS
Prof. dr. J.B.F. van Erp	TNO & Universiteit Twente
Prof. dr. H. Nijmeijer	Technische Universiteit Eindhoven
Prof. dr. ir. R.H.M. Goossens	Technische Universiteit Delft
Prof. dr.-ing. H. Vallery	Technische Universiteit Delft, reservelid

This research is supported by the Dutch Technology Foundation STW (Perspective project 12158 and VIDI project 14127), which is part of the Dutch Organization for Scientific Research (NWO), and which is partly funded by the Ministry of Economic Affairs.

Keywords: Telemanipulation, Haptic Feedback, Human Factors

Printed by: Gildeprint Drukkerijen

Front & Back: Rade Visual Art & Design

ISBN 978-94-6384-133-7

An electronic version of this dissertation is available at
http://repository.tudelft.nl/.

Resolve to perform what you ought;
perform without fail what you resolve.

Benjamin Franklin

PREFACE
VOORWOORD

Een aantal weken geleden maakte ik een wandeling met Joep, de dolblije, op eeuwige ontdekkingstocht zijnde labrador van vrienden. Als Joep snuffelt aan een grasspriet dan staat de wereld van Joep voor luttele seconden stil. Totdat daar een bloem is, een bij, een plant, of de geur van een andere hond, en nog een, en nog een... Joeps interesse is intens, maar van korte duur.

Ik begrijp Joep wel. Om te beginnen heeft mijn gesnuffel geleid tot een intense interesse in mens-machine interactie en het onderzoeksproces an sich - de aanleiding voor mij om een promotietraject te willen starten. Ook herken ik dit gedrag in de activiteiten die ik heb ontplooid: gedurende mijn onderzoek heb ik een dozijn aan verschillende experimenten uitgevoerd, links en rechts (mee-)gebouwd aan hardware setups, een klein voetbalteam aan afstudeerders (mede-)begeleid, en legio aan andere zaken uitgevoerd (zoals onderwijs, ScienceBattle, workshops). Ik ben trots op wat ik kan nalaten, en ik heb geleerd wat mijn valkuilen zijn, zoals dat een vork maar beperkt hooi kan nemen. Veel belangrijker, ik heb vriendschappen gemaakt voor het leven, bijzondere plekken op de wereld mogen ervaren en ik heb geleerd waar mijn krachten liggen. Ik had dit voor geen goud willen missen. Overigens had ik ook gewoon kunnen luisteren naar Elisabeth van Recess College, die mij vrijwel direct na kennismaking omschreef als een “happy puppy".

Ik hoop met mijn inzet een blijvend waardevolle bijdrage geleverd te hebben aan de (tele-)robotica, maar ook aan andere disciplines in het mens-machine-interactie domein. Laat mijn ontdekkingstocht de functie hebben gehad van een crossover operator in een genetisch algoritme.

CONTENTS

SUMMARY

Telemanipulation systems - in 1925 a vision to remotely treat patients, today widely adopted in a variety of applications - allow human operators to perform tasks which otherwise could not be performed, due to, for example, limitations with respect to distance (e.g., space), scale (e.g., surgery or micro-assembly) or hostile environments (e.g., subsea, nuclear). Effectively, a telemanipulation system functions as an extension to the human operator's motor apparatus, in which the mapping between motor commands and human hand is shifted to a mapping between motor commands and slave robot. Haptic feedback, both proprioceptive and tactile, is often essential for motor control and motor learning (i.e., building the 'mappings'), but may be distorted or even lost when not appropriately re-engineered.

There is, however, no consensus on how to design haptic feedback to best enable humans to perform practical telemanipulated tasks, as no theory or integrated view for human-in-the-loop design and evaluation of haptic feedback is available. Empirically, we know design guidelines 'depend' on aspects such as operator talent, training, the type of task or application, quality of the visual feedback, or task instruction. As a result, the design and evaluation of a telemanipulation system is heuristic: for each case, the required quality of haptic feedback is determined by trial-and-error. This lacuna in design guidelines based on human-in-the-loop theory makes telemanipulation performance suboptimal, and development slow and costly.

The aim of this thesis is to provide an integrated, human-centered view on the design and evaluation of haptic feedback, which can serve as a basis for generalized haptic feedback design. More specifically, this thesis is on the one hand focused on (i) assessment of haptic feedback design requirements for position and rate control within a uniform evaluation framework, and on the other on (ii) the development of a fundamental understanding of the role of haptic feedback on operator (neuromuscular) control mechanisms, and moreover, to generalize experimental findings by adapting existing motor-control paradigms and control-theoretic models. To do so, four key human-factor experiments were performed.

The first experiment focused on the benefit of haptic feedback for position controlled telemanipulation scenarios and the impact of task instruction and availability of visual feedback for several fundamental subtasks. In a second experiment the efficacy of four different haptic feedback interface designs for rate control was determined in a similar manner; both studies adopted a uniform evaluation framework, providing an integrated view on requirements for the haptic feedback.

We found that such a framework should incorporate at least a (abstract) task taxonomy, a baseline to compare against, task instruction, speed-accuracy trade-offs (i.e. what metrics to look at), performance-control effort trade-offs, operator training, and a

control on the quality of visual feedback. Furthermore, these studies showed that the best haptic feedback design to perform a given telemanipulation task predominantly depends on the required task workspace and task accuracy, and the need to reflect back contact transitions. Large workspaces are more easily (i.e. low workload) covered using rate control, where accuracy for positions and forces is higher using position control. Also, as an increase in device (i.e. haptic feedback) quality does not always correlate to an increase in task performance. This implies design of haptic feedback should be human-centered evaluation, both assessing the problem and validating the solution with the human in-the-loop.

Experiments three and four focused on the effects of haptic feedback on the human operator's motor control mechanisms when controlling a telemanipulation system in free-space. In study three, well-established cybernetic models were adopted to study trained movements, and the impact of slave dynamics and scaling of haptic feedback. In the final study, a reach-adaptation paradigm was used to study the role of haptic feedback when learning movements, and the impact of slave dynamics and bandwidth of the presented haptic feedback. These latter two experiments show that haptic feedback substantially affects an operator's underlying motor control mechanisms (i.e. feedback and feedforward control) when controlling a slave system. The effects were observed in both instantaneous improvements of task execution due to feedback of environmental forces or device dynamics, as well as also task execution improvements over longer periods of time due to improved internal models (i.e. learning); haptic feedback enhances the process of building 'mappings' between human input and a system's response. This suggests that improved haptic feedback quality improves learning rates (i.e. efficacy) and control responses (i.e. efficiency). Future studies should uncover the potential quantitative effects and time-scales at which these effects occur.

Additionally, study three showed that the amplitude of haptic feedback can be scaled down without harming task performance: human operators are capable of adjusting their (neuromuscular) control parameters independently of the absolute magnitude (i.e. gain) of the haptic feedback controller. However, when scaling, one should account for reasonable lower boundaries, that putatively may be given by Just Noticeable Differences (JNDs) to keep cues distinguishable. Upper boundaries may be given by individual constraints on comfort. These findings were confirmed by the second experiment.

Studies three and four illustrate that computational models and paradigms from the motor control literature can be adopted to provide generalizable descriptions of human operator behavior in telemanipulation. Here, we targeted free-space motions for systems like cranes and robot arms, and the tasks are representative for activities in domestic, nuclear or subsea environments. The cybernetic models enable for an exclusive understanding of the underlying operator control mechanisms (i.e. feedback and feedforward control) by looking in the frequency domain, as such complementing and enhancing the insights gained from the time-domain data. The reach adaptation paradigm enables to determine the extent to which haptic feedback bandwidth affects motor learning and generalization for different slave dynamics. Moreover, these model-based approaches enable extrapolation of findings and to predict outcomes when task characteristics change, such that informed a priori design considerations of haptic feedback

interfaces and, in the future, haptic support systems can be made.

SAMENVATTING

Telemanipulatie systemen – in 1925 een droombeeld om patiënten op afstand te behandelen, vandaag de dag breed toegepast in allerlei applicaties – stellen menselijke operators in staat taken uit te voeren die anders niet uitgevoerd hadden kunnen worden vanwege, o.a., afstandsbeperkingen (bijv. ruimtevaart), schaal (bijv. chirurgie of micro-assemblage) of vijandige omgeving (bijv. diepzee, nucleair). Een telemanipulatie systeem kan gezien worden als een verlengstuk van het menselijke bewegingsapparaat, waarbij de relatie tussen motorisch signaal en hand verlegd wordt naar een relatie tussen motorisch signaal en slave robot. Haptische feedback, zowel proprioceptief als tactiel, is in veel gevallen essentieel voor dit motorische systeem en het leren van de 'relaties', maar kan worden verstoord of zelfs verloren gaan wanneer deze niet gepast wordt (her-)ontworpen.

Echter, er is geen consensus over hoe haptische feedback te (her-)ontwerpen zodat operators zo goed mogelijk praktische telemanipulatie taken kunnen uitvoeren. Een theorie of integrale benadering voor het ontwerp en evaluatie van haptische feedback is niet beschikbaar. Empirisch weten we dat ontwerp richtlijnen afhangen van zaken als operator talent, training, het type taak of toepassing, kwaliteit van de visuele feedback, of taak instructie. Het ontwerp- en evaluatieproces van haptische systemen is daarmee heuristisch: voor elke situatie wordt de benodigde kwaliteit van de haptische feedback bepaald op basis van trial-and-error. Bovendien, dit gebrek aan ontwerp richtlijnen op basis van een eenduidige theorie resulteert in suboptimale prestaties van telemanipulatie systemen, en maakt het ontwikkelproces langzaam en kostbaar.

Het doel van deze thesis is om te voorzien in een integrale raamwerk voor ontwerp en evaluatie van haptische feedback, wat generaliseert over toepassing en taak. Hierbij staat de menselijke operator die een taak met het systeem moet uitvoeren centraal. Specifiek, focust deze thesis zich aan de ene kant op (i) assessment van de vereisten aan haptische feedback voor positie-en snelheidssturing binnen een uniform evaluatie raamwerk, en aan de andere kant op (ii) het ontwikkelen van fundamenteel begrip van haptische feedback en haar rol binnen het neuromusculaire system en, bovendien, het generaliseren van experimentele bevindingen door bestaande paradigma's uit het bewegingssturingsdomein en mathematische (c.q. cybernetische) modellen te adapteren. Hiertoe zijn vier sleutel human-factor experimenten uitgevoerd.

Het eerste experiment richtte zich op het bepalen van de waarde van haptische feedback in positie gestuurde telemanipulatie scenario's, en de impact van taak instructie en aanwezigheid van visuele feedback voor verschillende fundamentele subtaken. In een tweede experiment is de doeltreffendheid van vier verschillende ontwerpen voor haptische feedback in een snelheid-gestuurd telemanipulatie systeem op een vergelijkbare manier bepaald; in beide studies is een uniform evaluatie raamwerk geadopteerd, welke

een integraal zicht geeft op vereisten voor haptische feedback.

We hebben gevonden dat een dergelijk raamwerk ten minste een (abstracte) taak, een baseline, taak instructie, snelheid-nauwkeurigheid afwegingen (a.d.h.v. criteria), prestatie-werklast afwegingen, operator training en controle op de kwaliteit van visuele feedback moet bevatten. Daarnaast lieten deze studies zien dat het werkbereik, de nauwkeurigheid waarmee de taak dient uitgevoerd te worden, en de noodzaak contact overgangen te reflecteren de bepalende factoren zijn in het selecteren van het juiste haptische feedback ontwerp. Omvangrijke werkgebieden worden gemakkelijker (bijv. lagere werklast) bediend met snelheidssturing, terwijl de nauwkeurigheid van positie en krachten nauwkeuriger is met positiesturing. Ook leidt een verbetering van de kwaliteit van de haptische feedback niet altijd tot een verbetering van de taak uitvoering. Dit impliceert dat de menselijk operator integraal dient meegenomen te worden bij het evalueren van haptische feedback, zowel bij het definiëren van het probleem als het valideren van de oplossing.

Experimenten drie en vier richtten zich op de effecten van haptische feedback op het menselijk motorische systeem wanneer een telemanipulatie systeem in de vrij ruimte wordt bewogen. In studie drie zijn breed-gefundeerde cybernetische modellen geadopteerd om getrainde bewegingen, en de impact van slave dynamica en schaling van haptische feedback te bestuderen. In een laatste studie is een 'reach-adaptation' paradigma toegepast om de rol van haptische feedback bij het leren en generaliseren van bewegingen te bepalen, en de impact van slave dynamica en bandbreedte van de haptische feedback daarbinnen.

Deze laatste twee experimenten laten zien dat haptische feedback de onderliggende motorische mechanismen (feedback en feedforward sturing) substantieel beïnvloed wanneer een slave systeem wordt bestuurd. De effecten werden geobserveerd in zowel instantane verbeteringen van de taak uitvoering door terugkoppeling van omgevingskrachten en apparaat dynamica, als in verbeteringen van de taakuitvoering over langere termijn als gevolg van verbeterde interne modellen (motorisch leren); haptische feedback versterkt het leerproces van relaties tussen menselijk input en de responsie van een systeem. Dit suggereert dat verbeterde kwaliteit van de haptische feedback zorgt voor een versneld leerproces (effectiviteit), en verbeterde motorische input (efficiëntie). De kwalitatieve effecten hiervan, evenals de exacte tijdschalen dienen in nader onderzoek bepaald te worden.

Verder liet studie drie zijn dat de amplitude van de haptische feedback geschaald kan worden zonder dat dit invloed heeft op de uitvoering van de taak: menselijke operators zijn in staat hun (neuromusculaire) besturingsparameters aan te passen, onafhankelijk van de absolute magnitude van de haptische feedback. Let wel, wanneer geschaald wordt dienen redelijke ondergrenzen aan de krachten in acht genomen te worden, welke ingegeven kunnen worden door Just Noticeable Differences (JNDs) om zo onderscheid te kunnen blijven maken tussen signalen. Bovengrenzen kunnen worden gegeven door individuele beperkingen met betrekking tot comfort. Deze bevindingen werden bevestigd in experiment twee.

Studies drie en vier illustreren dat paradigma's uit het bewegingssturingsdomein en mathematische modellen geadopteerd kunnen worden om generaliseerbare beschri-

jvingen van het gedrag van de operator te verkrijgen. In deze studies is dit uitgevoerd voor bewegingen in de vrij ruimte voor systemen zoals kranen of robot armen, terwijl de taken representatief zijn voor activiteiten in onze dagelijkse omgeving, maar ook voor nucleaire of diepzee toepassingen. Het cybernetische model geeft exclusief begrip van onderliggende besturingsmechanismen (feedback en feedforward sturing) door naar het frequentie-domein te kijken, waarmee het begrip verkregen uit het tijd-domein gecompleteerd en versterkt wordt. Aan de hand van het reach adaptation paradigma's kan de mate waarin haptische feedback motorisch leer- en generalisatiegedrag beïnvloed bepaald worden voor verschillend slave systemen. Bovendien, door middel van deze model-gebaseerde aanpak kunnen resultaten geëxtrapoleerd worden en uitkomsten voorspeld wanneer taak eigenschappen veranderen, zodat a priori ontwerp overwegingen gemaakt kunnen worden met betrekking tot haptische feedback interfaces en, in de toekomst, haptische ondersteuningssystemen.

Chapter 1

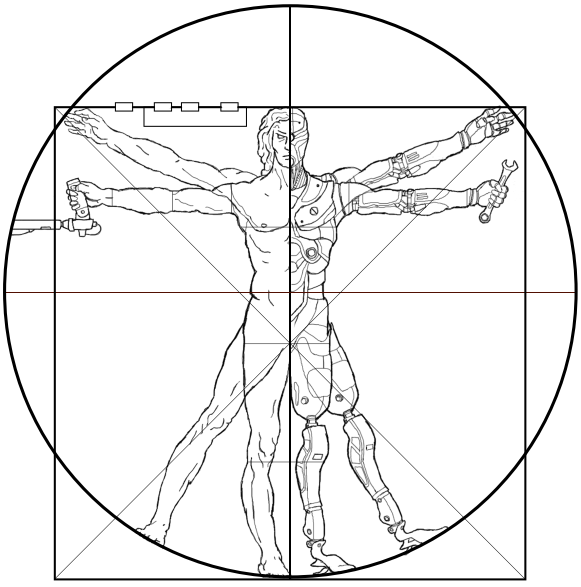

1

INTRODUCTION

1.1. A BRIEF HISTORICAL PERSPECTIVE ON TELEMANIPULATION

> *"The Teledactyl (Tele, far; Dactyl, finger - from the Greek) is a future instrument by which it will be possible for us to 'feel' at a distance. [...] This idea is not at all impossible, for the instrument can be built today with means available right now. It is simply the well known telautograph, translated into radio terms, with additional refinements. " — Hugo Gernsback in Science and Invention, February 1925*

It is 1925, merely five years after the first ever mention of robots ('robota' in R.U.R. by Karel Čapek). It is the year in which radio pioneer Hugo Gernsback predicts a robotic device for then year 1975 that allows doctors to not only remotely talk, but also remotely view and touch their patients. The device, the 'Teledactyl', consisted of two pairs of instruments and a screen, all of which connected by means of radio (see Fig. 1.1). Movements made by the doctor on the local teledactyl were transferred to the teledactyl at the patient's location. Similarly, when the patient's device met with resistance, the doctor's remote controls would replicate this resistance, allowing the doctor to 'feel' the patient. Hence, using the 'Teledactyl', doctors could diagnose and treat patients remotely; telemanipulation systems were born in thought.

Indeed, Gernsback's idea was not at all impossible. The earliest telemanipulation systems were developed in the 1950s by the Argonne National Laboratory in the USA. These mechanical manipulators consisted of a pair of robotic arms, with a master located at the local site, and a slave located at the remote site. While these first devices were mechanically coupled, from the 1970s the coupling became electrical. Push and pull rods were replaced by controllers, sensors and actuators. This allowed telemanipulators to be used not only in hostile environments (e.g. for maintenance in nuclear fission and fusion plants [87], space [10] and (sub-)sea [78, 115]), but also in environments with spatial constraints (e.g. minimally-invasive surgery [63, 107] or micro-assembly of micro-electro-mechanical systems [18]), as movements could be scaled.

1

Figure 1.1: The cover of technology magazine Science and Invention, February 1925. Radio pioneer Hugo Gernsback predicts the 'Teledactyl' for the year 1975, a device that allows doctors to diagnose and treat their patients remotely. Essentially, Gernsback predicted telemanipulation systems.

The transition from mechanical to electrical coupling from the 1970s onwards required the link between local and remote site to be 'mapped' and 'engineered' bilaterally. Force and positional information on either site were digitized and could be scaled, filtered and/or amplified. To facilitate (re)engineering of the link, numerous studies on analytic [52], control [9, 79] and hardware [29, 32] aspects of telemanipulation systems appeared. Focal point was the fidelity with which force and positional information were sent from the remote environment to the human operator, i.e. the haptic feedback quality or haptic 'transparency' [79, 138] of the system. Ideally, a telemanipulation system maps the contact forces of the slave with the remote environment one-to-one to the human operator, without any form of (electro)mechanical distortion. Over the years, many improvements with respect to the haptic feedback quality have been made, yet, to date, perfect transparent haptic feedback has not been realized. Apparently, there is more to telemanipulation systems than simply refining the 1925's precursor of the fax, the telautograph.

EVALUATING HUMAN-IN-THE-LOOP TELEMANIPULATION

Engineering perfect haptic transparency should not be a goal in itself. After all, it is not about the quality of the 'tool', but it as a matter of how well a human operator is able to execute a tasks utilizing the tool as an extension to his/her own limbs (i.e. task performance, or human-in-the-loop performance). In 1981, Brooks and Bejczy [22] were

among the first to refer to the human's perceptual and motor capabilities in telemanipulation specific literature. In their requirements definition for telemanipulation systems, human physiological characteristics (e.g. force capabilities) were taken as a baseline reference, or better, as an upper boundary for task performance; in their vision, engineering haptic feedback beyond the capabilities of the human is redundant and will not lead to task execution improvements. This was a design paradigm shift, and the 1980s became the cradle for studies evaluating human-in-the-loop telemanipulation (e.g [12, 128]). The existence of an upper task performance boundary limited by human characteristics, was later experimentally verified (e.g., [27, 55]).

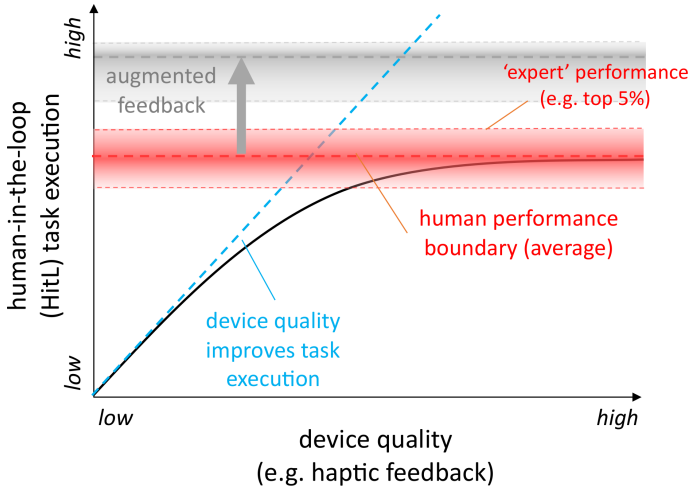

Figure 1.2: Abstract representation of device quality versus task performance. An upper boundary to task performance exists, which is given in by human operator characteristics. Engineering device characteristics (like haptic feedback) beyond this boundary is redundant and will not lead to task execution improvements [27, 55]. Augmented feedback or autonomous features allow to enhance the average task execution, and may assist novice operators to behave like experts.

What these human factor studies also revealed, was that telemanipulation systems required much-needed improvements. For example, in 1984 Vertut pointed out that performing the same task with a telemanipulation system takes typically two orders of magnitude (!) more time than performing a task with bare hands [128]. Obviously, telemanipulation systems allow amplification, scaling, filtering, and thereby human presence where it was previously impossible. But still, it is widely acknowledged that telemanipulated tasks are characterized by long task completion times, errors, unnatural or unintuitive interaction and frustration (e.g. [27, 51, 53]).

THE DIGITAL ERA: *augmenting* TASK EXECUTION

From the 1990s onwards, a trend to augment the perception-action loop is observed. Next to continues direct improvements to visual and audio feedback, digitization and by-wire techniques allow for, for example, compensation of tool weights, tracking of objects and constraining of trajectories (e.g. [50, 107]).

Well-known are the Virtual Fixtures (also called 'active constraints' [19]) by Louis Rosenberg ([107]), in which the user or operator was fully emerged in a 3D virtual environment and the slave could be constrained by simulated physical barriers, fields, and guides. Whereas Virtual Fixtures are passive and static, augmentation features may also be active and dynamic as in, for example, shared control [3] or shared autonomy.

Active constraints, shared control and shared autonomy are forms of *physical Human-Robot Interaction (pHRI)*. pHRIs describe the cooperation between human and an autonomous agent or robot to control a 'plant' (i.e., the system in the remote environment) [51]. Depending on environment specifications and individual capabilities of human and robot, pHRIs trade control between automation and human sequentially in time or 'share' control (i.e., continuously), and may support with low-level (i.e. physical feedback, workspace constraints or skill like tremor filtering) or high-level tasks (e.g. decision making, planning) [3]. One way or another, successful cooperation between robots and humans requires effective communication and interaction [93]. This challenge was already described in the early 50's by Fitts [46] and Wiener [131], and is still relevant today [100]. The introduction of an autonomous agent changes the nature of the human's task; the task shifts from being purely in-the-loop control, to supervisory control tasks like observing and monitoring the automation operating in the task environment. It is well known that this can lead to deteriorated task performance in off-nominal scenarios (i.e., unexpected events, or automation errors), due to, for example, loss of situation awareness, vigilance decrements or complacency (e.g., [43, 44, 81, 117, 118, 100]). Recently, such effects have been observed in the Defense Advanced Research Projects Agency (DARPA) Robotics Challenges, acknowledging that the ability for robots to be 'fully autonomous always and everywhere' is a myth [20] and the operator is a key system element [45].

It now is 2019. Concepts like *shared control*, *shared autonomy*, *human-robot symbiosis* and *interdependence* of human and automation are major topics within the (tele)robotic community, covering key notes and special sessions or issues. Telerobotic technology over-arches applications in aviation, vehicle navigation, surgical robotics, space robotics, maritime robotics and rehabilitation. However, even today, seemingly trivial tasks like opening a door [69] and exchanging a tile [17], are still extremely difficult to perform remotely, and the daily news showcases situations where humans and intelligent systems failed to cooperate effectively (e.g. the Uber and Tesla self-driving cars incidents, both March 2018). We could say technology has evolved faster than our understanding of how to interact with it.

Our current and future interaction with (remote) intelligent systems requires fundamental understanding of how humans control systems. These interactions will include monitoring the intelligent agent, correcting when errors occur, and taking over or even teaching (e.g. demonstrating) when a task is unfamiliar to or too complex for the intelligent agent. At the basis of this interaction is our haptic modality, which allows for low-level interaction and plays an essential role in the learning process of the interaction's dynamics. Interestingly, telemanipulation allows to engineer feedback catered towards the haptic modality, such that a natural or intuitive mapping between human and

telemanipulator is realized.

1.2. FROM *a posteriori* TO *a priori* DESIGN OF HAPTIC SYSTEMS

The haptic modality has received significant attention in telemanipulation literature. Specifically, the effects of haptic feedback can be categorized in effects that instantaneously affect task execution, and effects that show 'over-time', like learning and strategizing tasks.

First of all, feedback of the contact forces with a remote environment improves task execution (i.e. skill level) in terms of task completion time [38, 55, 85], contact force [38] and error rate [38, 55]. Also, haptic feedback reduces control effort measured in terms of cognitive workload [129] and energy consumption [55], compared to visual feedback only.

Secondly, there is strong evidence that the presence of haptic feedback changes neuromuscular planning and strategical learning. For example, when operators are provided with haptic feedback during manual excitation of a sprung mass [62], point-to-point movements with a spanner [133], or visuo-manual control over a system with up front unknown dynamics [56], their control changes in terms of the absolute amount or the frequency spectrum of the movements. Danion even reported that haptic feedback of the dynamics of the controlled system affected the movement strategy used by subjects, as well as their subsequent performance [33].

However, these statements are qualitative, or setup-or-task-specific at best, while device design requires quantitative information in the form of (concrete) requirements specifications. What is the extent to which haptic feedback affects task execution? And what quality of feedback is good enough to restore a functional mapping between human and telemanipulator? There is no consensus on the answers to these questions. All we know is that 'it depends', on aspects like operator talent, training, the type of task or application, quality of the visual feedback, task instruction, etc.. As a result, the design and evaluation process is heuristic (and a posteriori): for each case, the required quality of haptic feedback is determined by trial-and-error, and we cannot predict how changes to the telemanipulation system affect task execution, when, for example, the design is changed or autonomy is added. Generalization in the form of a uniform theory for human-centered design and evaluation is lacking. Telemanipulation is in need of a priori design guidelines.

Within this thesis, a contribution to a uniform modelling and evaluation framework and generalized design guidelines for haptic feedback is made, by:

- Developing guidelines for haptic feedback design within an uniform evaluation framework. The relevance of feedback is affected by factors like (sub)task-impact, visual feedback quality, and incorporates trade-offs like speed-accuracy and performance-control effort. Such a framework provides the design requirements (qualitatively), such that informed design specifications can be deduced (quantitatively).

- Performing key experiments to understand how haptic feedback contributes to

restoring a functional mapping between telemanipulator and human operator, such that the operator can intuitively control the device. Such understanding allows to predict the effects to task execution when task, task requirements (e.g. speed), telemanipulator parameters (e.g. haptic quality or device inertia) or even some additional intelligence, change.

A sensorimotor control perspective is adapted, as we believe that this field - describing how humans control their limbs - provides a body of experimental paradigms and mathematical models that can be extended to telemanipulation, and can form a basis for a priori telemanipulation design guidelines.

1.3. APPROACH: A SENSORIMOTOR CONTROL PERSPECTIVE ON HAPTIC FEEDBACK

Sensorimotor control describes the interaction between (sensory) perception and action (i.e. motor control) - it describes how we coordinate our movements in interaction with an environment or a tool. Sensory information can be visual (i.e. where is the door handle located, and what is its size?) or haptic (i.e. what is the door's inertia, where is its centre-of-rotation?). Actions are governed by predictions of dynamics and physiological parameters such as arm length or inertia. Moreover, our actions change over time as we train our behaviour and accommodate novel tasks or circumstances.

To ground and generalize experimental findings, sensorimotor studies often utilize mathematical models to describe limb movements (e.g. [13, 23, 46, 47]). Essentially, a telemanipulator functions as an extension to the human operator's motor apparatus, and can therefore be seen as an extension to these mathematical models. Hence, we believe sensorimotor control models and (experimental) paradigms can be applied to telemanipulation scenario's.

Fig. 1.3 describes a high-level control-theoretic framework of a human operator controlling a telemanipulation system. It describes perception and action as a closed-loop process, as common presented in neuroscience (e.g. [23, 64, 70]). The model is generic, rather than specific, and inclusive rather than exclusive. For example, common models to describe movement trajectories (e.g. optimal control [121] [Nisky et al., 2018], equilibrium point [13], minimum variance [57], or in-output models like McRuer's Crossover Model or Fitts' Law can be included in this framework.

The model shows the fundamental constructs of sensorimotor control. By integrating a goal (the slave's desired position, $x_{s,desired}$) and sensory data (e.g. visual and/or auditory), a desired command ($x_{m,desired}$) is generated and fed into the mechanisms that the motor commands; a feedforward and a feedback controller. Feedforward and feedback control (and their interactions) have been extensively studied in sensorimotor control literature. In the basis, when we first learn to control a system (i.e. in early learning), we mostly rely on feedback control. Over time contribution of the feedforward controller gradually increases by generating better estimates of the controlled dynamics, while at the same time reducing the feedback contribution ([47, 97]). This process, in which approximates of our own and external dynamics are generated (also called internal models) is called motor learning, and is fundamental to movements; it allows us to

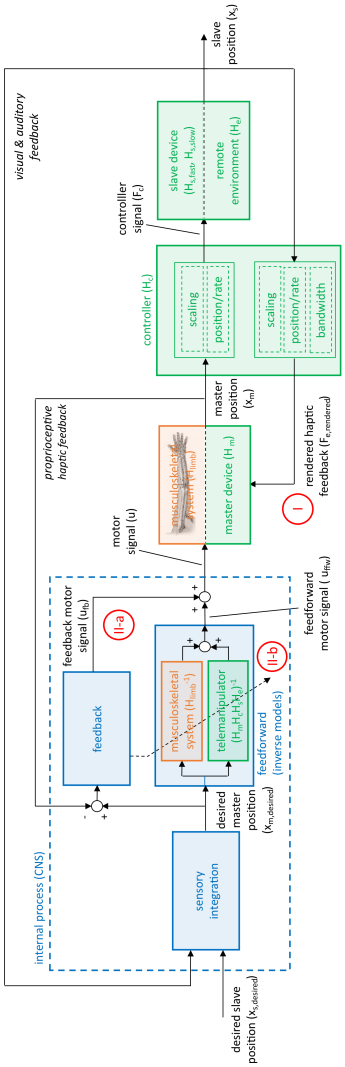

Figure 1.3: Simplified control-theoretic representation of a human operator (adapted from [64] [70]) controlling a telemanipulation system (hybrid notation [52]). Essentially, the telemanipulator (in green) functions as an extension to the human operator's motor apparatus (in blue) and allows to perform tasks which otherwise could not be performed. How should this extension be integrated with or mapped to the human's motor control system? Within this thesis several key-experiments are performed to study the mapping. Specifically, what are the requirements on the rendered haptic feedback quality for both position and rate control (Aim I-a and I-b)? And how are underlying motor control mechanisms (u_{fb} and u_{ffw}) affected by force feedback bandwidth and scaling (Aim II-a), and how is the formation of internal models (i.e. motor learning) affected by force feedback quality (Aim II-b)? A model-analytic approach is adapted, which allows to generalize the findings such that predictions can be made when task, device or environment changes, and well-informed device design requirements specifications can be formulated a priori. N.B.: for simplicity, the force contribution of prioprioceptive feedback nor tactile feedback are incorporated in this representation, and proprioceptive haptic feedback is only shown for position.

become more skilled in moving our own arms, or manipulating, for example, a telemanipulation system.

To what extent does haptic feedback allow for (restoring) a natural or intuitive interaction between human and telemanipulator? How does haptic feedback affect the fundamental motor control principles of feedforward and feedback? We do not know. Internal models may take years to perfect (as with a professional sports or musical instrument player), implying that motor learning effects cannot be analyzed in typical telemanipulation experiments. Also, accurate feedback control may only be evident for certain (sub)tasks and certain robotic systems, of which the effect is not lost in the bulk, noise and (inter-subject) variation.

Sensorimotor control literature provides us with qualified tools in the form of experimental paradigms (e.g. force-curl paradigm [47], pursuit tasks [86]) and mathematical models (e.g. [23, 64, 86]), to study these effects. Moreover, the models allow for generalization in the form of a uniform theory, such that we can predict how changes to the system affect task execution. Ultimately, such an approach will provide tools and guidelines for future human-centered design of telemanipulation systems.

1.4. THESIS GOAL & AIMS

The goal of this thesis is to develop a basis for generalized haptic feedback design by means of an uniform evaluation framework and control-theoretic operator models. Specifically these aims are:

- I-a To quantify haptic feedback bandwidth requirements in a generalized position controlled task, within a uniform evaluation framework (Chapter 2).
- I-b To evaluate haptic feedback design paradigms for rate-controlled telemanipulation systems, in a generalized rate-controlled task (Chapter 3).
- II-a To quantify the effect of haptic feedback scaling and slave dynamics on operator neuromuscular control mechanisms (feedback and feedforward control), and consequently task execution, using a cybernetic model (Chapter 4).
- II-b To quantify the extent to which haptic feedback contributes to telemanipulated motor adaptation (i.e. generation of internal models) in a reach adaptation experiment (Chapter 5).

To meet these aims, a series of human factor studies was performed. The implications of this research form the basis for design requirements for future haptic interfaces.

1.5. THESIS OUTLINE

The majority of this thesis (Chapters 2-5) consists of papers that have been either published or submitted to journals. The papers are presented in their original format. All Chapters can be read independently.

In **Chapter 2**, the impact of haptic feedback quality on the execution of telemanipulated (dis-)assembly tasks is evaluated, within an uniform evaluation framework. Similarly, feedback designs for rate-controlled telemanipulation are explored in **Chapter 3**; whereas feedback in slow, rate-controlled systems is not common, it is potentially beneficial, **Chapter 4** describes human operator control behaviour by means of a cybernetic model - how do haptic feeback scaling and slave system dynamics neuromuscular control mechanisms feedback and feedforward? Putatively, haptic feedback affects neuromuscular planning and coordination, as it affects the operator's ability to perform feedback control, especially for systems with low-power-over-inertia ratios.

The effects of haptic transparency on the rate and generalizability of motor learning are assessed in **Chapter 5**. Does haptic feedback enhance the generation of internal modals and therefore feedforward control? To answer this question, subjects performed a reach adaptation task under the effect of a viscous curl force field, while different levels of transparency were provided.

What is sufficient haptic feedback to restore a functional mapping between human and telemanipulator? This is the central question in **Chapter 6**, the Discussion. In addition, recommendations are made on design requirements for future haptic telemanipulation systems.

Finally, in **Chapter 7** conclusions are drawn on the extent to which haptic feedback affects telemanipulated tasks.

Chapter 2

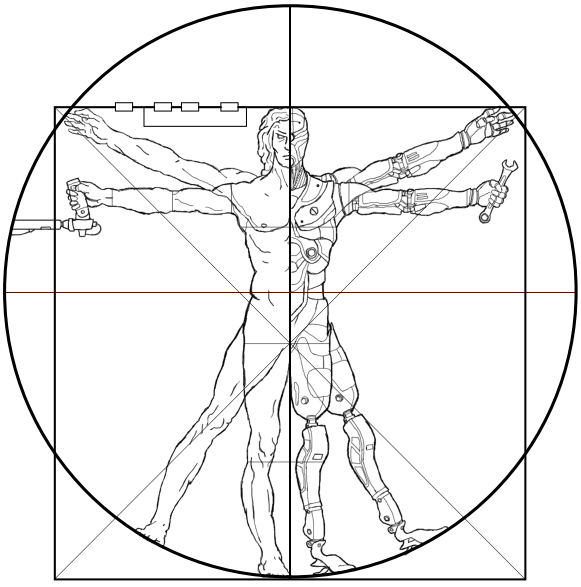

2

The Impact of Haptic Feedback Quality on the Performance of Teleoperated Assembly Tasks

In general, 'transparency' or 'rendered' haptic feedback is considered to improve task execution. Yet, it is not very well understood how important the quality of haptic feedback is. This chapter aims to quantify haptic feedback bandwidth requirements in a generalized position controlled task, within a uniform evaluation framework. For this purpose, subjects performed (dis-)assembly tasks in a hard-to-hard environment with different levels of haptic feedback quality (operationalized as bandwidth). Fig. 2.1 shows a simplified control-theoretic representation of the experimental conditions.

This chapter has been published in IEEE Transactions on Haptics Vol. 6, No. 2, 2013 [133]

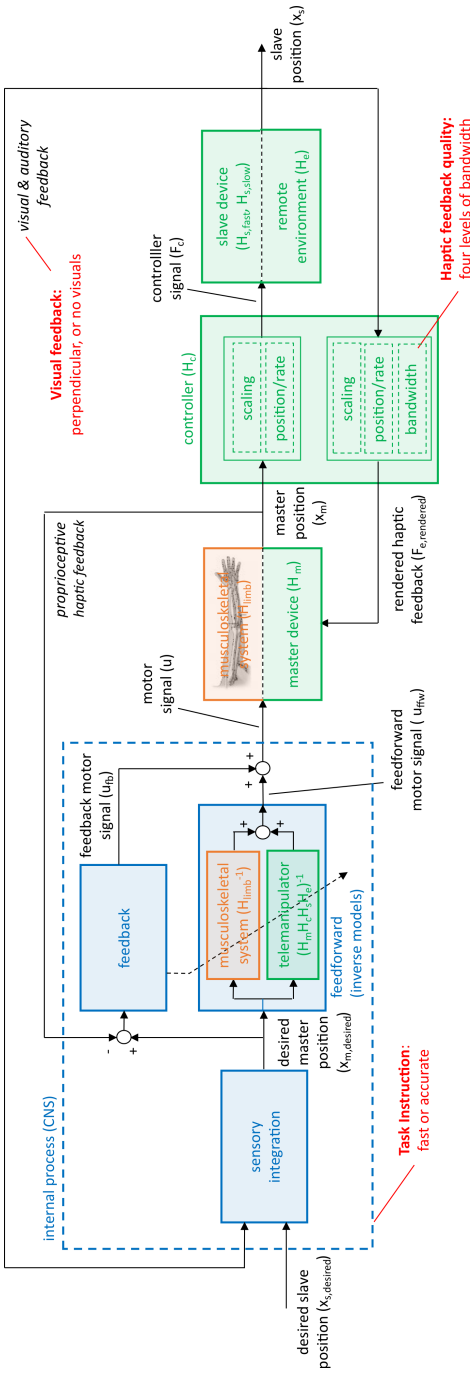

Figure 2.1: Simplified control-theoretic representation of the study as performed in this chapter. The effect of haptic feedback quality on task execution was quantified within a uniform framework which includes key-factors such as (sub)tasks, task instruction and visual feedback conditions. Task instruction, visual feedback and haptic feedback were modulated (shown in red).

ABSTRACT
In teleoperation, haptic feedback allows the human operator to touch the remote environment. Yet, it is only partially understood to what extent the quality of haptic feedback contributes to human-in-the-loop task performance. This paper presents a human factors experiment in which teleoperated task performance and control effort are assessed for a typical (dis-)assembly task in a hard-to-hard environment, well known to the operator. Subjects are provided with four levels of haptic feedback quality: no haptic feedback, low-frequency haptic feedback, combined low- and high-frequency haptic feedback, and the best possible-a natural spectrum of haptic feedback in a direct-controlled equivalent of the task. Four generalized fundamental subtasks are identified, namely: 1) free-space movement, 2) contact transition, 3) constrained translational, and 4) constrained rotational tasks. The results show that overall task performance and control effort are primarily improved by providing low-frequency haptic feedback (specifically by improvements in constrained translational and constrained rotational tasks), while further haptic feedback quality improvements yield only marginal performance increases and control effort decreases, even if a full natural spectrum of haptic feedback is provided.

2.1. INTRODUCTION

Telemanipulators allow humans to complete tasks in a remote environment, while preserving human judgement, skill, attention, and their ability to resolve unexpected situations [98]. The human is virtually relocated into the remote environment; "telepresence" as Sheridan [116] called it. A broad variety of teleoperated tasks exist, which all impose different requirements on the telemanipulator and its operator. While haptic feedback is generally considered to improve task performance for most tasks, it is not very well understood how important the quality of haptic feedback is.

A telemanipulator consists of a pair of robotic manipulators and a controller. Movements executed by the human operator on the master device are translated to the slave device, which interacts with the remote environment. Master and slave are interconnected through communication channels and a controller. The connected system of human operator, telemanipulator, and environment is referred to as the connected telemanipulator system [27]. This is illustrated in Fig. 2.2. To understand the significance of haptic feedback, it is important to understand the three main elements of the connected telemanipulator system: the telemanipulator, the human operator, and the remote environment.

In the middle of the connected telemanipulator system, the *telemanipulator* allows humans to make use of their unique capabilities in a remote environment, by inherently providing a bilateral information flow. Forces and movements are transferred from the human operator through the telemanipulator to the environment and vice versa. It has been shown that providing force feedback from the environment to the human operator yields a reduction in task completion time [38], [55], [84], energy consumption [55], error indices [38], [55], the magnitudes of the contact forces [38], and the users cognitive workload [129].

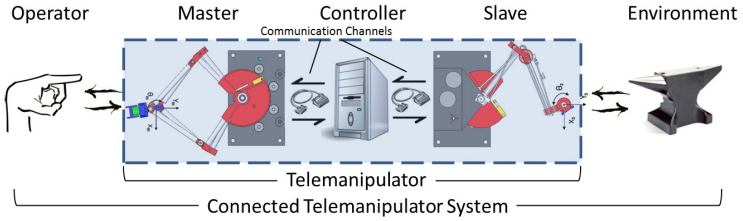

Figure 2.2: Elements of the Connected Telemanipulator System, adapted from Christiansson [27].

The quality of the force feedback is affected by both the haptic controller as well as the manipulator hardware. A strong focus on both aspects exists. Numerous architectures for control have been developed (e.g., [9], [27], [32], [40], [59], [79]). Models like the widely used two-port network analogy [52] allow for accurate evaluation of device performance and stability [32], [54] and for unambiguous comparison of different control architectures [9]. Whereas it is generally suggested that closed-loop control by means of force and position (four-channel control) yields superior performance [9], [27], [79], less sophisticated control architectures like the position-error controller are preferred in conservative fields where system availability is key [106].

The telemanipulator is often optimized toward a virtual rod with an infinitely small mass and an infinitely large stiffness (optimization toward transparency [40]). To optimize the overall connected telemanipulator system performance, however, this is not necessarily the right approach. For example, Christiansson [29] showed that an inferior controller in terms of device performance (e.g., bandwidth, stiffness) yields an increase in terms of task performance (e.g., task completion time contact forces) compared to the classic four-channel controller for a peg-in-hole task. This illustrates that improving the quality of the tool, and thus increasing device performance, does not necessarily improve task performance. Task performance is primarily determined by how effectively the human can use the feedback to control the system. What would be adequate haptic feedback to the human operator?

The *human* operator, the first element of the connected telemanipulator system, creates a somatosensory representation of the situation. This representation is often referred to as the body image or body scheme [25]. Ideally, tools (e.g., a telemanipulator) are included into the body scheme, such that the tools become “transparent”. In haptic teleoperation, this body scheme is most often built out of visual and haptic feedback; human’s two most effective modalities for manipulating objects [129].

While human operators are biased to attend vision, haptic feedback driven manipulation is subjected to less time lag than the visual equivalent [74]. For telemanipulators, the task determines the contributions of the feedback channels: If the task is familiar or requires coarse handling, vision will dominate. If the situation is unknown, delicate handling is required or if visual feedback is suboptimal, the human operator will increasingly rely on haptic information. Klatzky et al. [73] strengthen this, by stating that explorative tasks are generally performed fast and accurately when the bias to attend vision is removed.

Daniel and McAree [32] argue that there is a natural partition of the haptic modality based on physiological properties. Below ~20 Hz, proprioceptors (interoceptive haptic receptors) like Golgi tendon organs and muscle spindles, observe the highly energetic information of the low-frequency haptic channel. Above ~30 Hz, mechano-receptors (exteroceptive touch receptors) construct the information conveying segment of the haptic modality: the high-frequency haptic segment. Situated in the muscles, proprioceptive receptors are the dominating sensors in coordinating movements. Mechanoreceptors, in contrary, contribute to the awareness of systems and surroundings. With a high sensitivity for low-amplitude high-frequency signals (vibrations), these receptors provide unique environmental information [119]. How would the bandwidths of these physiological systems relate to teleoperated task performance? At what bandwidth would task performance saturate?

The third element of the connected telemanipulator system is the environment in which a task is remotely performed. In, for example, nuclear [87], space [10], and (deep-)sea applications, the human is preferably on a remote location with respect to the manipulated objects due to the hostile environment. Telemanipulators used in micro-assembly or (minimal invasive) surgery have the ability to improve the precision and dexterity with which operators can position their instruments, for example, by filtering hand tremor [63]. Some tasks involve accurate positioning of components (e.g., assembly), while other tasks require low-accurate forces to enable a precise trajectory (e.g., applying a torque with a spanner). These two tasks are typical examples of the distinct parameter sets humans apply when executing different tasks. When accurately positioning, humans will act stiff through co-contraction to minimize overshoot due to their own movements or external perturbations. When applying a torque, humans will approximate a tangential force, while they will act compliant in axial and radial directions; humans can comply with external disturbances to minimize undesirable loads [6]. The bolt-and-spanner task cannot be executed if the human would act stiff. This is just one example of the dynamic task behavior of humans. Situations of humans quickly adapting their proprioceptive feedback gain to changing environmental conditions (e.g., force perturbations [125] or damping [36]) have also been reported.

The task-dependent adaptive behavior of visual and haptic feedback complicates the assessment of generic task performance; an arbitrary task A yields different requirements from an arbitrary task B. Hence, a fundamental span of tasks needs to be defined, describing the wide variety of tasks. Aliaga acknowledged this problem and proposed a set of four device parameters that are representable for the task span: free motion impedance, position tracking in free movement, force tracking in hard contact tasks, and maximum transmittable impedance [9]. However, human-in-the-loop performance is not an integral part of this analytical approach. Nonetheless, the set can be extrapolated to a set of fundamental tasks, oriented to define task performance instead of device performance. It is proposed that many tasks, but specifically tasks where hard-hard contact occurs (e.g., nuclear remote handling, (deep-)sea or space operations) can be separated in the following four fundamental tasks:

1. Free-space movement tasks are the tasks for which the external forces on the slave device are zero, with or without tool.

2. Contact transition tasks are the transitional stages in between free-space movement tasks and environmental interaction. Adequate perception of contact establishment can be crucial to determine spatial position and orientation of objects.

3. Constrained translational tasks are tasks in which a movement along an axis is performed, requiring a high level of position control. This can either appear by mechanical constraints (e.g., coaxial sliding of pipes) or a constrained distance to an object (e.g., welding).

4. In constrained rotational tasks, a hard mechanical linkage constrains the degrees of freedom to rotations along a precise trajectory around a pivot point. The task requires to control forces on the linkage, tangential to the trajectory. Examples are bolting actions, opening lids or valves and turning a door handle.

On the basis of the human's physiological properties, Brooks [21] stated that a force feedback signal should have a minimal bandwidth of 20-30 Hz for "meaningful perception," while "near-optimal performance" is achieved for ~400 -Hz bandwidth. Experimental assessment of task performance has shown that for a peg-in-hole task, low-frequency haptic feedback reduces impact forces, but does not influence environmental contact forces or task completion time [28]. This same research shows that high-frequency haptic feedback does not improve task performance, while the combination of low- and high-frequency feedback reduces subjective workload and increases subjective task performance. Providing high-frequency feedback information improves the performance of material identification tasks [76], [2]. However, these studies concern small task segments, which have only limited meaning on overall, operational task performance.

The main objective of this research is to understand how the quality of haptic feedback influences human-in-the-loop task performance. We limit the study to what is useful for tasks performed in a hard-to-hard environment, well known to the operator. Subjects are presented with four haptic feedback conditions that address the complete haptic feedback spectrum: teleoperated control with no haptic feedback (TC_{NF}), low-frequency haptic feedback (TC_{LF}), and combined low- and high-frequency haptic feedback (TC_{LFHF}), while natural haptic feedback is presented in a direct-controlled equivalent (DC). The main question of this research is: To what extent does the quality of haptic feedback contribute to human-in-the-loop task performance, using a telemanipulator as a tool?

Brooks [21] itemizes the bandwidth of environmental signals, by estimated slow skin motion at ~0Hz, compressive stresses at ~10Hz, controlled slip at ~30Hz, and vibrations up to ~400Hz. With these properties as a starting point, it is expected that free-space movement tasks will not benefit from any form of haptic feedback. Contact transition tasks, however, yield compressive stresses and high-frequent vibrations on impact, and therefore both low-frequency and high-frequency haptic feedbacks are expected to increase task performance. For constrained translational and constrained rotational tasks, slow skin motions, compressive stresses, and controlled slip will occur; it is expected that providing low-frequency feedback improves task performance. The hypotheses have been summarized in Tab. 2.1. Notice that teleoperated task execution without haptic feedback (TC_{NF}) has been defined as the baseline scenario.

Fundamental Subtask	Haptic Feedback Quality TC_{NF}	TC_{LF}	TC_{LFHF}	DC
Free-Space Movement	0	0	0	0
Contact Transition	0	+	++	++
Constrained Translational	0	+	+	++
Constrained Rotational	0	+	+	++

Table 2.1: Hypothesized task performance effect of haptic feedback quality per fundamental task. '+' and '++' denote two levels of performance improvements with respect to baseline task performance (symbolized by '0') without haptic feedback.

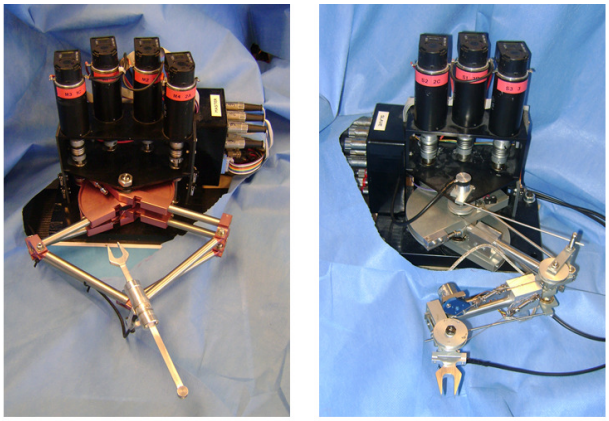

a) b)

Figure 2.3: The Munin master (a) and slave (b) devices.

2.2. METHODS

2.2.1. SUBJECTS

Ten subjects with an age range of 23 to 28 years participated in a within-subject designed experiment.Three subjects had previous experience with telemanipulators, while the other seven had no experience at all. The subjects were given an introduction to the system and were, after practice, asked to complete a teleoperated bolt-and-spanner task. All subjects gave their informed consent.

2.2.2. EXPERIMENTAL SETUP

The experiments were performed on a 3-DoF planar teleoperation system. The system consists of a double-rhomb force-redundant parallel master (Fig. 2.3a) and a serial slave device (Fig. 2.3b), as first discussed in [27]. The system runs on a Mathworks xPC Target real-time operating system at 1 kHz, with an estimated time delay between master and slave of 1.5 ms.

On both master and slave a spanner interface was constructed. The master was instru-

mented with a ATI Nano 17-SI 12 6-DoF force sensor to measure the operator's input. A Setra Model 141 accelerometer was mounted on the slave side to measure the high-frequency contact forces.

Impedance models of the master ($Z_m = F_m/V_m$) and slave (Z_s) have been estimated separately for the translations (x, y) and rotation (Θ):

$$Z_{m,xy} = m_{m,xy}s + b_{m,xy}, \text{ with } m_{m,xy} = 0.23\ Ns^2/m \text{ and } b_{m,xy} = 4.5\ Ns/m,$$

$$Z_{m,\Theta} = m_{m,\Theta}s + b_{m,\Theta}, \text{ with } m_{m,\Theta} = 0.025 \cdot 10^{-3}\ Ns^2/m \text{ and } b_{m,\Theta} = 0.02\ Ns/m,$$

$$Z_{s,xy} = m_{s,xy}s + b_{s,xy}, \text{ with } m_{s,xy} = 0.28\ Ns^2/m \text{ and } b_{s,xy} = 6\ Ns/m,$$

$$Z_{s,\Theta} = m_{s,\Theta}s + b_{s,\Theta}, \text{ with } m_{s,\Theta} = 0.025 \cdot 10^{-3}\ Ns^2/m \text{ and } b_{s,\Theta} = 0.04\ Ns/m.$$

A generic (two-channel PD) position-error controller was implemented, as this is the baseline for most industrial telemanipulators due to its robustness [106]. The PD gains have been set equal for master and slave: $K_{pd,xy} = 400/s + 0.02$ for the translations and $K_{pd,\Theta} = 0.4$/s+0.002 for the rotations.

Using the two-port network modeling framework [52] and the HapticAnalysis package [27], device performance and stability were evaluated. It was calculated that, among other metrics, the bilateral force and positional bandwidth are ~7 Hz, the transparency error is ~68 [-] and the Zwidth is 31 [-]. According to the passivity [54], absolute stability [108], and closed-loop stability [27] criteria, the controller is stable.

In addition, the stiffness of the telemanipulator was measured for four instances for each of the degrees of freedom. The mean for the x-direction is 449 N/m with a standard deviation (σ) of 7.5 N/m. For the y- and Θ-directions, a stiffnesses of, respectively, 380 (σ=64) N/m and 0.261 (σ=0.013) Nm/rad were obtained. Notice that the measured stiffnesses in x- and y-direction are respectably close to the analytical stiffness of 400 N/m (the translational P-gain), while the rotation stiffness seems to suffer substantially from mechanical compliance (0.4 Nm/rad calculated versus 0.261 Nm/rad measured stiffness). A more detailed analysis of performance and stability of this particular setup is performed in [132].

The environment with which the telemanipulator interacts consists out of a M6 bolt constructed on an aluminum plate. The implementation of the environment on the slave side is shown in Fig. 2.4. The moment on the bolt is created artificially with a spring, such that the tightening torque is constant. The tightening torques to overcome the static and dynamic friction were measured for 20 instances. The mean of the static friction is 35.7 Nmm, with a standard deviation (σ) of 2.0 Nmm. For the dynamic friction a mean of 31.6 (σ=6.1) Nmm was measured.

2.2.3. TASK DESCRIPTION

The subjects were asked to complete a modified bolt-and-spanner task, starting at point A and moving subsequently to B and C (see Fig. 2.4). A, B, and C were located at (x y Θ =

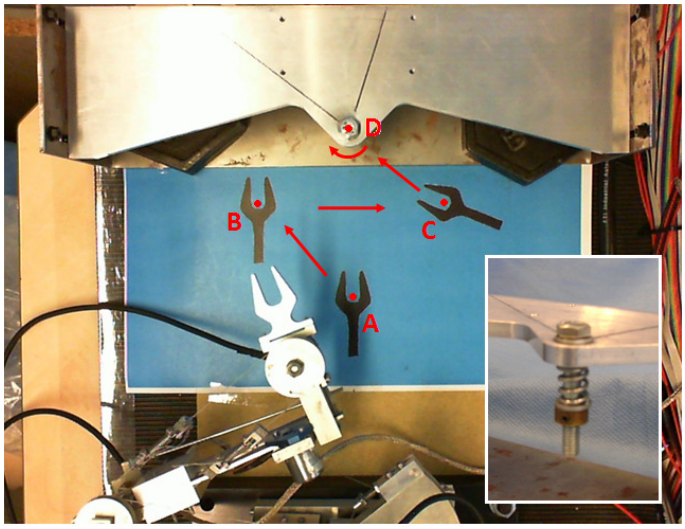

Figure 2.4: Implementation of the bolt-and-spanner task, slave side (scale approximately 1:10).

(0 0 0)), (-0.06m 0.08m 0°), and (0.06m 0.08m -60°), respectively. From C, the subjects had to slide the spanner over the bolt, which was located at D = (x y = 0m 0.12m). Finally, an 80-degree stroke had to be made. Reference points and angles were all visually indicated.

The bolt-and-spanner task contains the four fundamental subtasks. Free-space movement is performed when moving from A to B to C (see Fig. 2.5). Contact transition is started at C and is considered completed when the contact evolves to a sliding motion. The sliding motion over the bolt is considered a constrained translational task. A constrained rotational task is executed when identifying the compliance center of the rotation, while minimizing forces perpendicular to the circular trajectory.

2.2.4. EXPERIMENT DESIGN

Three experimental conditions are discriminated, namely haptic feedback quality, visual feedback, and task instruction.

HAPTIC FEEDBACK QUALITY

The subjects were presented with four levels of haptic feedback:

1. TC_{NF} (teleoperated control without force feedback). Effectively, this is achieved by setting the slave-to-master PD gains to zero.

2. TC_{LF} (teleoperated control with low-frequency haptic feedback). It is provided by a classic position-error controller. The analytical bandwidth of the force signal presented to the human operator is approximately 7 Hz [132].

3. TC_{LFHF}. A high-frequency signal is superimposed on the existing low-frequency force feedback. The signal is hand tuned to provide an intuitive feeling. Measured

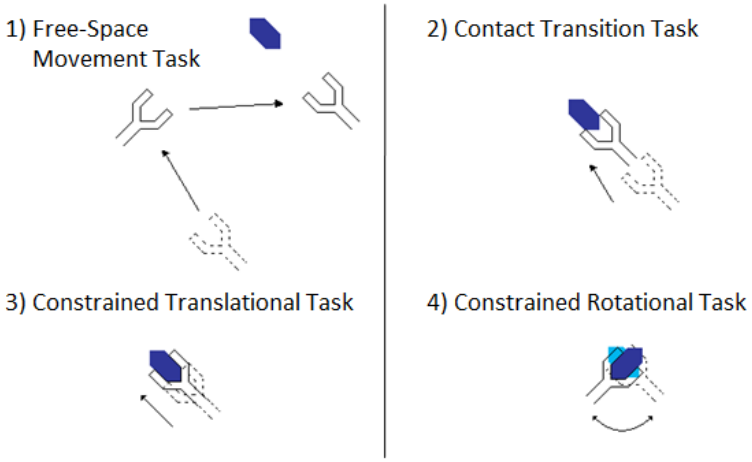

Figure 2.5: The four fundamental subtasks as identified in a bolt-and-spanner task.

contact accelerations are passed through a fourth-order high-pass Butterworth filter with a cutoff frequency of 30 Hz; the boundary of Daniel and McAree's partition of the haptic modality [32]. When the filtered signal exceeds a threshold of 0.015 m/s2, a signal containing a 50-Hz and a 100-Hz sinusoid (frequencies the manipulator can display, while being above the 30-Hz boundary) is generated and displayed with a delay of 2-3 ms for the duration of one 50-Hz period (20 ms). Notice that the amplitude is proportional to the impact acceleration.

4. *DC*. The direct-controlled equivalent of the bolt-and-spanner task. A rigid spanner interconnects human and task, therefore attaining a force feedback bandwidth in the order of thousands of Hertz. The environment is relocated to the master side and the task is executed while holding the master, but now with decoupled slave. The *DC* condition allows for reference comparison to the telemanipulated conditions.

VISUAL FEEDBACK

Suboptimal camera views are often encountered in teleoperation. For example, the view suffers from depth perception issues or the line of sight is blocked by the manipulated object. Therefore, two opposites of visual feedback are tested. Either a perpendicular view of the scene is provided for optimal visual feedback, or no visual feedback is provided at all such that the subject has to perform the task blind. The perpendicular view is displayed on a computer screen next to the setup using a Microsoft Lifecam Cinema webcam. Fig. 2.4 shows the view the subject is provided with.

The subjects are not asked to perform the task blind in the TC_{NF} condition. Furthermore, if the task is to be completed blind, the free-space movement task is not performed and the subject will start its trial at point C (see Fig. 2.4).

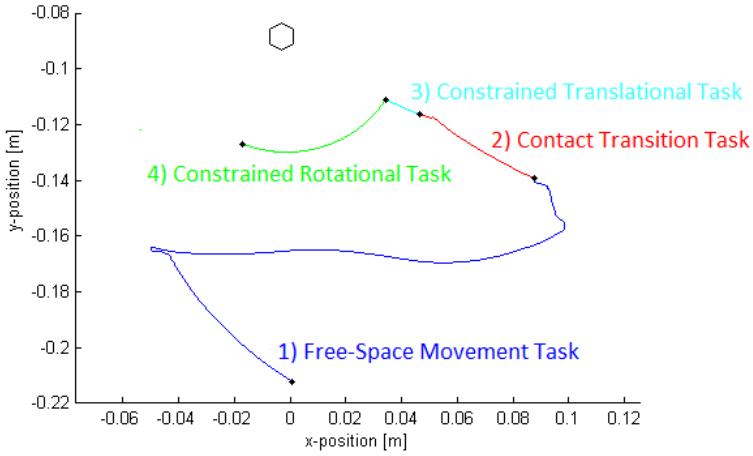

Figure 2.6: Trajectory plot of the manipulator endpoint position, showing the four fundamental subtasks.

TASK INSTRUCTION

When performing a task, subjects have a natural preference for a certain control strategy. Often, these strategies are trade-offs between force magnitude, positional accuracy, and/or time. Hence, the subjects are given two opposing task instructions:

1. *Accurate*, to evoke task execution optimized toward low forces and positional accuracy, or
2. *Fast*, to evoke task execution optimized toward time.

2.2.5. DATA ACQUISITION AND TASK PERFORMANCE METRICS

The positions of master and slave are recorded with an accuracy of 0.03 mm. On the master side, a force sensor is placed, which measures the forces and torques between the human operator and master device in three degrees of freedom. All data are recorded at 1 kHz. Fig. 2.6 shows a typical example of a subject completing the bolt-and-spanner task: The free-space movement task is represented by the blue-colored trajectory, the contact transition task is colored red, while the constrained translational and constrained rotational task are, respectively, colored cyan and green. Based on the recorded data, task performance is evaluated in terms of *task completion time*:

- t_{tct} task completion time s, the time in seconds it requires for the subject to complete the task.

Two metrics for control effort are defined:

- $F_{i,m}$ maximum input force N, maximum interaction force between operator and master.
- n_{rr} reversal rate [-], the amount of steering corrections by the operator as a measure for his mental effort [83]. The input forces of the operator are passed through

a 10-Hz low-pass (fourth-order Butterworth) filter, and the amount of sign changes is counted. Trained operators tend to steer smoothly, resulting in a low n_{rr}.

Furthermore, for each haptic feedback condition, the following metrics are tracked:

- The self-reported workload is captured using the NASA Task Load Index on a scale from 0 to 100 [49]. A lower score represents a lower subjective workload.
- The subjects are asked to grade their performance on a 20-point scale from 1 to 10, where 1 represents failure and 10 represents perfection. This is the self-reported performance.

2.2.6. DATA ANALYSIS

The comparison of experimental conditions was made on basis of populations, assuming a normal distribution. Using a repeated measure design, 10 subjects were asked to repeat each combination of experimental conditions eight times. The order with which the haptic feedback conditions and combinations of visual feedback and task instruction was presented was randomized. The data were analyzed using a two-way analysis of variance, with factors representing haptic feedback quality and subject inter-variance. A post hoc analysis was executed to compare the haptic feedback quality levels. Only the post hoc results will be presented in the results section. The self-reported workload and self-reported performance scores were evaluated using a paired T-test. Results with a p-value below 0.05 are considered significant (α=0.05). The significance of the results is presented as "•••", "••," and "•" for, respectively, p≤0.001, p≤0.01, and p≤0.05.

The parameters of the experiment are summarized in Table 2.2.

2.3. RESULTS

Fig. 2.7 shows a bar chart of the mean task completion time (t_{tct}) for the complete bolt-and-spanner task, separated for the means of the different subtasks. The following results are obtained:

- VA. For the *visual* and *accurate* condition, TC_{LF}, TC_{LFHF}, and DC show a decreased task completion time compared to TC_{NF} (respectively, p=0.042, F=5.6; p=0.018, F=8.3; p<0.0001, F=55.1). There are no differences between TC_{LF}, TC_{LFHF}, and DC (p≥0.068, F≤4.3).
- VF. For the *visual* and *fast* condition, both TC_{LFHF} (p=0.011, F=10.1) and DC (p=0.015, F=9.1) show a decrease in task completion time compared to TC_{NF}.
- BA. Compared to TC_{LFHF}, DC shows a decrease in task completion time (p=0.009, F=11.3) when performed *blind* and *accurate*.
- BF. When performed *blind* and *fast*, no differences were found.

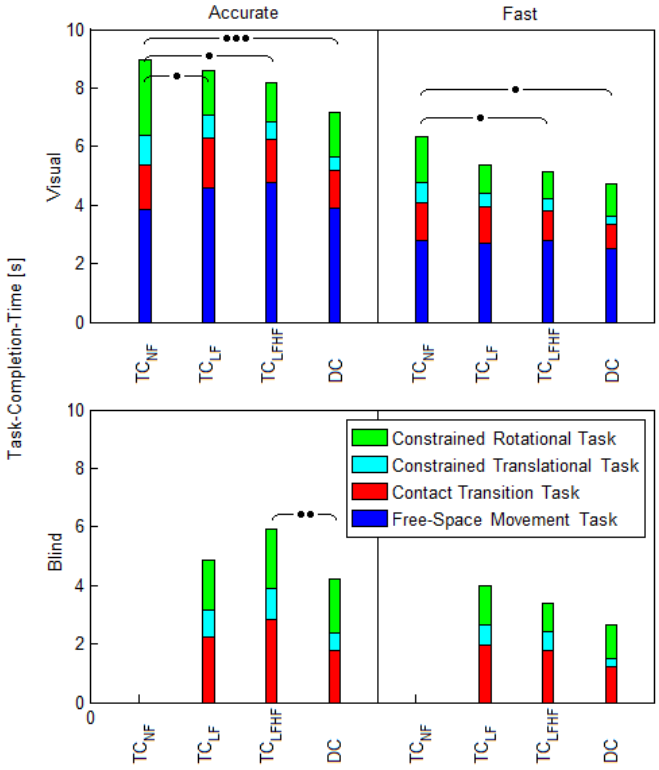

Figure 2.7: Task performance—mean task completion time of the entire bolt-and-spanner task. Each bar graph shows the mean contribution of the four fundamental subtasks. "•••," "••," and "•", respectively, denote the significance of $p \leq 0.001$, $p \leq 0.01$, and $p \leq 0.05$.

Summary of the Experimental Design	
Task:	four fundamental subtasks (Free-Space Movement, Contact Transition, Constrained Translational and Constrained Rotational Tasks), performed in a single bolt-and-spanner task
Conditions:	haptic feedback Quality (TC_{NF}, TC_{LF}, TC_{LFHF}, DC), Visual feedback (*Visual, Blind*) and Task Instruction (*Accurate, Fast*)
Metrics:	task-Completion-Time, Maximum Input Force, Reversal Rate, Task Load Index, Self-Reported Performance
Group size:	10 subjects (3 with basic experience with telemanipulators, 7 with no experience)
Practice:	5 minutes general practice with the setup, task instruction and visual conditions
Repetitions:	8 for each combination of conditions
Breaks:	a 10 second break in between each repetition, a 1 minute break after each set of 8
Design:	within-subject and randomized conditions

Table 2.2: Summary of the Experimental Design.

The mean of the NASA Task Load Index for the TC_{NF}, TC_{LF}, TC_{LFHF}, and DC condition was, respectively, 61, 51, 50, and 38. A clear ranking is obtained: TC_{LF}, TC_{LFHF}, and DC yield a lower workload compared to the baseline TC_{NF} (respectively, p =0.012, p =0.002, and p<0.0001). Between TC_{LF} and TC_{LFHF}, there is no difference (p=0.900), while DC yields a lower workload than TC_{LF} (p≤0.0001) and TC_{LFHF} (p=0.007). Thus, the following ranking toward task performance is obtained: TC_{NF}> TC_{LF}=TC_{LFHF}> DC. The mean of the self-reported performance was 5.6 for TC_{NF}, 6.8 for TC_{LF}, 7.1 for TC_{LFHF}, and 7.9 for DC. Eight out of 10 subjects rated their performance higher when more haptic feedback was available. The two participants that reported a higher subjective workload for TC_{LFHF} compared to TC_{LF}, also rated their performance lower. No difference was found between TC_{LF} and TC_{LFHF} (p=0.425). The TC_{NF} condition was rated the lowest performance (p=0.024, p≤0.0001, and p≤0.0001 for, respectively, TC_{LF}, TC_{LFHF}, and DC), whereas DC yields superior performance (p=0.022, p≤0.0001, and p≤0.0001 for, respectively, TC_{LFHF}, TC_{LF}, and TC_{NF}). Hence, also for the self-reported performance, the ranking $TC_{NF} > TC_{LF} = TC_{LFHF} > DC$ holds.

The task performance (t_{tct}) and control effort ($F_{i,m}$ and n_{rr}) metrics are separately presented for each of the fundamental subtasks in the upcoming paragraphs.

2.3.1. FREE-SPACE MOVEMENT TASK

For the free-space movement task, performance in terms of the task completion time (ttct) and control effort in terms of reversal rate (nrr) are not influenced by the haptic feedback quality. The maximum input force (Fi,m), however, shows differences for both task instruction conditions.

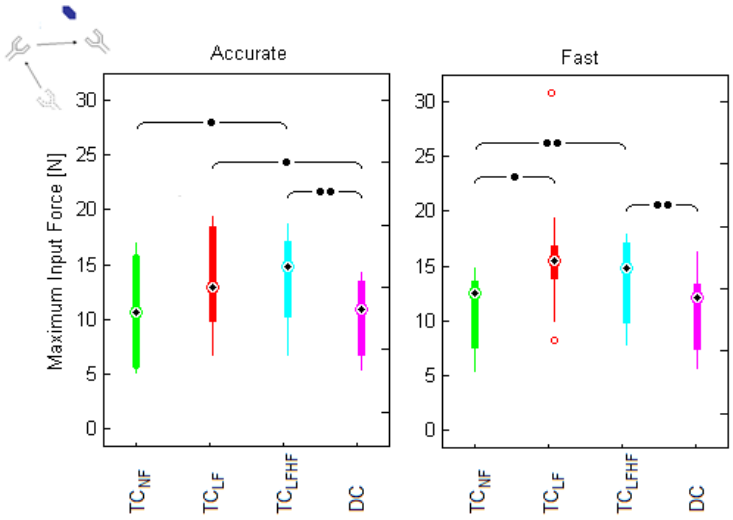

Figure 2.8: Free-space movement task—maximum input force. TC_{LF} and TC_{LFHF} yield higher operator input forces compared to TC_{NF} and DC. Each boxplot shows the data for 10 subjects, averaged for eight repetitions per subject. A boxplot displays the median of the data set, the 25th and 75th percentiles, while the whiskers extend to 1.5 times inter-quartile range. The circles represent outliers.

Fig. 2.8 shows box plots of the operator's maximum input force for the free-space movement task. In the accurate condition, the operator provides higher input forces when position-error control is enabled: TC_{LFHF} shows an increase compared to TC_{NF} (p=0.040, F=5.8), while both TC_{LF} and TC_{LFHF} show an increase compared to DC (respectively, p=0.013, F=9.5; p=0.0003, F=31.9). When performed fast, a similar phenomenon is observed; TC_{LF} shows a higher maximum input force compared to TC_{NF} (p=0.0459, F=5.4), whereas the input force during TC_{LFHF} is higher for both TC_{NF} (p=0.0005, F=27.3) and DC (p=0.009, F=11.2).

2.3.2. CONTACT TRANSITION TASK

The contact transition task shows no differences for task-completion time and reversal rate. Fig. 2.9 shows the maximum input force for this fundamental subtask. In general, it can be seen that performing the task blind or fast yields higher input forces than, respectively, visual or accurate task execution. Also, when performing the task accurately, haptic feedback quality does not influence the input force ($p \geq 0.082$, $F \leq 3.8$). For the visual and fast condition, however, TC_{LF} and DC both show an input force increase compared to TC_{NF} (respectively, p=0.0008, F=24.2; p=0.0098, F=10.6), while DC shows an increase compared to TC_{LFHF} (p=0.012, F=9.9). When performed blind and fast, DC shows higher input forces compared to both TC_{LF} (p=0.0043, F=14.4) and TC_{LFHF} (p=0.0005, F=27.7), most likely due to the direct contact with the environment. Hence, the expected performance increase of TC_{LFHF} compared to TC_{LF} was not found for any of the conditions.

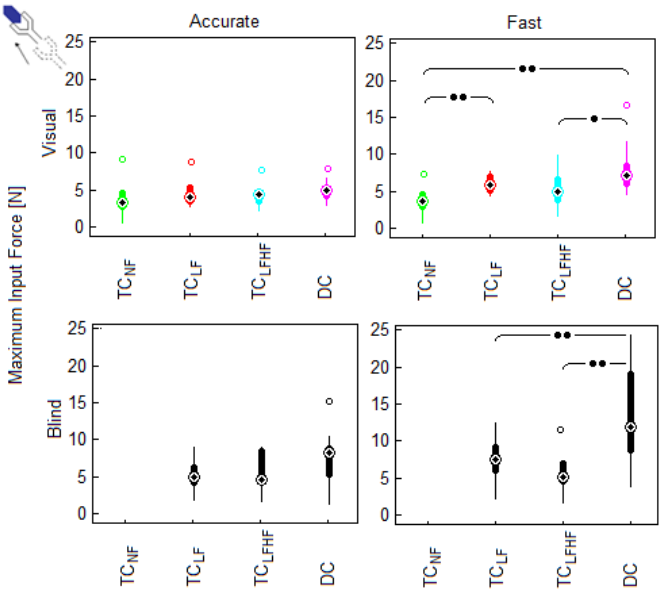

Figure 2.9: Contact transition task—maximum input force. A performance increase of TC_{LF} with respect to TC_{LFHF} cannot be found.

2.3.3. CONSTRAINED TRANSLATIONAL TASK

All task performance and control effort metrics show similar results: TC_{LF}, TC_{LFHF}, and DC all are superior to the TC_{NF} condition. TC_{LF} and TC_{LFHF} show no measurable differences, while DC yields superior performance. This ranking is illustrated by Fig. 2.10. The task completion time is reduced for TC_{LF} compared to TC_{NF} when performed accurate (p=0.0034, F=6.21) as well as when performed fast (p=0.028, F=6.8). TC_{LFHF} feedback does not yield an improvement compared to TC_{LF} (p≥0.187, F≤2.0). DC shows a further reduction of task completion time (p≤0.044, F≥5.5). As stated, the same classification of haptic feedback holds for maximum input forces and reversal rate.

Fig. 2.11 shows that providing low-frequency haptic feedback (TC_{LF} and TC_{LFHF}) reduces the reversal rate compared to the baseline TC_{NF} (p≤0.017, F≥8.5). DC is superior for all conditions (p≤0.045, F≥5.4), while no differences can be found between found between TC_{LF} and TC_{LFHF} (p≥0.27, F≤1.4).

2.3.4. CONSTRAINED ROTATIONAL TASK

Performing the constrained rotational task without haptic feedback (TC_{NF}) yields inferior task performance compared to the other haptic feedback quality conditions (p≤0.001, F≥24.4 for accurate and p≤0.011, F≥10.5 for fast), whereas no differences are found between TC_{LF}, TC_{LFHF}, and DC. Box plots of the task completion time are shown in Fig. 2.12. For the reversal rate, similar results are obtained; TC_{LF}, TC_{LFHF}, and DC all show a decrease in the reversal rate compared to TC_{NF} (p≤0.002, F≥18.7 for accurate and

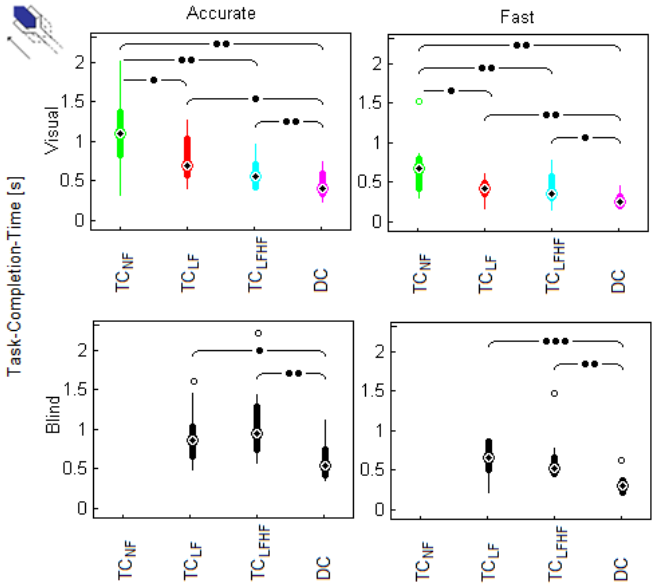

Figure 2.10: Constrained translational task—task completion time. TC_{NF} performance is inferior, TC_{LF} and TC_{LFHF} show no measurable difference, while DC yields superior performance.

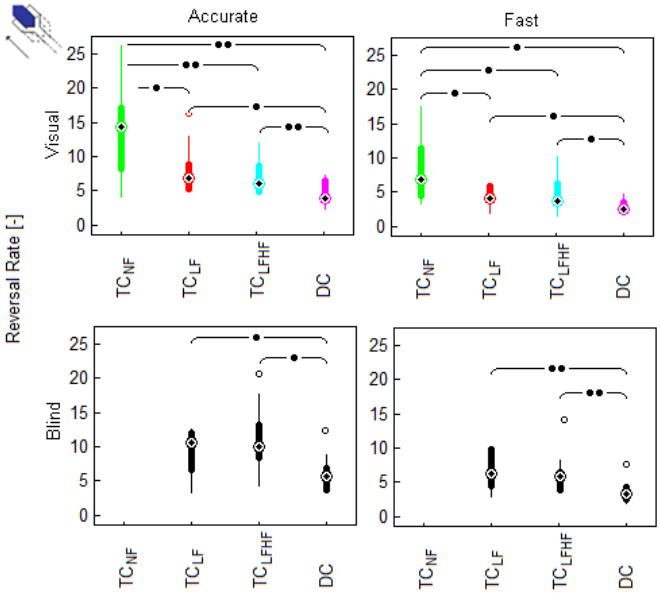

Figure 2.11: Constrained translational task—reversal rate. Control effort classification: $TC_{NF} > TC_{LF} = TC_{LFHF} > DC$.

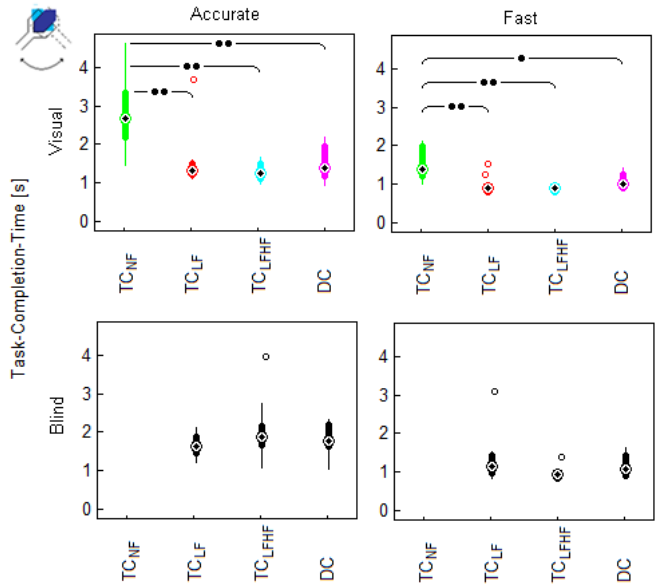

Figure 2.12: Constrained rotational task—task completion time. TC_{NF} shows inferior performance, whereas no differences are found between TC_{LF}, TC_{LFHF}, and DC.

p≤0.007, F≥12.2 for fast), whereas in between TC_{LF}, TC_{LFHF}, and DC no differences are found. This is illustrated in Fig. 2.13. The operator's maximum input force differs from this pattern. For DC compared to TC_{LFHF}, the maximum operator input force is increased for the visual and fast condition (p=0.0034, F=15.6), while for blind conditions the input force is decreased (p≤0.031, F≥6.5). Visual and accurate shows no differences.

2.4. DISCUSSION

In general, increasing haptic feedback quality improves task performance, regardless of operator and strategy. However, many significant differences found in the analyzed, broad spectrum of haptic feedback only show a relatively small magnitude of change: The largest improvement is a 54 percent reduction in task completion time, when comparing the extreme situation of full natural haptic feedback with no haptic feedback (DC compared to TC_{NF}). Moreover, the differences of TC_{LF} and TC_{LFHF} with DC are much smaller than expected. Even for the constrained rotational task, which describes a complex path, the tasks could be performed fairly well for all conditions. Apparently, the quality of haptic feedback does not substantially affect task performance.

For the free-space movement task, different haptic feedback conditions did not lead to differences in task completion time and reversal rate, while the operator's maximum input forces are higher for TC_{LF} and TC_{LFHF} compared to TC_{NF} and DC. This is an artifact of the haptic controller; the position-error controller partially reflects the slave's inertia in TC_{LF} and TC_{LFHF}, but not in TC_{NF} (no feedback controller) and DC (no slave).

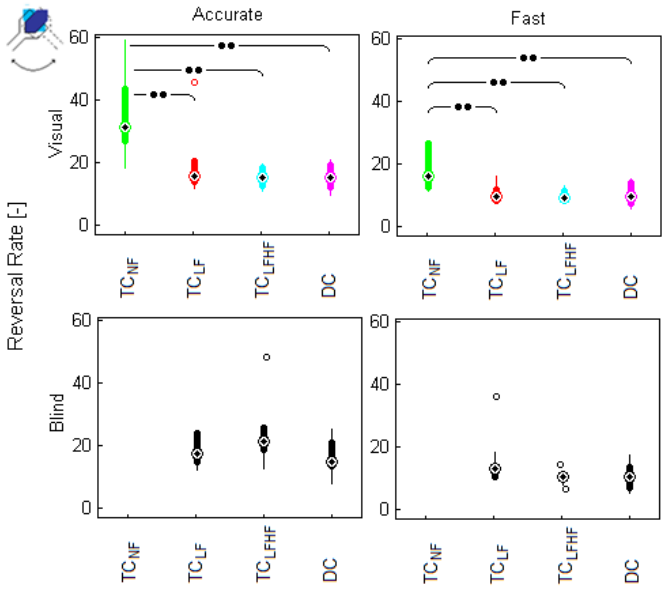

Figure 2.13: Constrained rotational task—reversal rate. Again, TC_{NF} shows inferior performance compared to the other conditions: $TC_{NF} > TC_{LF} = TC_{LFHF} = DC$.

Also, interaction forces between bolt and spanner propagating through the tool to the operator face a higher stiffness, lower inertia, and lower damping in DC (a rigid spanner) compared to TC (a two-bar linkage). Hence, one could argue that for DC, besides a now perfect transparent haptic controller, the hardware has also become more transparent.

The combination of contact transition and constrained translational tasks shows many similarities with common peg-in-hole tasks; the operator is to align the relatively long spanner properly, whereupon it is slid over the bolt. Peg-in-hole tasks are surprisingly difficult to perform using robotic manipulators, partly due to the limited mechanical compliance of the robotic device [24]. Telemanipulators, in general, are a relative compliant type of robotic manipulators. For example, Christiansson [28] pointed out that due to its compliance, the predecessor of the device used in this research seemed to facilitate peg-in-hole tasks. Therefore, the stiffness of the critical, rotational degree of freedom was increased by a factor of ~4-5 to 261 Nmm/rad (n=4, σ=13) compared to previous studies. Still, it could be possible that, during teleoperated conditions (TC_{NF}, TC_{LF}, and TC_{LFHF}), the manipulator facilitates peg-in-hole tasks to an extent where the importance of a mating strategy, and thus haptic feedback quality, is reduced. For the constrained position task, the second part of a peg-in-hole task, this compliance does not seem to substantially reduce the usefulness of haptic feedback; providing feedback in telemanipulated conditions (TC_{LF} and TC_{LFHF} compared to TC_{NF}) improves performance and control effort, but performing the task with a rigid manipulator (DC com-

pared to TC_{LF} and TC_{LFHF}) improves the task execution even more. This is in agreement with previous studies showing that peg-in-hole tasks benefit from haptic feedback [55], [28]. For the contact transition task, a similar effect is seen, but only for the control effort of fast executed trials. Thus, for the contact transition task, instead of an effect of haptic feedback, it could also be the compliance that affects performance, in general, and control effort for accurately performed trials.

Low-frequency haptic feedback improves performance for constrained translational and constrained rotational tasks, but not for free-space movement nor contact transition tasks. Further improvement of the haptic feedback quality, by providing additional high-frequency haptic feedback (TC_{LFHF}) or by allowing direct control (DC), does not substantially improve task performance. O'Malley and Goldfarb [95] state that while the lower boundary of connected telemanipulator system performance is limited by the tool (telemanipulator) capabilities, the upper boundary is limited by the human operator himself. In other words, there are certain minimum requirements to the content of the information projected at the master side, but it is redundant to provide more information [27]. Apparently, for the tested tasks, providing low-frequency haptic feedback suffices the requirements to optimize the performance of the connected telemanipulator system. Hence, low-frequency haptic feedback out of all haptic feedback is predominantly responsible for improvements in task performance for the experimental conditions studied.

Humans, in general, are biased to use their visual channel for task control [74]. The same holds for the subjects that participated in this experiment; they struggled to verify the correctness of their movements in the absence of visual feedback, shown by the increase in task completion time (for constrained translational, and constrained rotational tasks), maximum input force (for contact transition and constrained translational tasks), and reversal rate (for contact transition, constrained translational, and constrained rotational tasks). Their movements show characteristics of explorative tasks, with indecisiveness and unstructured motion control. Hence, in most cases, subjects are quite right to bias visual feedback. However, if subjects are forced to perform the contact transition task under tight time constraints, the task completion time is equal for blind performed tasks compared to tasks with visual feedback. This indicates that, specifically for the fast executed contact transition task, the haptic channel dominates regardless of the visual feedback conditions.

The four generalized fundamental tasks as defined in this study are mainly relevant for maintenance and (dis-)assembly tasks. Typical examples are the remote handling activities as currently performed at fusion reactor JET [87] and as foreseen at future fusion reactors [106]. Here, thoroughly offline planned and rehearsed tasks are performed in a hard-to-hard environment, well known to the operator. For teleoperated tasks like those in the medical field, soft tissue discrimination tasks are of vital importance. Hence, the implementation of the high-frequency haptic feedback and the definition of the fundamental tasks may need application-specific adjustment.

Another important acknowledgment is that the repeating nature of experiments, in general, and this bolt-and-spanner task specifically could lead to a situation where subjects are able to include the telemanipulator dynamics and task instructions into their body scheme, to an extent where the focus shifts from feedback-based task control to control on the basis of feedforward. While this partially is what is strived for, in practice, when tasks are extensively offline rehearsed, feedforward control through extensive practice can hinder the analysis of isolated task segments. In this experiment, feedforward control has been observed in all subtasks (the blind condition actually evokes feedforward control deliberately). While the task cannot be performed decently without any form of haptic and visual feedback (purely feedforward), the task performance on basis of solely haptic or visual feedback is fair. Apparently, the subjects were well aware of the telemanipulator dynamics and could therefore include the telemanipulator dynamics into their body scheme fairly well for this particular task and setting.

Although the bolt-and-spanner task is, in principle, a three degree of freedom task (3 DoF), containing two translations and one rotation, performing a similar task in 6 DoFs would be fundamentally more difficult. A planar 3 DoF environment can be optimally visualized using only one perpendicular camera view, whereas for 6 DoF one would need at least three camera views for verification of the three translations and rotations. Hence, tracking all 6 DoF simultaneously via the visual channel adds complications in (depth) perception and introduces virtual translations between the camera views; implications that do not occur when making the same transition for the haptic cue. Therefore, it is expected that operators will be much more dependent on the haptic channel for 6 DoF manipulation tasks than they are for 3 DoF tasks.

The results suggest that, for the tasks studied, limited task performance improvements may be expected when further pursuing optimal transparency. A promising alternative strategy is to support the operator by providing additional virtual feedback information, either visually (e.g., augmented reality [11]) or haptically (e.g., virtual fixtures [107]). An example that stands out in literature is shared control, first described by Steele and Gillespie [120]. Shared control offers the ability to highlight preferred control strategies to enhance performance or safety in dynamic work environments, for example, by providing haptic guidance signals [7]. Haptic shared control shows promising results in the automotive domain (e.g., lane changing [7]), and recently also in teleoperation (e.g., obstacle avoidance [68]). By looking at the task requirements, shared control directly and continuously supports the operator in his task. As a result, it improves performance of the system as a whole. Improving transparency on the other hand mainly focuses on a single element of the connected telemanipulator system (the telemanipulator), which according to this study, leaves only marginal space to improve the system's overall performance. Illustrative is the research by Boessenkool et al. [14], which shows that augmented feedback on basis of solely shared control is more effective than feedback based on transparency optimization.

This study suggests that only by combining state-of-the-art developments in control techniques and thorough understanding of human motion control with sophisticated

support strategies like shared control, the task performance of the connected telemanipulation system can be optimized.

2.5. CONCLUSIONS

The influence of haptic feedback quality on teleoperated task performance and control effort has been assessed for a typical (dis-)assembly task in a hard-to-hard environment, well-known to the operator. Four fundamental subtasks have been identified, namely: 1) free-space movement, 2) contact transition, 3) constrained translational, and 4) constrained rotational tasks. For the experimental conditions studied, it can be concluded that compared to baseline task performance without haptic feedback:

- Overall task performance is substantially improved by providing low-frequency haptic feedback, while further increasing the haptic feedback quality yields only marginal improvements, even if a full natural spectrum of haptic feedback is provided.
- Improvements due to low-frequency haptic feedback occur during constrained translational (a reduction in task completion time, maximum input force, and reversal rate) and constrained rotational subtasks (a reduction in task completion time and reversal rate).
- Compared to low-frequency haptic feedback, providing a full spectrum of haptic feedback improves constrained translational tasks (in terms of task-completion time, maximum input force, and reversal rate) and fast executed contact transition tasks (in terms of maximum input force), while the performance and control effort of constrained rotational tasks remains unaffected.

CHAPTER 3

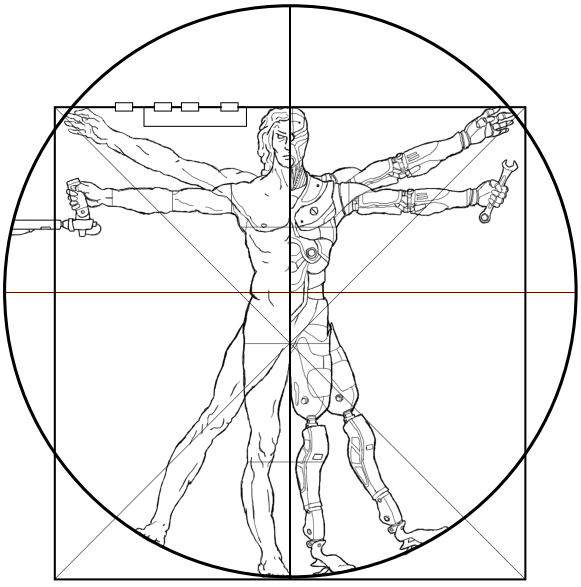

3

Exploring Haptic Feedback Designs for Rate Controlled Systems

The design of haptic feedback in rate control is challenging as the input (i.e. master) does not match the controlled system's (i.e. slave) output, in terms of physical quantity as well as order of magnitude. Therefore the measured interaction forces of the controlled system with its environment cannot be reflected directly to the human operator. In this chapter the efficacy of four different haptic interface designs for rate control is determined for free-space, contact transition and force-level tasks. Fig. 3.1 shows a simplified control-theoretic representation of the experimental conditions.

This chapter was submitted for review to IEEE Transactions on Haptics

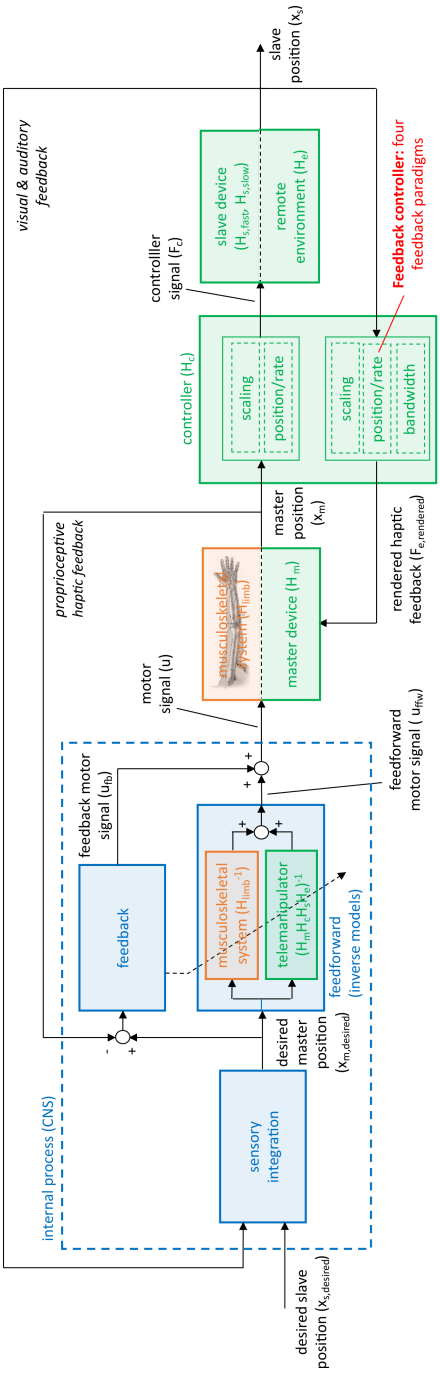

Figure 3.1: Simplified control-theoretic representation of the study as performed in this chapter. In order to study the efficacy of haptic feedback design for a rate-controlled task, four haptic feedback designs (shown in red) were evaluated within a uniform framework including (sub)tasks, task instruction and visual feedback.

ABSTRACT
In rate control, the position of the operators input device commands a desired velocity for the controlled machine. This type of control is the industry standard for operators controlling heavy machines over large workspaces. The operator usually only has visual feedback and feels no haptic feedback concerning the machine dynamics, or its interaction forces with the environment. Where haptic information potentially makes task execution more intuitive and easier to control, especially with complex machine dynamics. This study explores four design options for providing an operator with haptic feedback on the input device, 1) a basic spring stiffness to convey manipulator position, 2) the basic spring with an additional deadband force around zero, 3) an approach from literature to feedback the derivative of the machine's measured interaction forces, and 4) a novel method to feedback the interaction forces by manipulating the stiffness of the input device. Subjects (n=12) used a haptic manipulator to control a virtual slow dynamic system with rate control, performing three generic subtasks: goal-directed movements, minimizing impact force during contact transitions, and controlling the level of slave force when in contact with a visco-elastic environment. The results show improvements for offering an advanced static spring to the basic spring during goal-directed movements, but equal results for reflecting environment feedback compared to the advanced spring. For reflecting environment forces as additional stiffness, improvements were found when conducting force level tasks. We conclude that the novel stiffness feedback provides operators most advantages in task performance and control effort over the entire range of task types.

3.1. INTRODUCTION

Teleoperation of large heavy machines such as excavators or cranes, is often performed using rate control; where the position of the operators input device (e.g. joystick) commands the desired velocity remote machine (hereafter called slave) [113, 115, 116]. Rate control allows the slave's movement to be commanded over a large (theoretically infinite) workspace, as opposed to the position control encountered in bilateral telemanipulation [72, 42]. Typically, in rate controlled large heavy machines, visual feedback of task-related information is available on screens. The control device is typically passive, with a static centring stiffness [113, 80]. Therefore the operator feels no feedback on the control device concerning the machine dynamics, or its interaction forces with the environment (e.g. soil or attached loads). Such important information can then only be perceived by ambient cues (sounds and vibrations).

This paper focuses on feedback of the interaction forces during rate control, with the aim to contribute to improvements in task execution for rate controlled large heavy machines [96]. Previous work on force feedback in position controlled slow dynamic systems has shown understanding and predicting the dynamic behaviour. This has led to improvements in task execution and control effort for slow dynamic systems during free space tasks [133]. The goal of this paper is to experimentally evaluate different haptic feedback designs to facilitate operators during rate control of heavy slaves. Literature describes two methods to translate interaction forces between slave and environment to a master device held by the operator: force-based feedback and stiffness-based feedback [80, 109, 102, 110]. Both types of feedback methods are illustrated in Fig. 3.2.

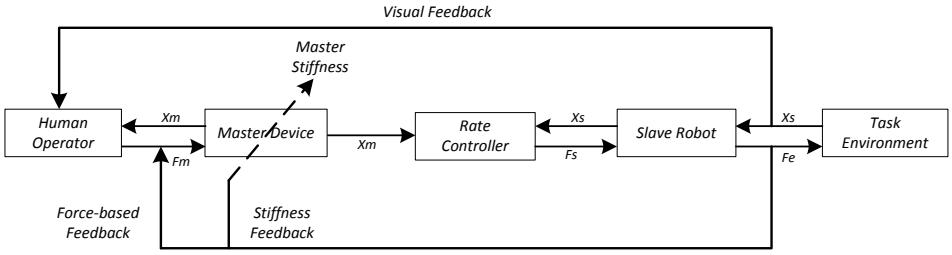

Figure 3.2: Schematic representation of a human controlling a rate controlled remote machine with two methods of haptic feedback visualized, adapted from Salcudean [9]. Note that the rate controller block is modified to be able to separately visualize the environment interaction force Fe directly. Fe is either directly fed back as a force (or its derivative) on the master device or as an adapting factor of the master stiffness.

Two main information channels (position error and interaction forces) can be reflected with haptics when the four-channel structure in position control is used (based on the work of [138] and [52]). The same approach is used for rate control by Salcudean et al. [110, 139] by reflecting the velocity error and the measured environment forces to the human operator. The velocity error informs the operator about the dynamics of the controlled machine, by reflecting the difference on the acquired velocity to the commanded velocity. This informs the state of the vehicle of (de)accelerations. Reflecting the dynamic information seems most informative when operating slow dynamic vehicles in free-space tasks [133]. Reflecting the measured environment forces informs the operator of the interaction of the vehicle with the environment.

The theoretical design of haptic feedback during rate control has been extensively investigated by Salcudean et al. [80, 102, 110, 139, 109]. One of the things they suggested is that the derivative of the measured force should be reflected instead of the force itself. Reflecting forces in a rate controlled task shows promising results for velocity and force tracking in theory [110, 139]. This concept solves the potential problems of direct force feedback that lead to possible instabilities because the feedback drives the input device out of its neutral point of zero input. The practical applicability of reflecting these derivative forces has been questioned, because it results in no longer a natural feel of the occurring contact forces [80, 102].

Another way of overcoming this problem was suggested by [102]. He proposed stiffness feedback to indicate a clear neutral point and maintain stability also for zero inputs. Similar effects for stiffness feedback compared to direct force feedback has been researched for car driving applications by [4], to maintain stability for a haptic guidance systems using shared control [90]. Stiffness feedback remains the general centring stiffness around the central neutral point clearly informed to the human operator, therefore stability is easily maintained as well. [88] investigated the stability when reflecting forces in rate control and compared this for various methods. They found for moderate time delay problems that reflecting an estimated environment impedance as a form of stiffness feedback to improve transparency while remaining robust stability. However to maintain stability under time delay, [101] used velocity error to reflect forces to the operator. They found also when colliding with objects that robust stability was guaranteed

with variable time-delays by means of an energy-bounding algorithm. Combining velocity error feedback with environment forces incorporated as stiffness feedback seems promising to overcome instability by maintaining the general centring stiffness.

Besides the importance of the method of reflecting haptic information to the operator, another important question is what information type (e.g. velocity error and/or measured environment forces) is relevant to the operator? To study this question, a useful classification for tele-operated task execution is the division in three main task types: free-space, contact transition and force level tasks, based on [133]. Rate con-trolled operations are most often conducted in free-space tasks and typically controls large heavy machines with a slow dynamic system response. Therefore, controlling these machines might benefit most from a reflected velocity, informing its dynamic response. However, when making contact in a contact transition task, informing the environment interaction forces might indicate the impact more clearly. And controlling a specific force level onto the environment during a force level task could also benefit from information about the environment forces.

The objective of this study is to understand the extent to which different feedback paradigms affect task execution in rate control. It seems most beneficial for stability and satisfactory to remain a clear neutral point of zero input [102]. Therefore, it is hypothesized that offering stiffness feedback is most useful of either the velocity error or environment forces. It is also hypothesized that when offering only haptic feedback of the state of the input device (i.e. static spring), a clear neutral point of zero input has to be noticeable when using rate control.

In this study, a human factors experiment is conducted to evaluate the different feedback designs. In section 3.2 the four designs are described: two static springs, force-based feedback and stiffness feedback. The methods are described in section 3.3 and the results for each task type are described separately in section 3.4. The discussion and conclusion can be found in section 3.5 and 3.6 respectively.

3.2. HAPTIC FEEDBACK DESIGN

Usually, during rate control the only forces an operator feels on the control interface are due to the passive dynamics (mainly a static spring). No task-related feedback of the controlled machine is given, such as its achieved velocity or encountered environment force. This section details four different approaches to design haptic feedback on the control interface; two static spring designs, force-based and stiffness feedback. This section also includes the tuning of each approach for subsequent human-in-the-loop experiments as described in section 3.3.

3.2.1. TWO STATIC SPRING DESIGNS

In rate control the input device position corresponds to a commanded slave velocity. Hence, it is helpful to have a centring stiffness to help indicate the difference between a zero-velocity command, accelerating or decelerating. A basic static spring can increase the knowledge of the commanded velocity, due to the absolute position information from the spring force [89]. Implementation of such spring force is common in rate control because of its simplicity and not requiring any additional sensory feedback.

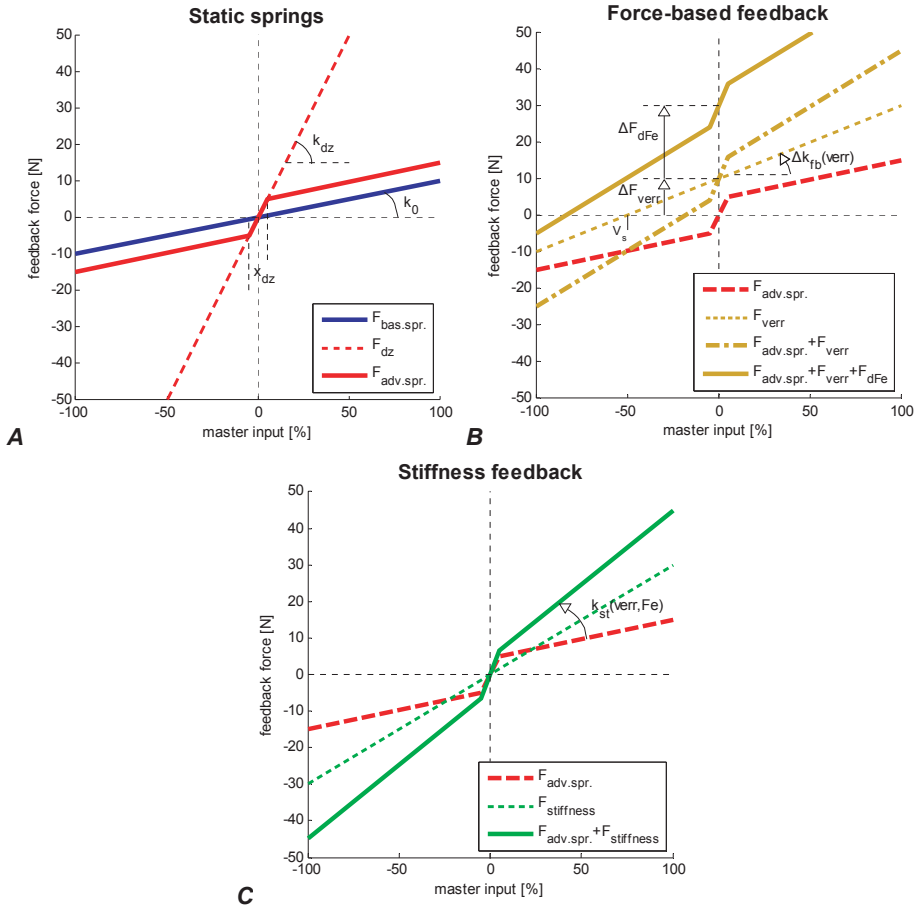

Figure 3.3: The static relation between master force Fm and master input x_m for the four haptic feedback design methods (the thick solid lines) and relevant design components (dotted and dashed lines). A) Two static spring designs with a basic spring ($F_{bas.spr.}$) and advanced spring with clear zero indication ($F_{adv.spr.}$). B) Force feedback designs based on literature, including the baseline spring ($F_{adv.spr}$), with added velocity error ($F_{adv.spr.} + F_{verr}$) and derivative of environment ($F_{adv.spr.} + F_{verr} + F_{dFe}$). C) Stiffness feedback design including the baseline spring ($F_{adv.spr.}$), with added stiffness ($F_{adv.spr.} + F_{stiffness}$).

In Fig. 3.3 A the blue thick solid line indicates the most basic spring, as typically implemented in academic research (e.g. [80, 102, 110, 88]). The basic spring merely consists of a stiffness gain k_{spr} on the input position xm, as given in Eq. (3.1). In the block diagram as shown in Fig. 3.4, this static spring is depicted with H_{spr} which effectively creates the impedance of the master dynamics H_{master}. The stiffness gain k_{spr} is tuned to 40 N/m to result in approximately 8 N of force at maximal input, therefore enabling to augment other forces (as clearly seen in Fig. 3.11 at item II). The damping gain b_{spr} is set to 6 Ns/m, to achieve a closed loop damping ratio of 0.3.

$$F_{bas,spr} = k_{spr} \cdot x_m + b_{spr} \cdot \dot{x}_m \tag{3.1}$$

Industry practice typically incorporates an out-of-zero switch in the joystick mechanism, to ensure zero input at a certain deadband (e.g. Gessmann GmbH industrial joystick mechanism [111]). This also gives a much better indication of the zero position at an overall low spring stiffness. This nonlinear spring characteristic was implemented by overlaying a much higher stiffness within a small deadband, as given in Eq. (3.2). The deadband position x_{db} of 4 mm, 1% of maximal stroke, contained a stiffness k_{db} tuned to 1500 N/m to result in 3 N of constant force outside the deadband.

$$\begin{aligned} F_{adv,spr} &= k_{spr} \cdot max(|x_m| - x_{db}, 0) \cdot sign(x_m) + k_{db} \cdot min(|x_m|, x_{db}) + b_{spr} \cdot \dot{x}_m \\ b_{adv,spr} &= \begin{cases} b_{db}, & |x_m| < x_{db} \\ b_{spr}, & |x_m| \geq x_{db} \end{cases} \end{aligned} \tag{3.2}$$

This advanced spring gives a clear zero velocity indication inside the deadband for a complete stop of the slave velocity. In Fig. 3.3 A the red thick line indicates the advanced spring with deadband force indication. The thin red dashed line indicates the increases stiffness k_{db} which is limited to the deadband position x_{db}. The damping $b_{adv.spr.}$ is kept equal to the basic spring for outside of the deadband and within set to 37 Ns/m to maintain an equal damping ratio of 0.3.

3.2.2. FORCE-BASED FEEDBACK DESIGN

Information of the state of the slave can also be reflected to the operator. These states include the velocity error (between commanded and realized slave velocity), and the measured interaction force between slave and environment (e.g., mud, rock and tools).

The velocity error v_{err} is defined as the difference in the commanded velocity (based on the master position xm) and the realized system velocity v_s Eq.(3.3). Because the slave operates at a larger workspace then the master device is capable of, a scaling factor G_{scale} of 0.2 is implemented. The block diagram in Fig. 3.4 shows that the velocity error not only can be reflected to the operator, but also is used to control the slave $H_{control}$. Therefore the scaling factor G_{scale} also determines the commanded desired slave velocity based on the master position x_m in Fig. 3.4.

$$v_{err} = v_s - \frac{x_m}{G_{scale}} \tag{3.3}$$

The feedback force of the velocity error is comparable to the controlled slave force F_C as shown in Fig. 3.4, therefore includes the controller gains K_P and K_D, based on [110].

This force is reduced with a force feedback gain $G_{fb,verr}$ of 0.1 to keep the forces tangible to the operator, as shown in Eq.(3.4). This velocity error feedback force is shown in Fig. 3.3 B as the thin brown dashed line, which essentially creates a spring stiffness around the acquired velocity v_s of the slave.

$$F_{err} = G_{fb,v_{err}} \cdot \left(K_P \cdot v_{err} + K_D \cdot \frac{\partial v_{err}}{\partial t} \right) \tag{3.4}$$

The measured contact environment force F_{env} is fed back to the operator as a derivative in time, for a transparent four channel system [110]. This is implemented with gain $G_{fb,\dot{F}e}$ of 0.05 on top of the scaling gain G_{scale}, as shown in Eq.(3.5), for which the environment force F_{env} is filtered with a 50 Hz lowpass second order Butterworth filter.

$$F_{dFe} = G_{fb,\dot{F}e} \cdot \left(F_{env} \cdot \frac{\partial v_{err}}{\partial t} \right) \tag{3.5}$$

The total force feedback based on literature using the complete four channel approach is a combination of the static spring $F_{adv,spr.}$ of Eq.(3.2), the velocity error $F_{v_{err}}$. and the environment force $F_{\dot{F}e}$ as shown in Eq.(3.6). The summation of feedback for these two different information channels is also depicted in Fig. 3.4 with the two parallel blocks for force-based feedback.

$$F_{force,lit} = F_{adv.spr.} + F_{v_{err}} + F_{\dot{F}e} \tag{3.6}$$

The thick brown dash-dotted line in Fig. 3.3 B shows that when adding the velocity error force $F_{v_{err}}$ to the static spring force $F_{adv.spr.}$, the neutral point shifts from the acquired velocity v_s of the slave towards zero. The addition of the environment force derivative may cause substantial oscillations in the neutral point after impact due to the nature of this signal. This results in loss of a clear zero point of commanded slave velocity.

3.2.3. STIFFNESS FEEDBACK DESIGN

The fourth haptic feedback design is based on the work of [102], whom also applied stiffness feedback instead of force-based feedback to maintain stability in hard environments. However in this study the additional stiffness gain is based on both the velocity error $k_{st,v_{err}}$ and the environment force $k_{st,Fe}$, as shown in Eq.(3.7).

$$F_{stiffness} = \left(k_{st,v_{err}}\{x_m, v_s\} + k_{st,Fe}\{F_{env}\} \right) \cdot x_m \tag{3.7}$$

The stiffness gain $k_{st,v_{err}}$ is a function of the absolute velocity error as stated in Eq.(3.8), with a gain $G_{st,v_{err}}$ of 0.2.

$$k_{st,v_{err}} = G_{st,v_{err}} \cdot \left| v_s - \frac{x_m}{G_{scale}} \right| \tag{3.8}$$

The stiffness gain $k_{st,Fe}$ is a function of the absolute measured scaled environment force with a gain $G_{st,Fe}$ of 0.7, as stated in Eq.(3.9).

$$k_{st,Fe} = G_{st,Fe} \cdot |F_{env} \cdot G_{scale}| \tag{3.9}$$

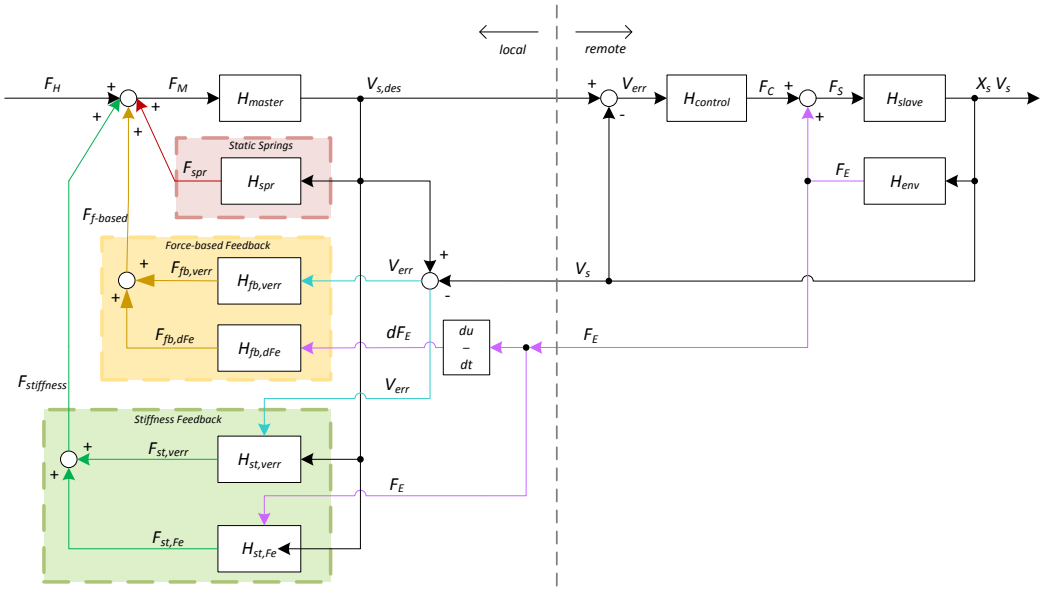

Figure 3.4: Block diagram demonstrating the three haptic feedback design types, static springs (red), force-based feedback (yellow) and stiffness feedback (green). The block diagram consists of a local master device from which a human force is converted into an input position, and scaled to a desired slave velocity. From this a closed loop controller actuates the remote slave device with a controller force, which again interacts with a remote environment. Both the achieved slave velocity and interaction forces are fed back to the lower two feedback designs types.

The stiffness force $F_{stiffness}$ of Eq.(3.7) is based on the input position x_m and is a linear stiffness around zero as shown with the thin green dashed line in Fig. 3.3 C. The total stiffness feedback design is a combination (shown in Eq.(3.10)) of both the static spring of Eq.(3.2) and the additional stiffness force of Eq.(3.7), shown in Fig. 3.3 C with the thick solid green line.

$$F_{stiffn,des} = F_{adv.spr.} + F_{stiffness} \tag{3.10}$$

The stiffness force of Eq.(3.7) consists of two parts (velocity error and environment force), depicted in the block diagram in Fig. 3.4 with the two parallel blocks for stiffness feedback. However the environment force $F_{st,Fe}$ only gives feedback when in contact with an environment. And when in contact the slave velocity would be near zero, thus the feedback would not inform clearly on the system dynamics. Therefore the feedback is designed to switch off the velocity error feedback when making contact, essentially switching between environment forces and velocity error feedback.

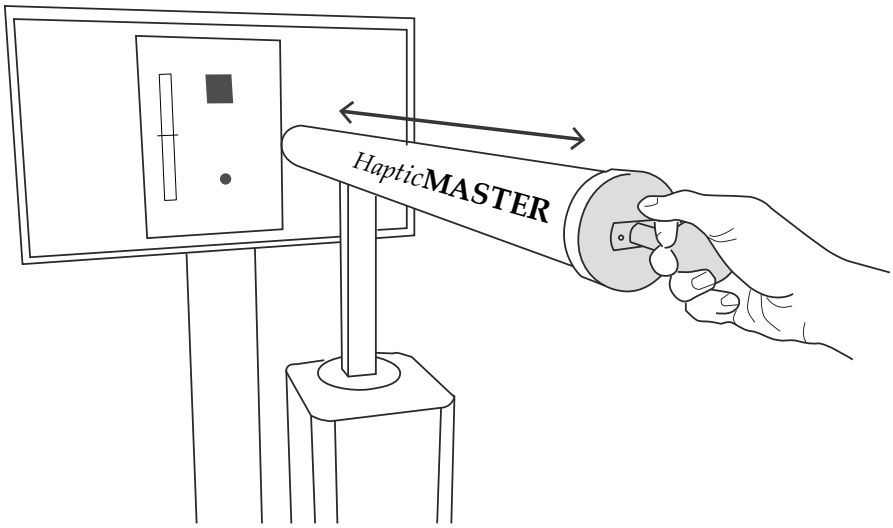

Figure 3.5: Experimental Setup. The subject holds the master input device *Haptic*MASTER of Moog Inc. while executing a single degree of freedom task in rate control.

3.3. EXPERIMENTAL METHODS

3.3.1. SUBJECTS

Twelve subjects, with an average age of 27.8 years and 5.5 year standard deviation, volunteered for the experiment. None of the subjects had previous experience with teleoperation and were naive about the experiment. All subjects gave their written informed consent prior to the experiment. The setup and experiments were approved by the local ethics committee of the Delft University of Technology.

3.3.2. APPARATUS

The experiments were performed on the *Haptic*MASTER (FCS Moog Inc.) as shown in Fig. 3.5, on which the four feedback designs were implemented. The *Haptic*MASTER is 3 DoF, but was constrained to only allow movement along the radial-axis of the device, which was aligned with the sagittal plane of the subject (fig. 3.5). The admittance-controlled *Haptic*MASTER has a position resolution of $12e^{-3}$ mm, a stiffness of 10 kN/m, force sensitivity of 10 mN and frequency response of 25 Hz [126]. The virtual inertia and damping of the master device were respectively set at J_m of 2.5 kg and B_m of 5 Ns/m. The manipulator was controlled with a VxWorks RT operating system running at 2048 Hz.

The slave system H_s, designed in Matlab Simulink, was simulated on an additional real-time controller by Bachmann GmbH. This virtual slave was implemented according to Eq. 3.11. We aimed at a bandwidth of H_s of approximately 0.6 Hz, as large heavy machines such as excavators or cranes can be typically described having a 0.2-1 Hz cutoff frequency (e.g., [80, 113, 115, 116]). We chose inertia J_s of 200 kg, and then - limited by closed-loop stability - settled with a damping B_s of 800 Ns/m, proportional gain K_P of

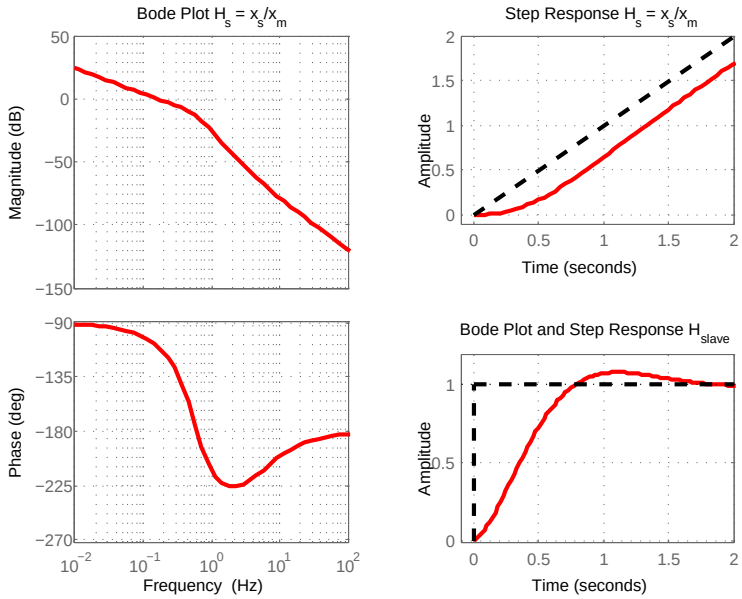

Figure 3.6: Bode plot and step response of the slave system (open-loop). The Bodeplot on the left is showing the cut-off frequency of approx. 0.57 Hz of a first order system with second order dynamics. This is also shown in the right for the step response shown for slave position and the derivative to a step input on the master position.

2000, derivative gain K_D of 70, and a scaling factor G_{scale} of 0.2. This gives the slave system H_s a bandwidth of approximately 0.57 Hz, as shown in Fig. 3.6 with plots of frequency and time responses. Notice that, in simulation, the the absolute values of the parameters of H_s is irrelevant, and it is about their relative proportions.

The real-time controller runs at 1000 Hz and logs its (state) data at the same frequency. The visualization on the display was updated at a rate of 25 Hz.

$$H_s = \frac{x_s}{x_m} = \frac{1}{G_{scale}} \cdot \frac{K_D \cdot s + K_P}{J_s \cdot s^3 + (K_D + B_s) \cdot s^2 + K_P \cdot s} \tag{3.11}$$

3.3.3. EXPERIMENT DESIGN

While controlling the virtual slave subjects were offered with each of the four feedback designs from section 3.2, static springs, force-based and stiffness feedback. These designs were tested in three general task types, free-space, contact transition and force level. In Fig. 3.7 the visualization of each task type is given and in table 3.1 above are the corresponding condition explanations. The content of each experimental condition depends on the conducted task (e.g. in free-space there is no measured environment force).

The *Free-Space task* (FS) consisted of four experimental conditions: 1) baseline condition of a simple spring, 2) industry practice of an advanced spring with clear zero ve-

Table 3.1: Description of Experimental Conditions per Sub-Task

	Free Space Task	**Contact Transition Task**	**Force Level Task**
1. Bas. Spr.	Basic static spring	-	-
2. F-based	Advanced static spring with deadband indication	Advanced static spring with deadband indication	Advanced static spring with deadband indication
3. F-based	Advanced static spring with velocity error as force-based feedback	Adv. static spring with vel. error and derivative of environment force as force-based feedback	Adv. static spring with vel. error and derivative of environment force as force-based feedback
4. Stiffness	Advanced static spring with velocity error as stiffness feedback	Adv. static spring with vel. feedback in free-space and environment force when in contact as stiffness feedback	Adv. static spring with environment force as stiffness feedback

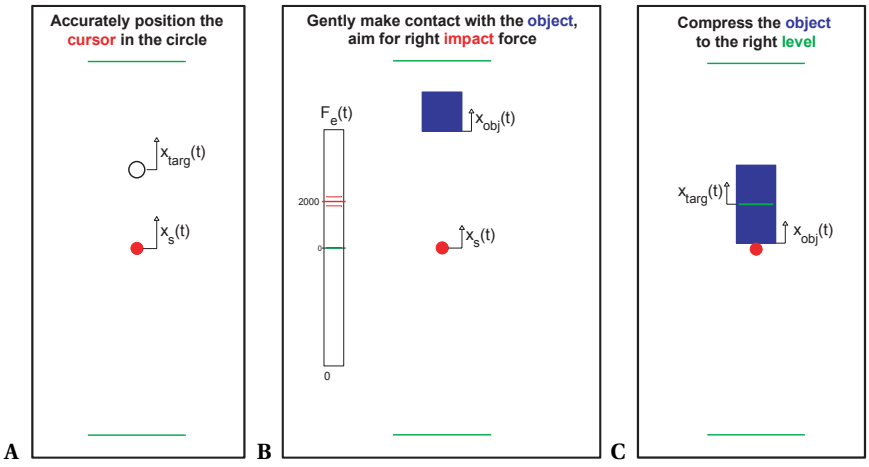

Figure 3.7: Visualizations of the three subtasks. A) Free-Space task, the red dot indicates the slave position and the black circle the target position. B) Contact Transition task, the blue block represents the object and the three small red lines in the rectangle on the left the required target impact force. C) Force Level task, the blue block represents the object that needs to be compressed up to the thin green line.

locity indication, 3) velocity error as force-based feedback and 4) as stiffness feedback. The target to reach varied in free-space step size of 20% and 30% of screen size in both directions for unpredictability of task execution to the subjects. Only the small step size was used for analysing task execution to emphasize on the final positioning and reduce noise during the travelled distance, where the target size is 1.25% of the smaller step size.

The *Contact Transition task* (CT) consisted of three experimental conditions: 2) industry practice of an advanced spring, 3) velocity error as force-based feedback plus the derivative of the measured environment force, and 4) both velocity error and environment force as stiffness feedback. The margin to the objects to make contact with varied in free space distance of 19% and 28% of screen size in both directions. Only the largest margin was used for analysing task execution to emphasize on the achieved impact force. The object consisted of a stiff spring-damper properties of respectively 100 kN/m and 2 kNs/m, combined with the slave damping and inertia resulting in a second order system with a 3.6 Hz natural frequency and damping ratio of 0.32.

The *Force Level task* (FL) also consisted of three experimental conditions: 2) industry practice of an advanced spring with clear zero velocity indication, 3) velocity error as force-based feedback plus the derivative of the measured environment force and 4) environment force as a stiffness. The object had to be compressed to half its size as indicated with the green thin line (which consisted of 10% of the screen size). The stiffness of the blocks that had to be compressed varied accordingly to the target interaction force levels of 2750 N and 1833 N for equal compression distance. Only the largest force level was used for analysing task execution. For the feedback to the operator the interaction force was scaled using the designs as described in section 3.2, for an equivalent direct force feedback as example this scaling would be approximately 1% of this force to the operator.

During the experiment, each experimental condition was tested using eight repetitions of either of the three task types to be completed. These eight repetition consisted of two variations for each task types, applied in two directions. The order of the three or four experimental conditions and the order of the three subtasks were both counterbalanced using a Balanced Latin Square Design (BLSD) [48]. Variations with each task type and direction were also counterbalanced using a BLSD.

3.3.4. PROCEDURE

Each subject was asked to stand in front of the input device, *Haptic*MASTER, and hold the black knob with one hand as depicted in Fig. 3.5. The display behind the input device showed either of the three subtasks as shown in Fig. 3.7, indicating the free-space, contact transition or force level task. The subjects were asked to conduct the task as fast as possible and each prior task execution time was shown to the subject. For the free-space task subjects had to hold the operated red dot within the black target circle for one second until the next target appeared. The contact-transition task was instructed and trained to aim for the target impact force as indicated and was constant throughout the experiment. The force level task was instructed to compress the blue rectangular block with the red controlled dot up to the green indicated target line. When subjects completed each repetition of either of the subtasks a short beep was given auditory to indicate the completion of the repetition.

Prior to each experimental condition, the subjects were presented with a training sequence also consisting of eight repetitions of the subtask to be conducted. Also, prior to each subtask the subjects were presented with a familiarization task, which consisted of the baseline condition for that particular subtask (basic or advanced spring). The familiarization trial also consisted of the eight repetitions, but was repeated until consistent task execution of under 10 seconds was achieved.

3.3.5. MEASURED VARIABLES AND METRICS

Task performance is measured with *settling time* and *overshoot* for both the free-space (FS) and force level (FL) task. Settling time is the time elapsed from the start of the step input until the operator stayed within the target. Overshoot of the target is defined as the percentage of distance the target was exceeded outside of the boundaries. For the contact transition (CT) task the *time-to-contact* and *impact error* were used as performance metrics. The time it took before making contact is the time the operator had actively control over the task. After making contact the time of the task was defined by a fixed impact measurement time of 200 ms. The impact force is relevant for what the operator did during contact, which had a target interaction impact force of 1000 N and the error between what was maximally realized, is defined as impact error.

For all three subtasks *steering reversals* and *master force* are used as objective metrics for control effort. Steering reversals is defined as the amount of zero crossings of the operator force input, using a second order Butterworth filter with a 5 Hz cutoff frequency, a deadband threshold of 25 mN and a minimum of 250 mN between each reversal was required to filter out unintentional noise on the signal, similar to [14] and [78]. Physical effort was calculated as the mean of the amount of force applied to the input device.

For subjective measures the Van der Laan questionnaire was used to capture the *usefulness* and *satisfying* score of the feedback design for all three subtasks [30]. The usefulness consisted of 5 components: useful, good, effective, assisting and raising alertness. The satisfying consisted of four components: pleasant, nice, likeable and desirable. Subjects rated the usefulness and satisfying components on a five point scale from -2 to +2. Usefulness and satisfying scores were calculated by averaging respective components.

3.3.6. DATA ANALYSIS

For each subject and form of support system, the metrics are computed per trial and averaged subsequently over the four repetitions. Per metric, the means are compared between the forms of support using a repeated measures analysis of variance (RM-ANOVA). A Greenhouse-Geisser correction was applied when sphericity was violated. For significant main effects ($p<0.05$), post-hoc comparisons with Bonferroni correction for multiple comparisons was applied.

3.4. RESULTS

The results of all metrics as explained in section 3.3.5 are given for the task type free-space, contact transition and force level in tables 3.2, 3.3, 3.4 respectively. For clarity, the results presented in Fig. 3.8, 3.9, 3.10 only include the results of the two most relevant performance metrics, an objective effort metric and subjective metrics. The data tables

include the detailed result and statistical results for each metric in each task type.

3.4.1. FREE-SPACE TASK

In the free-space task subjects had to perform the task as fast as possible. This resulted in a tradeoff for performance of speed and accuracy of reaching the target. In Fig. 3.8.A are therefore the results shown of the overshoot and settling time in a two dimensional graph, where overshoot is a metric of accuracy and settling time of the speed tradeoff. Results show a significant difference in settling time (p=.005, F=8.2) and post-hoc comparisons show a reduced settling time when offering an advanced static spring with clear zero velocity indication compared to a basic spring (31% mean reduction, p=.028). No difference in overshoot was found as also given in table 3.2.

Control effort obviously increased for physical effort by the measured master force when offering more feed-back (p<.001, F=67). Interestingly mental effort increased when offering feedback of the state of the slave, as shown in 3.8.B with a difference in steering reversals (p<.001, F=9.4). This can be seen by the increased steering reversals when offering force-based feedback compared to the baseline static spring (36% mean increase, p=.014) or advanced spring (45% mean increase, p=.003). And this can also be seen with an increase for stiffness feedback to the basic spring (35% mean increase, p=.017).

Subjective measures show a clear increase in satisfying (p=.005) and usefulness (p=.039) of the advanced spring compared to the basic spring. Usefulness also increased when offering stiffness feedback compared to the basic spring (p=.003).

Table 3.2: Results of Free Space Task

	T settling [s]	Overshoot [%]	Reversals [-]	F master [N]	Usefulness [-]	Satisfying [-]
1. Basic Spring [1]	7.86 (6.46, 9.25)	4.06 (1.76, 6.35)	15.75 (13.35, 18.15)	1.81 (1.62, 2.00)	-0.38 (-0.80, 0.04)	-0.63 (-1.25, 0.00)
2. Adv. Spring [1]	5.45 (5.05, 5.86)	2.87 (1.25, 4.48)	14.81 (13.61, 16.01)	4.26 (4.05, 4.46)	0.55 (0.10, 1.00)	1.06 (0.70, 1.43)
3. F-based Feedback [1]	6.13 (5.58, 6.67)	3.64 (2.40, 4.87)	21.48 (18.77, 24.19)	6.53 (5.96, 7.11)	0.35 (-0.04, 0.74)	0.13 (-0.29, 0.54)
4. Stiffness Feedback [1]	6.15 (5.75, 6.56)	1.88 (1.23, 2.53)	19.92 (17.50, 22.34)	6.17 (5.14, 7.20)	0.62 (0.35, 0.89)	0.29 (-0.15, 0.74)
Statistics [2]	p=.005 (F=8.2)	p=.191 (F=1.7)	p<.001 (F=9.4)	p<.001 (F=67)	p=.001 (F=7.5)	p<.001 (F=8.8)
Post-hoc [3]	1 to 2, p=.028	-	1 to 3, p=.014 2 to 3, p=.003 2 to 4, p=.017	all, p<.01 except 2 to 4, p=.024 3 to 4, p>.1	1 to 2, p=.039 1 to 4, p=.003	1 to 2, p=.005 2 to 3, p=.033

Main mean results of all evaluation metrics for performance, control effort and subjective measures, accompanied with their statistical results for free-space tasks.
[1] Group mean (95% Confidence Interval).
[2] Statistics are shown with a p and F value for a Repeated Measures ANOVA with Greenhouse-Geisser corrections when sphericity was violated.
[3] Post-hoc comparisons were applied using Bonferroni compensation.

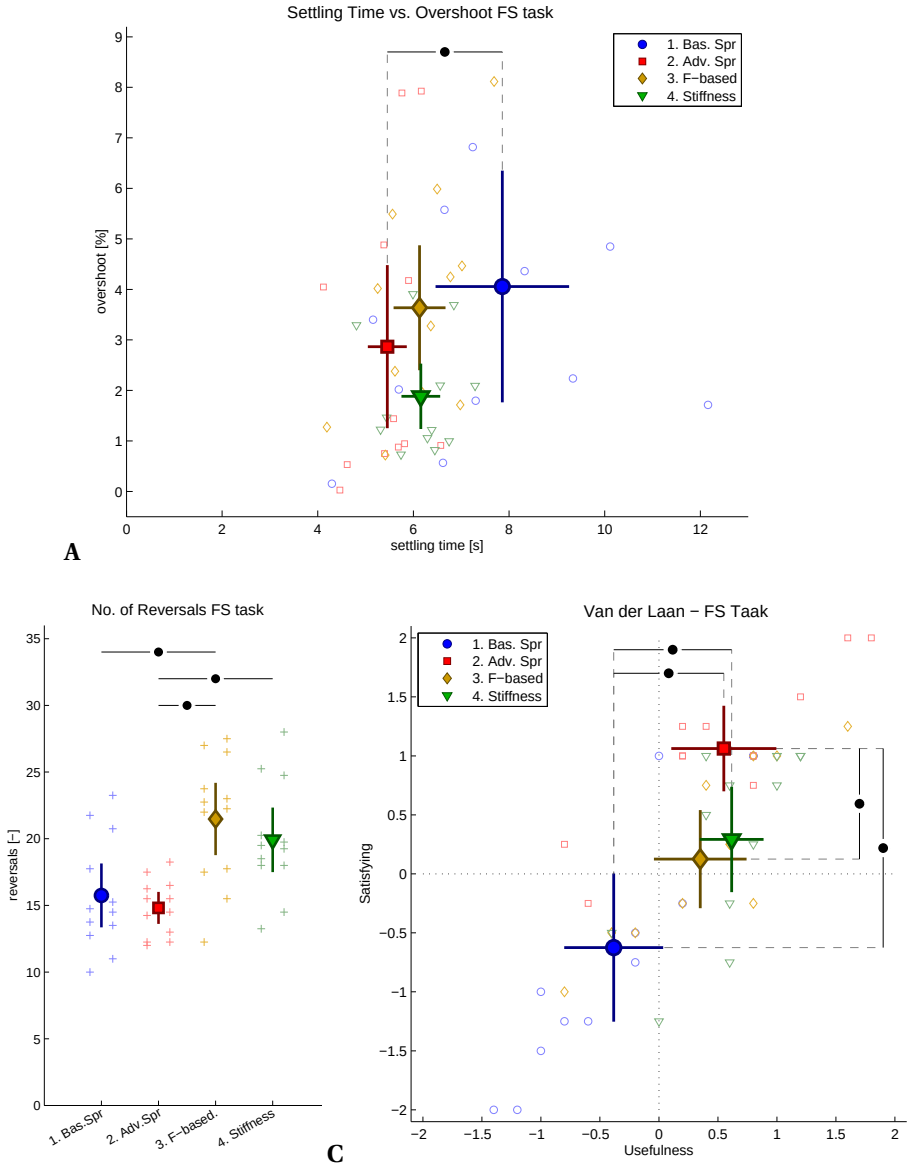

Figure 3.8: Results of **free-space task** for all four conditions applied. A) settling time (x-axis) versus overshoot (y-axis). B) number of steering reversals. C) subjective Van der Laan measure. All results are shown of the group mean (thick filled marker) and their 95% confidence interval (thick error bars), combined with individual subject means (thin markers). The horizontal bars indicate a significant difference over the factor environment or support, where "•" denote the significance level of $p<0.05$.

3.4.2. CONTACT TRANSITION TASK

In the contact transition task subjects had to make contact with the object with a given impact force as fast as possible. This gives a tradeoff in time to complete and accuracy

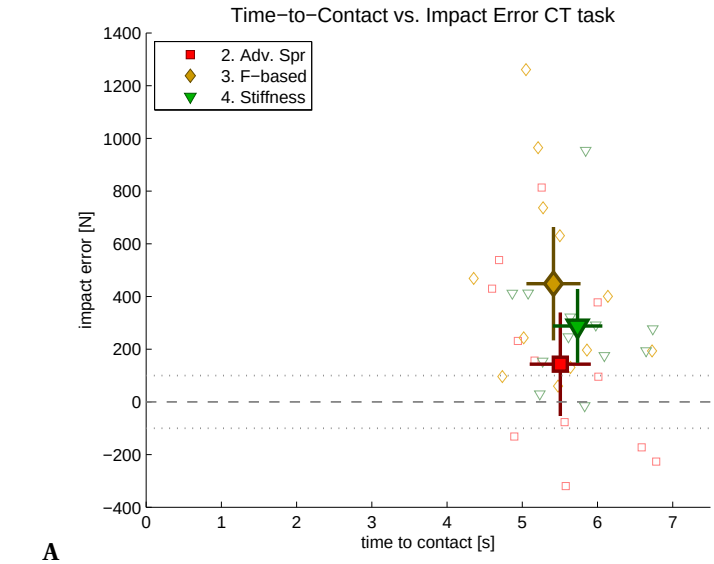

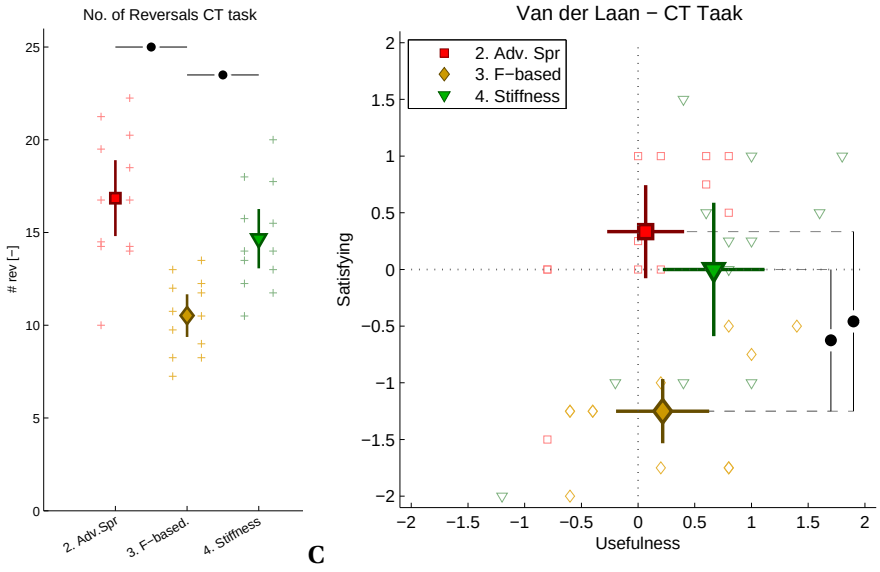

Figure 3.9: Results of **contact transition task** for all three conditions applied. A) time to contact (x-axis) versus impact error (y-axis), with the dashed lines representing the given impact force range indication. B) number of steering reversals. C) subjective Van der Laan measure. General figure representations of metrics are described in the caption of Fig. 3.8

of achieving the impact force. In 3.9.A this is shown for the time to contact and impact error results, in a two dimensional graph but with no statistical significant difference.

Control effort however reduces when offering force-based feedback compared to both the advanced static spring and stiffness feedback (mean reduction of 38% and 28% respectively, both p<.001) as can be seen in 3.9.B. Physical effort also increases when offering force-based or stiffness feedback (p<.001).

Subjective measures however show a clear reduction of satisfying for when offering force-based feedback to the static spring and stiffness feedback (p<.001 and p=.003 respectively) as can be seen in 3.9.C.

3.4.3. FORCE LEVEL TASK

In the force level task subjects had to compress the object to a specific point and therefore corresponding force level. This resulted in a tradeoff between speed and accuracy which can be seen in settling time and overshoot respectively as can be seen in 3.10.A. Results show a large reduction of overshoot when offering stiffness feedback compared to an advanced static spring (77%, p=.038). However this comes with an increased settling time for stiffness feedback compared to the static spring (10%, p=.017).

Control effort reduces when offering information regarding the state of the slave, both force-based and stiffness feedback have reduced reversals compared to the advanced static spring (both 37%, p<.01).

Subjective measures show a clear difference in both satisfying and usefulness of the static spring compared to offering force-based and stiffness feedback. Both force-based and stiffness feedback have a reduced satisfying score (p=.029 and p=.007 respectively).

Table 3.3: Results of Contact Transition Task

	T contact [s]	Impact err. [N]	Reversals [-]	F master [N]	Usefulness [-]	Satisfying [-]
2. Adv. Spring [1]	5.50 (5.10, 5.91)	142.8 (-53.7,339.3)	16.85 (14.8, 18.9)	6.20 (5.93, 6.47)	0.07 (-0.27, 0.41)	0.33 (-0.08, 0.74)
3. F-based Feedback [1]	5.41 (5.06, 5.77)	448.4 (233.2,663.6)	10.52 (9.4, 11.7)	8.88 (8.18, 9.57)	0.22 (-0.19, 0.63)	-1.25 (-1.53, -0.97)
4. Stiffness Feedback [1]	5.73 (5.41, 6.06)	288.0 (147.8,428.2)	14.67 (13.1, 16.3)	9.81 (8.63, 10.98)	0.67 (0.22, 1.11)	0.00 (-0.59, 0.59)
Statistics [2]	p=.210 (F=1.7)	p=.118 (F=2.7)	p<.001 (F=20)	p<.001 (F=29)	p=.091 (F=2.7)	p<.001 (F=16)
Post-hoc [3]	-	-	2 to 3, p<.001 3 to 4, p<.001	2 to 3, p<.001 2 to 4, p<.001	-	2 to 3, p<.001 3 to 4, p=.003

Main mean results of all evaluation metrics for performance, control effort and subjective measures, accompanied with their statistical results for free-space tasks.
[1] Group mean (95% Confidence Interval).
[2] Statistics are shown with a p and F value for a Repeated Measures ANOVA with Greenhouse-Geisser corrections when sphericity was violated.
[3] Post-hoc comparisons were applied using Bonferroni compensation.

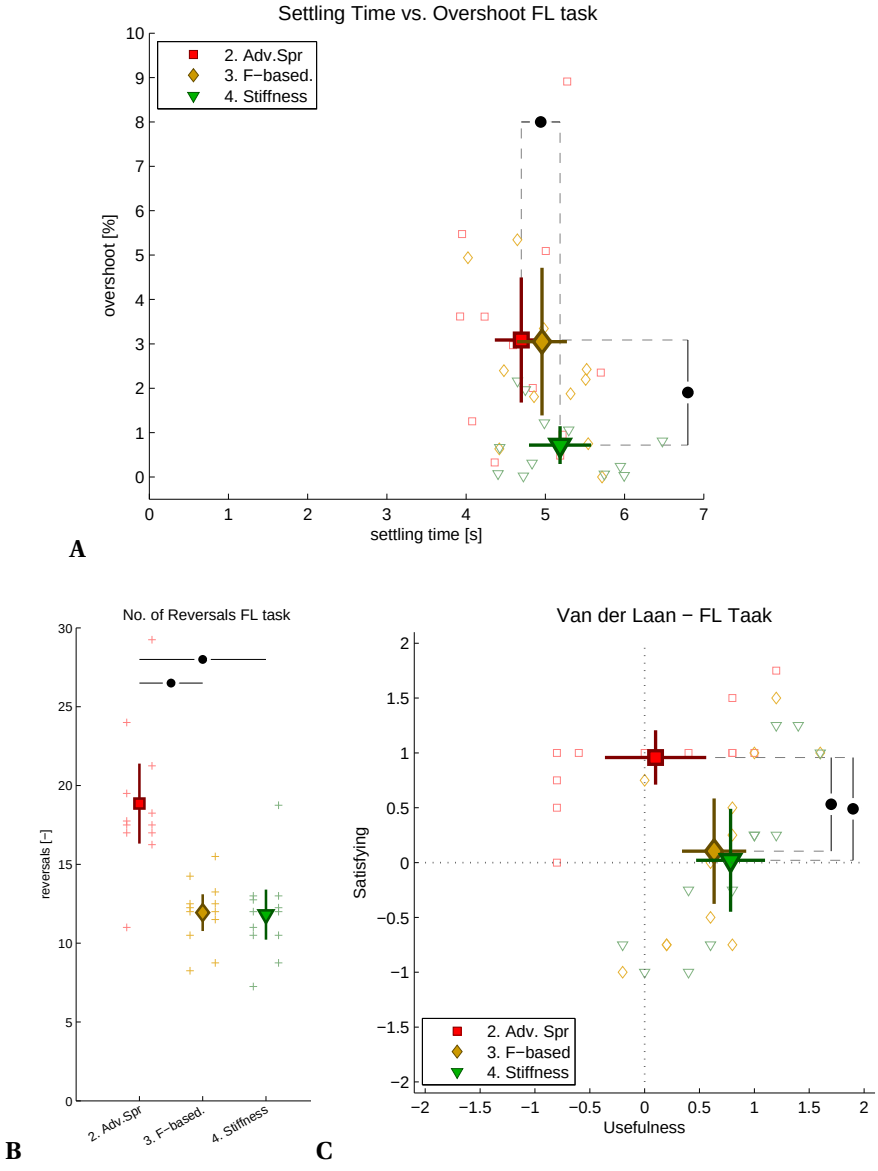

Figure 3.10: Results of **force level task** for all three conditions applied. A) settling time (x-axis) versus overshoot (y-axis). B) number of steering reversals. C) subjective Van der Laan measure. General figure representations of metrics are described in the caption of Fig. 3.8

3.5. DISCUSSION

The tested control interface designs substantially affected the execution of rate controlled tasks. The analysis focused on analysing the impact of different interface designs for three generic subtask types: free-space, contact transition and force level tasks.

The free-space task was most challenging to execute with the basic spring (lowest reported usefulness and satisfaction), which evoked large inter-subject variability. The advanced spring (with clear zero velocity indication) improved rate control compared to the basic spring, both in terms of settling time and in reported usefulness and satisfaction. Interestingly, in research static springs are typically only implemented as a basic spring (e.g. [80, 102, 110, 88]) and not as an advanced spring as usually implemented in industry (e.g. Gessmann GmbH [111]). This research shows that implementing this simple nonlinear spring characteristic into a static spring already shows clear improvements for task execution.

The two designs that feedback information regarding the state of the slave (i.e. force-based and stiffness feedback conditions) entailed a higher number of steering reversals. This increased control effort could suggests a higher mental load, due to the additional information offered to the operator. The participants rated both the force-based and stiffness feedback conditions as more useful than the basic spring, although force-based feed-back was reported to be less satisfying. In terms of objective metrics, stiffness feedback seemed to result in similar small settling times and lower overshoot as the advanced spring but did not differ significantly to the basic spring. No difference in performance was found between the force-based and the other three designs. This corresponds to results found in simulation by [139], who showed accurate tracking results during free motion and improved transparency when offering force-based feedback. [110] also found

Table 3.4: Results of Force Level Task

	T settling [s]	Overshoot [%]	Reversals [-]	F master [N]	Usefulness [-]	Satisfying [-]
2. Adv. Spring [1]	4.70 (4.36, 5.03)	3.09 (1.68, 4.50)	18.85 (16.32, 21.39)	5.37 (5.08, 5.65)	0.10 (-0.36, 0.65)	0.96 (0.71, 1.21)
3. F-based Feedback [1]	4.96 (4.64, 5.27)	3.05 (1.39, 4.71)	11.94 (10.77, 13.10)	19.42 (18.44, 20.41)	0.63 (0.34, 0.93)	0.10 (-0.38, 0.58)
4. Stiffness Feedback [1]	5.19 (4.79, 5.58)	0.72 (0.29, 1.14)	11.81 (10.23, 13.40)	17.10 (16.44, 17.75)	0.78 (0.47, 1.10)	0.02 (-0.45, 0.49)
Statistics [2]	p=.018 (F=4.9)	p=.010 (F=5.7)	p<.001 (F=16)	p<.001 (F=532)	p=.028 (F=4.2)	p=.002 (F=8.2)
Post-hoc [3]	2 to 4, p=.017	2 to 4, p=.038 3 to 4, p=.083	2 to 3, p=.009 2 to 4, p=.001	all, p<.001 except 3 to 4, p=.004	2 to 4, p=.105 -	2 to 3, p=.029 2 to 4, p=.007

Main mean results of all evaluation metrics for performance, control effort and subjective measures, accompanied with their statistical results for free-space tasks.
[1] Group mean (95% Confidence Interval).
[2] Statistics are shown with a p and F value for a Repeated Measures ANOVA with Greenhouse-Geisser corrections when sphericity was violated.
[3] Post-hoc comparisons were applied using Bonferroni compensation.

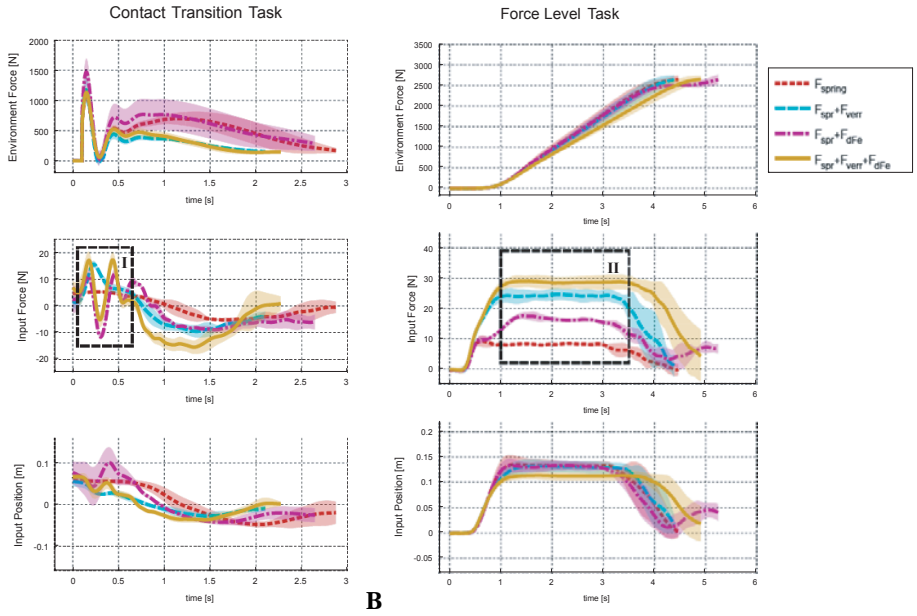

Figure 3.11: Time trace results of each component of force-based feedback, obtained from a typical subject for A) in contact task. B) force level task. Force-based feedback (solid brown lines) consist of a static spring component (red short-dotted lines), combined with velocity error feedback (cyan long-dotted lines), or combined with the derivative environment force (magenta dashed-dotted lines).

accurate tracking results with experimental data up to 8 Hz when offering force-based feedback.

Both force-based and stiffness feedback did not yield in substantial benefits compared to the advanced spring, for the additionally required sensors and controllers to enable this type of state feedback. Concluding, for pure free-space tasks an advanced spring would be the best choice.

The contact transition task was most frustrating to control when force-based feedback was offered and was rated with lower satisfaction scores, although it did not result in larger errors. This may be due to oscillatory forces at impact resulting in instabilities and user discomfort. These oscillations are a result of feeding back the derivative of force, an effect that is not mentioned in the simulation studies of [110]. The oscillating effect occurs in human-in-the-loop contact transitions during force-derivative feedback, this is shown for a typical subject in 3.11.A in box I. A similar effect is seen when offering only the derivative component as for the all components combined. In the top sub figure of Fig. 3.11.A it can be seen that equal task execution was performed when offering each individual component of force-based feedback (velocity error and derivative environment force feedback). The derivative of the environment force shows a strong oscillating effect for approximately 500 ms. The number of steering reversals was reduced for the force-based feedback, possibly indicating subjects were hesitant of the oscillating feedback when making contact.

Similar oscillating results during force-based feedback were found by [110]. They

showed force tracking performance for a single operator while interacting with a flexible and rigid environment. During initial contact with both environment types, their results show similar oscillating forces. [102] demonstrated that stiffness feedback avoided such oscillations during contact transitions due to the inherently stabilizing factor of finite restoring force of stiffness feedback.

In the force level task a significantly lower overshoot and increased settling time was found during stiffness feedback compared to the advanced static spring. The beneficial decrease in overshoot (77% reduction in means) is substantial compared to the relatively small increase of settling time (10% increase in means). 3.10.A illustrates this trade-off of a relatively large reduced overshoot, which comes with an increased settling time. Both interface designs that feedback information about the physical interaction with the environment (force-based and stiffness feedback) have the lowest workload in terms of number of reversals and rating of usefulness and satisfaction.

Similar control inputs are given for the varying individual feedback components as illustrated in the lowest sub figure of Fig. 3.11.B, resulting in similar force-level task executions as shown in the top sub figure. Box II in 3.11.B shows that the velocity error component of force-based feedback results in substantial additional static stiffness during in-contact, even though using similar control inputs when offered individual feedback components. When combined feedback is given, the velocity error dominates the feedback signal and does not add important information to the operator during this task execution. During stiffness feedback the velocity error component is switched off when environment contact forces are detected, therefore not having this issue. And because stiffness feedback is based on the absolute contact interaction force and not its derivative, the feedback remains increasing for increasing contact forces.

[110] found comparable experimental results for force tracking up to 8 Hz. During static inputs the derivative of interaction forces becomes constant when in-contact. This is proven mathematically as perfect transparency by Hashtrudi-Zaad [58, 88], based on the perfect transparency control law of [79] for position control. To increase the awareness of the environment interaction forces [58] suggests to reflect the contact force itself instead of the derivative, which might lead to an unnatural feel [88, 102]. Offering stiffness feedback as proposed by [102], avoids this problem, which our human-in-the-loop study confirms.

In our study subjects performed rate control during abstracted (sub)tasks, which allows detailed evaluation of task performance, but complicates generalization of the findings to real-world tasks. The relatively small benefits of offering feedback of the state of the slave found in this study are expected to be more substantial in more realistic tasks, such as controlling a remote subsea vehicle or operating container cranes. Based on this study, it is recommended to offer the stiffness feedback design from this study when rate-controlled task consist of all three tested subtasks. When information regarding the state of the slave is not present or costly to obtain, an advanced static spring with clear zero indication as used in this study is recommended.

3.6. CONCLUSION

A human factors experiment was conducted to determine the efficacy of four different haptic interface designs for rate control: two passive designs based on springs (standard

and advanced) and two designs reflecting physical interaction in the remote environment (based on velocity error or on measured environment forces). The four designs were tested during rate control of a slow virtual slave for three abstract subtasks: free-space (FS), contact transition (CT) and force level (FL) tasks. For the experimental conditions studied, the following is concluded:

- Compared to a basic spring, the advanced spring design with clear zero velocity indication improves task performance (i.e. overshoot) and is rated as more useful and satisfying (FS task).
- Feedback of velocity error either as force-based or additional stiffness does not improve task performance and increases control effort (FS task).
- Feedback of the derivative of the environment force requires less control effort, but is also rated less satisfying as a support (CT task).
- Reflecting the environment force as additional stiffness, improves task performance (i.e. over-shoot) and costs less control effort (i.e. steering reversals) (FL task).

These results indicate that passive spring designs are sufficient for rate-controlled tasks where free-space sub-tasks dominate. Feeding back information about the physical interaction is beneficial for in-contact tasks and force level tasks, where stiffness feedback results in benefits over feedback back the derivative of the environment interaction force.

CHAPTER 4

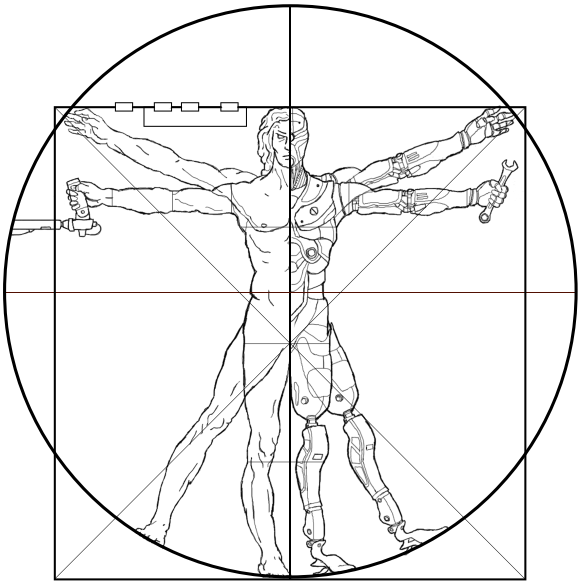

4

A Cybernetic Approach to Quantify the Effect of Haptic Feedback on Operator Control Behavior in Free-Space Telemanipulation

The extent to which haptic feedback affects operator control behaviour for trained movements is only partially understood. This chapter describes a key experiment aimed at quantifying the role of haptic feedback during free-air telemanipulation tasks. A well-established cybernetic modelling framework was adopted, within which the effect of haptic feedback scaling and slave dynamics on operator neuromuscular control mechanisms (feedback and feedforward control), and consequently task execution, was evaluated. Fig. 4.1 shows a simplified control-theoretic representation of the experimental conditions.

This chapter was submitted for review to IEEE Transactions on Cybernetics

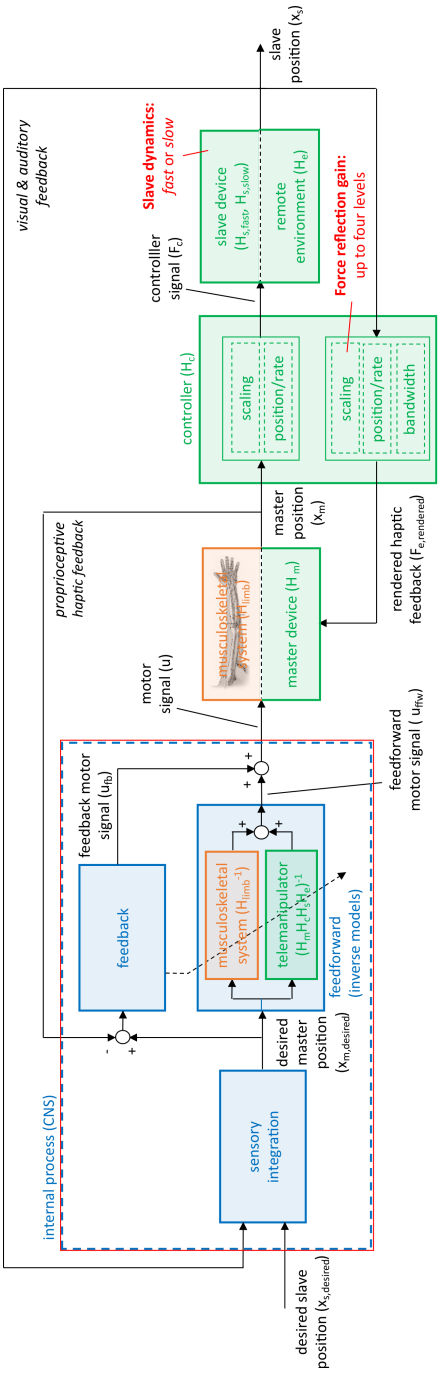

Figure 4.1: Simplified control-theoretic representation of the study as performed in this chapter. The effect of haptic feedback scaling and slave dynamics on operator neuromuscular control mechanisms (framed in red) was studied within a well-established cybernetic modeling framework. Slave dynamics and force feedback gain (shown in red) were modulated.

ABSTRACT

Telemanipulation encompasses applications with a wide variety of slave dynamics, ranging from minimally-invasive surgery to large-scale nuclear maintenance. Hence, the haptic feedback from the remote site - which is considered essential to effectively perform tasks - is often scaled. The objective of this study is to quantify the effect of slave dynamics and such scaling of haptic feedback on task execution, and to identify the corresponding changes in underlying control behavior of the operator using a cybernetic model. In a human factors study, subjects (n=13) used a haptic master device to control a virtual slave in a 1 DoF pursuit task with preview. The simulated slave dynamics were either *fast* or *slow* with respect to human operator dynamics. Four levels of haptic feedback scaling were provided, namely 0%, 25%, 50% or 100%. The experimental results indicate that task execution was only marginally affected when manipulating haptic feedback for fast dynamic systems. For slow dynamic systems, full haptic feedback substantially improved task execution compared to no haptic feedback, but at the cost of increased operator physical workload. Interestingly, these effects persisted for scaled haptic feedback. Additional frequency domain analysis for the slow dynamic system revealed that, compared to no feedback, any haptic feedback level enables operators to generate phase lead, allowing for improved compensation of the slow slave system's lag. A quasi-linear cybernetic control model was fit to the data to quantify underlying control behavior; the operator's effective time delay and future viewpoint were substantially reduced for all haptic feedback conditions, compared to no haptic feedback. We conclude that the proposed model accurately describes the effect of slave dynamics and haptic feedback on operator control behavior, namely that scaled haptic feedback allows operators to adapt their feedback and feedforward responses, such that slow slave systems can be controlled more accurately in free-space, with a higher bandwidth.

4.1. INTRODUCTION

Teleoperation entails a wide variety of tasks to be performed. Operators may use the master device to control a slave directly (where movements may be scaled), with rate-control, or through set-points to a semi-autonomous system. In many real-world teleoperation applications haptic feedback is absent, especially during rate control, set-point control – and scaled direct control. This paper focusses on *bilateral* teleoperation, where the slave is under direct control from the master device, but where control and haptic feedback may be scaled. In subhuman-scale applications (e.g., micro-assembly of micro-electro-mechanical systems [18] or minimally-invasive surgery [34]), master device movements need to be scaled down and force feedback in the slave environment needs to be scaled up in order for the operator to be able to perceive and respond to it. Note that in this case the human arm dynamics are dominant over the slave manipulator dynamics. Conversely, when manipulating a superhuman-scale slave (e.g., in nuclear [15] or sub-sea environments [77]), master device movements need to be scaled up, and force feedback on the master device needs to be scaled down. Note that in this case the slave dynamics dominate the human arm dynamics and unscaled coupling of the dynamics on the master device would make movement impossible.

When available, haptic feedback from the remote environment is often considered

essential to effectively perform tasks with these systems, while different forms of augmented haptic feedback (e.g. [8] [68] [98]) are seen as promising methods to improve task execution. However, how the quality and quantity of haptic feedback affects task execution is not well understood. Similarly, the operator response to augmented forces is not fully comprehended. As a result, the design and evaluation of haptic interfaces and augmented support systems is often subjected to trial-and-error.

This study focuses on measuring and modeling operator control behavior of free-space tasks while controlling a system with substantial dynamics (e.g., cranes, large slave robots, vehicles). A formalized understanding of the effects of haptic feedback and system dynamics on operator control behavior, captured in a computational modeling framework, is expected to help with model-based design of haptic feedback and augmented support systems.

'Haptics' is often referred to as our sense of touch: tactile feedback via our skin that provides information on forces (e.g., pressure, vibrations), but also temperature, humidity and pain. However, haptics also includes kinesthetic or proprioceptive feedback via our muscles and tendons, that provides feedback on muscle stretch and tendon forces, and by integration: feedback on orientation of our body and interaction forces with the environment. A telemanipulation system reflects haptic information from the remote site to the local site, and vice versa. The quality and quantity of this haptic feedback transfer is often captured by 'transparency', commonly defined as the fidelity with which force and positional information is sent from remote (or slave) side to local (or master) side [40] [79] [138]. The haptic feedback to the operator can comprise both the reflected dynamics of the slave (i.e. the inertia and damping of the slave are partially felt by the operator), as well as the contact forces of the slave in the remote environment.

The fact that we can control many devices with only visual feedback often obscures the benefits of haptic feedback. However, the benefits of haptic feedback are substantial: when in physical contact with the remote environment, haptic feedback has shown to improve task execution in terms of task completion time [38] [55] [85], contact forces [38] and errors [38] [55], and reduces control effort measured in terms of reversal rate [133], cognitive workload [129] and energy consumption [55], compared to solely visual feedback.

But even when there is no physical contact of the slave system with the remote environment (i.e. free-space tasks), haptic feedback gives the operator a feel of the dynamics of the controlled system (e.g., the slave device and any objects held). In visuomanual control of a system with a priori unknown dynamics [56] and manual excitation of a sprung mass [62], operators improved their control input when haptic feedback was available. Danion et al. [33] conclude that haptic feedback enhances the control of non-rigid objects. Also, several studies (e.g. [65] [114]) suggest that haptic feedback improves high-level neuromuscular planning; it enhances building the causal relation between operator input, system dynamics and subsequent system response . To this extent we found that an operator's ability to generalize beyond a set of pre-experienced motions in an abstract curl force field increases when the quality of the fed back haptic information is (close to) natural [134].

In short, while the effects of haptic feedback during free-space task execution are

widely acknowledged, it is not well understood how the feedback affects underlying operator dynamic control behavior. Computational models would help to understand and quantitatively describe the effects of, among others, slave dynamics or reflected haptic feedback. Specifically, such computational models would help to describe and predict changes in human operator control behavior, such that haptic interfaces and systems with augmented feedback can be optimized a priori. However, contrary to pilot (e.g. [86] [124]) or driver behavior (e.g [104]), operator models for telemanipulation are not readily available.

Control-theoretic models have been widely accepted in the field of neuroscience (e.g. [65] [103] [122]). These models describe how basic movements (i.e. reaching movements) are performed and learned, and incorporate mechanisms for feedforward control, feedback control and learning; our central nervous system learns associations between action and sensory feedback, either by reconstructing the motion from sensory feedback (inverse dynamics), or by translating desired behavior into motor commands (forward dynamics) [122]. These neuroscience models describe the execution of the actual limb movement, but only with a-priori knowledge of the goal. The models do not describe how this goal is derived from dynamic sensory information (i.e. perception).

A more unifying approach addressing perception-action coupling is given by the theory of *successive organization of perception* [75]. This theory is based on the premise that human operators control a device based on high-level control strategies derived from (dynamic) sensory information. The theory classifies three types of control strategies, namely compensatory, pursuit, and precognitive control. In compensatory control the operator can only use feedback control, which is often realized by solely visualizing the error between reference target and system output to the human operator. During pursuit control, the operator combines feedback with feedforward control, typically by visualizing both output and reference target, such that the operator may use past experience and knowledge of the near future. In precognitive control the human operator acts as an open-loop controller and performs purely feedforward.

Operator control behavior during compensatory tracking tasks is accurately modeled by the 'crossover model' by McRuer and Rex [86]. Depending on the plant dynamics, this quasi-linear model characterizes the operator as a gain with a time delay and elements for lead-lag equalization. For pursuit tasks, Wasicko et al. [130] suggested an extension to the crossover model, which used a combination of feedback control based and feedforward control to control the plant. However, Wasicko et al. did not formulate a generic model. Only recently, feedforward models were developed and validated with experimental data for pursuit tasks with predictable reference signals [39], and for pursuit tasks with preview [124]. The model by van der El et al. [124] extends the quasi-linear operator model for compensatory tracking tasks, with two points of the previewed reference as input to the human operator (i.e., a look-ahead controller).

In practice, telemanipulation tasks are rarely performed purely based on feedback information, or purely based on feedforward information; an operator uses an estimate of the system's dynamics to plan its movements, while any distortions are corrected using feedback control. Hence, in order to study operator control behavior in telemanipulation tasks, it is important to use a model which incorporates both feedforward and

feedback: the pursuit model.

The pursuit models show that, in the human-machine system's frequency range most critical to its performance and stability, the human operator has the capability to adjust or equalize his behavior such that the closed-loop characteristics yield some desired command-response relationship, disturbances can be suppressed, variations and uncertainties can be minimized and adequate closed-loop stability margins can be attained [86]. In telemanipulation, the controlled device dynamics for, for example, space, nuclear [15] and sub-sea [77] tasks, are often in the range of, or even larger than, human operator dynamics. Control of such systems is characterized by large control lag, typically caused by large inertias combined with relatively low power actuators. This means that, from a dynamics point of view, the slave system being controlled is the limiting factor in the closed-loop human-machine system [72]. What is the extent to which human operators can adjust or equalize their behavior such that the basic requirements of any good feedback control system are fulfilled (e.g., adequate command-response relations and closed-loop stability margins [86])? And how does haptic feedback affect operator control parameters, given certain slave dynamics?

The objective of this study is to quantify operator control mechanisms underlying haptic feedback in visuo-motor coordination. A control-theoretic approach is adopted to measure and model operator responses, yielding quantitative insights of observed operator control behavior. As such this study expands on previous work [134], in which mainly time domain metrics were analyzed. Subjects were subjected to a visuo-motor control task, in which a previewed reference trajectory was to be tracked using a (virtual) telemanipulation system, with either fast or slow dynamics. The dynamics of the controlled system were fed back fully (i.e. the slave's dynamics are directly presented to the operator), scaled (i.e. the slave's dynamics are scaled before being presented to the operator) or not at all. Besides metrics derived in the time domain, a black-box identification method was used to quantify causal relationships in operator control behavior, and a recently published cybernetic model [124] was fit to the data.

We hypothesize that when either full or scaled haptic feedback is provided, operators are able to more accurately control the slave system compared to not providing haptic feedback. We expect reductions in tracking errors and mental control effort, as haptic feedback may improve the operator's estimates of the system's state. The root of these effects may be found in improvements of the operator's feedback and feedforward responses; we expect that haptic feedback allows a reduction of the effective time delays, because of the generally faster sensorimotor response to haptic stimuli compared to visual stimuli.

4.2. MATERIALS & METHODS

4.2.1. SUBJECTS

Thirteen healthy, right-handed subjects aged between 24 and 35 years all affiliated with the Delft University of Technology were recruited. The participants had none or limited experience with robotic systems. All subjects gave informed consent. The study was approved by the Delft Human Research Ethics Committee.

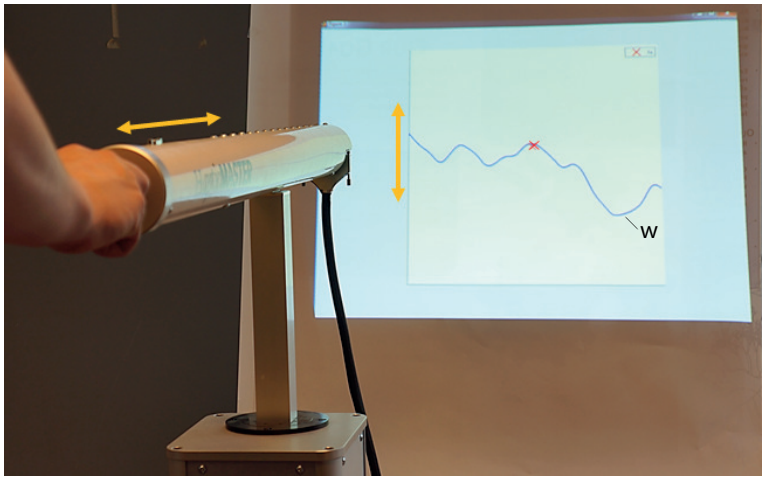

Figure 4.2: The experimental setup showing master device, virtual slave system (red cross) and reference trajectory w (blue line) in a pursuit display with preview. Subjects were standing in front of the HapticMASTER, which was aligned with the sagittal plane of the subject. Pushing the master device forward moves the slave system upwards, pulling it moves the slave system downwards. Subjects were instructed to track the reference as accurately as possible.

4.2.2. APPARATUS

The experiments were performed on the 3 degree-of-freedom admittance-controlled FCS Moog HapticMASTER with a simulated slave device. The HapticMASTER was constrained to only allow movement along the forward/backward-axis of the device, which was aligned with the sagittal plane of the subject (Fig. 4.2). The HapticMaster has a position resolution of <12e-6 m, a stiffness of >10 kN/m and a force sensitivity of 100 mN [82]. The virtual inertia and damping of the master device were respectively set at J_m = 2.5 kg and B_m = 5 Ns/m. The manipulator was controlled with a VxWorks RT operating system running at 2048 Hz. The slave system, designed in Matlab Simulink, was simulated on an additional real-time controller by Bachmann GmbH. This industrial controller runs at 1000 Hz and logs position and force at the same frequency. The visualization was updated at a rate of 30 Hz.

4.2.3. EXPERIMENTAL DESIGN

TASK DESCRIPTION

Subjects controlled a second-order virtual slave system (a mass-damper), actuated via a servo actuator, with the goal of tracking a multisine reference trajectory w as accurately as possible. A forward movement in the sagittal plane of the subject allowed control of the vertical position of the slave system (Fig. 4.2). The scaling between movement and visualization was approximately 1:1. Reference trajectory w was displayed as a pursuit display with two seconds of preview and history. The multisine signal consisted of 10 logarithmically distributed frequency pairs ranging from 0.03 to 4 Hz. In order to represent a realistic tracking task, the power spectrum of the reference trajectory contained a significant amount of power at the lower frequencies, with a second-order roll-off (20

dB/decade) [31]. To achieve this, the reference trajectory was filtered with a second-order Butterworth filter with a cutoff frequency of 0.5 Hz. Six different random phase time domain signals were generated all with a duration of 35 s. Two signals were solely used for training purposes and four for the measurement trials. All subjects performed the trials with the same signals, while the order in which the signals were presented was randomized. Fig. 4.3 shows a time trace and the auto spectrum of w.

EXPERIMENTAL CONDITIONS

The two independent variables were slave dynamics (*fast* or *slow*) and force reflection gain (K_{fb}=0 ∨ 1 for the *fast* system and K_{fb}=0 ∨ 0.25 ∨ 0.5 ∨ 1 for the *slow* system).

The dynamics of the second-order mass-damper slave system were chosen with respect to the frequency range of the operator's voluntary control inputs. The human's neuromuscular system only allows for precision movements up to approximately 1 Hz, with voluntary inputs up to several Hertz (up to 6-8 Hz for skilled professionals like pilots [130]). As such, the dynamics of the *fast* and *slow* dynamic systems were chosen to have a cutoff frequency - the point at which the output of the system drops -3 dB relative to the nominal value - of f_c = ~8 Hz and f_c = ~1.5 Hz, respectively. Hence the *fast* dynamic system predominantly appears to the human operator as a gain, whereas the *slow* dynamic system appears as a second-order system (a mass-damper) above its cutoff frequency, substantially affecting closed-loop human-machine performance. The transfer function of the second-order slave system and its position servo actuator is given by:

$$H_s(s) = \frac{x_s(s)}{x_m(s)} = \frac{k_d s + k_p}{J_s s^2 + (B_s + k_d)s + k_p} \tag{4.1}$$

Here x_m and x_s represent master and slave position, respectively. Slave inertia J_s and damping B_s were set at 2.5 kg and 10 Ns/m for the *fast* system and 50 kg and 200 Ns/m for the *slow* system. The systems were tuned to be critically damped. Limited by closed-loop stability, proportional gain k_p and derivative gain k_d were set at 2000 [-] and 80 [-], respectively, for the *fast* and 2500 [-] and 300 [-] for the *slow* dynamic system. Fig. 4.4 shows a bode plot and step response for the two controlled dynamics.

The force reflection gain K_{fb} was selected to be K_{fb}=0 or 1 for the *fast* and K_{fb} = 0, 0.25, 0.5 or 1 for the *slow* dynamic system. The equation for the force feedback is given by:

$$F_{fb}(t) = K_{fb}\Big(\big(x_s(t) - x_m(t)\big)k_p + \big(\dot{x}_s(t) - \dot{x}_m(t)\big)k_d\Big) \tag{4.2}$$

Thus for K_{fb}=0, no haptic feedback is provided to the human operator, whereas for K_{fb}=1, the servo system tries to equate $x_m(t)$ with $x_s(t)$.

EXPERIMENTAL PROTOCOL

Each of the six experimental conditions were performed in blocks of four repetitions. Each block was preceded by four training trials. The two blocks with *fast* and the three blocks with *slow* system dynamics were grouped. When the switch between slave dynamics was made, subjects performed another four training trials. The order in which conditions were presented to subjects, and the order of reference trajectories within a block of four repetitions, were randomized by means of a balanced Latin square for the

first twelve subjects and randomized for the thirteenth subject. Subjects rested and relaxed their arm between trials.

4.2.4. DATA PROCESSING

DATA ACQUISITION

Force and position data of the master device, as well as position data of the simulated slave were logged at 1 kHz. Fig. 4.5 shows a typical example of the tracking behavior of a subject. For each trial, the first and last second were discarded. Based on the recorded signals, time domain analysis was performed for both the *fast* and *slow* dynamics system. System identification and parameter estimation was performed for the data for the *slow* dynamic system.

TIME DOMAIN ANALYSIS

For both the *fast* and *slow* dynamic system, task performance and control effort were evaluated in terms of:

e_m Mean tracking error in mm of the slave position (x_s) with respect to reference trajectory w.

n_{rr} Number of reversals [-]. The amount of steering corrections by the operator as a measure of his mental effort [83]. n_{rr} was calculated by counting the number of sign changed of the filtered operator input force (second-order Butterworth with 5 Hz cutoff).

$F_{i,m}$ Mean interaction force N between operator and master device.

Additionally, for the *slow* dynamic system, the mean tracking error (e_m) was evaluated for frequencies < 0.5 Hz and frequencies ≥ 0.5 Hz. To do so, the data was anti-causally filtered [5] according to: $X(f) = X(f_{<0.5}) + X(f_{\geq 0.5})$, where $X(f)$ is the Fast Fourier Transform of $x(t)$. Subscripts indicate frequency bands < 0.5 and ≥ 0.5 Hz, of which the boundaries are not absolute.

FREQUENCY DOMAIN ANALYSIS

A) Nonparametric Analysis A closed-loop identification method was adopted to estimate the Frequency-Response Functions (FRFs) from reference trajectory to control input ($\hat{H}_{wc}$) and from control input to slave position ($\hat{H}_{cx}$). As such, the recorded time data of each trial was transformed to the frequency domain using the Discrete Fourier Transform (DFT), according to $w(t) \Rightarrow W(f)$, $c(t) \Rightarrow C(f)$ and $x_s(t) \Rightarrow X(f)$. The DFTs were used to estimate cross- and autospectral densities ($\hat{S}$), which were averaged over frequency bands and over repetitions to reduce variance due to noise. The FRFs were estimated of these spectral densities:

$$\hat{H}_{wc} = \frac{\hat{S}_{wc}}{\hat{S}_{ww}} \tag{4.3}$$

As a measure for the linearity between the signals the coherence (Γ) between input (w) and output (x_s) was estimated. A high coherence (i.e., close to 1) indicates linear

behavior and justifies the use of quasi-linear operator models.

$$\Gamma_{wx} = \sqrt{\frac{|\hat{S}_{wx}(f)|^2}{\hat{S}_{ww}(f)\hat{S}_{xx}(f)}} \tag{4.4}$$

B) Model Structure The model used to quantify the operator control behavior is adapted from van der El et al. [124], which is an extension to of the quasi-linear operator model for compensatory tracking tasks by McRuer et al. [86], and is depicted in Fig. 4.6. This model [124] incorporates an operator describing function ($H_{o,e}$), models for both a near ($H_{o,n}$) and a far ($H_{o,f}$) viewpoint response to a previewed reference trajectory, and an element modeling physical interaction of human operator and master device (H_{PI}). The near viewpoint response ($H_{o,n}$) is omitted, as its contribution to the operator control behavior is limited [123]. Also, parameter estimations were performed up to the FRFs at 1.63 Hz (i.e., the highest two FRF estimates at 2.55 and 4.01 Hz have been omitted). This is in line with [124], which only validated the model to describe human control behavior up to 1.84 Hz.

The operator describing function $H_{o,e}$ modulates an operators' response to a tracking error, just as in McRuer's crossover model [86]. The dynamics of the controlled system affect $H_{o,e}$. For the *slow* dynamics system, which appears to the human operator as a gain for the lowest frequencies and as a second order system at higher frequencies, $H_{o,e}$ is given by a lag system:

$$H_{o,e}(s) = K_e \frac{1}{T_{Ie}s+1} e^{-\tau_v s}, \tag{4.5}$$

with gain K_e, lag time constant T_{Ie} and effective time delay τ_v. The Laplace operator is given by s.

Far viewpoint response $H_{o,f}$ modulates an operators response to a future point on the reference trajectory, located τ_f seconds ahead. The future signals are weighted with gain K_f and low-pass filtered with lag time constant T_{If}, according to:

$$H_{o,f}(s) = K_f \frac{1}{T_{If}s+1} e^{\tau_f s} \tag{4.6}$$

The operator's intrinsic muscle visco-elasticity, limb mass and the interaction dynamics with the haptic master device are lumped in a physical interaction model H_{PI}. H_{PI} is parameterized using a second-order model:

$$H_{PI}(s) = \frac{\omega_{PI}^2}{s^2 + 2\zeta_{PI}\omega_{PI}s + \omega_{PI}^2} \tag{4.7}$$

As can be derived from Fig. 4.6, the transfer from visual reference trajectory w to control input c is given by:

$$H_{wc}(s) = \frac{H_{o,f}(s)H_{o,e}(s)H_{PI}(s)}{1 + H_{o,e}(s)H_{PI}(s)H_{cx}(s)}, \tag{4.8}$$

where H_{cx} is the (pre-defined) response from control input to slave output. H_{cx} thus equals the dynamics of the *slow* dynamic system as given by Eq. (1).

Notice this model structure represents the far viewpoint response $H_{o,f}$ and the operator describing function $H_{o,e}$ in series - the visual reference signal w is processed before being fed to the feedback controller). Thus the open-loop response, which can be interpreted as a feedforward component, is given by $H_{o,f}H_{o,e}$, whereas the feedback response is described by $H_{o,e}$. This deviates from typical motor control literature (e.g. [64, 70]) which presents feedforward (H_{ffw}) and feedback (H_{fb}) as parallel processes, in which the error between reference and target ($w - x_s$) is directly fed to the feedback controller (thus $x_s/w = (H_{ffw} + H_{fb})/(1 + H_{fb})$). The two representations are mathematically exchangeable ($H_{fb} = H_{o,e}$ and $H_{ffw} = H_{o,f}H_{o,e} - H_{o,e}$), but care should be taken on, specifically, the interpretation of feedforward as a construct.

C) Parameter Estimation The operator control model (H_{wc}, Eq. (4.8)) was fitted to the FRFs of the data ($\hat{H}_{wc}$, Eq. (3)) in the frequency-domain, using a grid search methodology. Random initial conditions for the optimization procedure were generated within the parameter space spanned by 0-5 [-] for K_e, 0-2 s for T_{Ie}, 0-0.3 s for τ_v, 0.05-5 [-] for K_f, 0-0.5 s for T_{If}, 0.2-0.8 s for τ_f, 1-3 Hz for ω_{PI} and 0-0.4 [-] for ζ_{PI}, which is in agreement with previous work [123] [124].

Parameter estimates were evaluated by minimizing a least-squares error criterion in the frequency domain for each of the initial condition sets (m):

$$\epsilon(m) = \sum_k f(k)(log\frac{H_{wc}(k)}{\hat{H}_{wc}(k)})^2, \tag{4.9}$$

in which $f(k)$ is the frequency vector. The best fit was selected according to $min(\epsilon(m))$.

D) Model Validation The variance accounted for (VAF) was calculated to obtain a validity index for the quantified parameters. A VAF of 100% indicates that the linear model fully describes the measurements. Noise, non-linearities and other unmodelled behavior reduce the VAF. Low coherence (noise or non-linearities) result in low VAFs. To calculate the VAF the model is simulated in time with the reference trajectory w as input and the simulated operator control input $\check{c}(t)$ as output for each time sample n:

$$VAF\big(c(n),\check{c}(n)\big) = \Big(1 - \frac{\sum_n ||c(n) - \check{c}(n)||^2}{\sum_n ||c(n)||^2}\Big) * 100\% \tag{4.10}$$

DATA ANALYSIS

Experimental conditions were compared using a repeated measures ANOVA, assuming normal distributions and variance homoscedasticity. A p-value of 0.05 or below was deemed significant (α = 0.05). Results for the *fast* and *slow* dynamic system are presented independently.

Table 4.1: Mean (μ) and standard deviation (σ) of the metrics mean tracking error (e_{mean}), number of reversals (n_{rr}) and mean operator interaction force ($F_{i,m}$), for each of the experimental condition. The metrics are calculated from a population of 13 subjects each with 4 repetitions per condition.

		μ (σ) for $K_{fb}=0$	μ (σ) for $K_{fb}=0.25$	μ (σ) for $K_{fb}=0.5$	μ (σ) for $K_{fb}=1$
Fast	e_m [-]	10.19 (1.49)	-	-	10.11 (1.69)
	n_{rr} s	133 (13)	-	-	121 (15)
	$F_{I,m}$ s	1.65 (0.21)	-	-	2.38 (32)
Slow	e_m [-]	18.83 (2.46)	17.36 (2.19)	17.51 (2.70)	17.06 (1.90)
	n_{rr} s	130 (14)	83 (9)	76 (9)	82 (10)
	$F_{I,m}$ s	2.09 (0.31)	7.04 (0.50)	13.0 (1.2)	25.3 (3.0)

4

4.3. RESULTS

4.3.1. TIME-DOMAIN RESULTS

Means (μ) and standard deviations (σ) for the time domain metrics e_{mean}, n_{rr} and $F_{i,m}$ for each of the experimental conditions are shown in Tab. 4.1.

For the mean tracking error (e_{mean}) of a *fast* dynamic system there is no difference when providing haptic feedback compared to not having haptic feedback (K_{fb}=1 versus K_{fb}=0; p=0.82, F=0.05), as shown by Fig. 4.7a. The mean tracking error for the *slow* dynamic system is affected by the force reflection gain (p=0.001, F=6.64): K_{fb}=0.25, K_{fb}=0.50 and K_{fb}=1 yield an approximately 8% lower mean error than K_{fb}=0 (p<0.035, F>5.67). The is no difference between the conditions with haptic feedback (p>0.25, F<1.92).

The number of reversals (n_{rr}, shown in Fig. 4.7b) for a *fast* dynamic system is about 9% lower when feedback is provided (p<0.001, F=28.5). Similarly, the force reflection gain affects the number of reversals (p<0.001, F=193) for the *slow* dynamic system. The post-hoc analysis shows that compared to not having haptic feedback (K_{fb}=0), any feedback substantially reduces the number of reversals (p<0.001, F>264) by about 40%. Between the conditions with feedback, K_{fb}=0.5 yields a lower number of reversals than K_{fb}=0.25 and K_{fb}=1 (p<0.022, F>6.98).

Haptic feedback increases the mean operator interaction force ($F_{i,m}$, Fig. 4.7c) for both the *fast* (p<0.001, F=86) and the *slow* dynamic system (p<0.001, F=675). For the *slow* dynamic system, the mean interaction force proportionally increases as the force reflection gain increases (p<0.001, F>419); K_{fb}=0.5 yields almost double the interaction forces as K_{fb}=0.25. Similarly, K_{fb}=1 almost doubles the forces compared to K_{fb}=0.5.

Anti-causal filtering of the signals shows that for perturbations below 0.5 Hz, there are no differences in the mean tracking error (e_m) between haptic feedback conditions for both the *fast* and *slow* dynamic system (p=0.34, F=0.97 and p=0.25, F=1.41 respectively).

Also above 0.5 Hz, there is no difference between K_{fb}=0 and K_{fb}=1 for the *fast* dynamic system (p=0.66, F=0.21). For the *slow* dynamic system however, haptic feedback affects the mean tracking error (p=0.012, F=4.20); compared to K_{fb}=0, haptic feedback reduces the error for K_{fb}=0.25, K_{fb}=0.5 and K_{fb}=1 (p<0.030, F>6.1) by about 9-13%. Between conditions with feedback, there is no difference (p>0.20, F<1.9).

4.3.2. FREQUENCY-DOMAIN RESULTS

The identified operators' FRFs are taken from reference trajectory w to operator control input c. Fig. 4.9 shows these FRFs for the *slow* dynamic system, averaged over all operators. Squares indicate the estimated magnitude and phase for the condition without feedback ($K_{fb} = 0$). Similarly, circles denote the estimated magnitude and phase for conditions with feedback (K_{fb}=0.25, K_{fb}=0.5 and K_{fb}=1). The errorbars (in black) represent the 95% confidence interval of the population mean. For the condition without feedback ($K_{fb} = 0$), the phase for the highest two frequencies in the reference trajectory at approx. 1.0 and 1.6 Hz is 22 and 5 degrees, respectively, whereas for the conditions with feedback the phase for these two frequency points is about 30 and 25 degrees, respectively.

Coherences of the FRFs were calculated of the power spectral densities, based on averages over two adjacent frequencies. Coherence is >0.9 for the lowest seven frequency points and >0.8 for the highest frequency (see Fig 4.13), indicating linear operator control behavior.

The parameters of the operator's control model were fitted to the identified response functions per subject. Parameters estimations for the population of 13 subjects are shown in Tab. 4.2 and displayed in Fig. 4.10

For the parameters of the operator error response model $H_{o,e}$, no differences are found for K_e and T_{Ie} (p=0.79, F=0.34 and p=0.42, F=0.95, respectively). τ_v is affected by haptic feedback (p<0.001, F=7.71). A post-hoc analysis reveals that compared to K_{fb}=0, τ_v decreases from 0.087 to 0.032, 0.026 and 0.029 for K_{fb}=0.25 (p=0.008, F=7.7), K_{fb}=0.5 (p=0.008, F=9.9), and K_{fb}=1 (p=0.014, F=8.3), respectively. Between conditions with feedback, there is no difference (p>0.39, F<0.77).

For the far-viewpoint response $H_{o,f}$, no differences are found for K_f and T_{If} (p=0.41, F=0.98 and p=0.81, F=0.32, respectively). The mean of τ_f is reduced from 0.527 s for $K_{fb} = 0$ to 0.461, 0.473 and 0.475 s for $K_{fb} = 0.25$ (p=0.008, F=10.11), $K_{fb} = 0.5$ (p=0.005, F=11.5) and $K_{fb} = 1$ (p=0.047, F=4.9), respectively. Again, between conditions with haptic feedback no differences are found (p>0.31, F<1.2).

The neuromuscular model $H_{o,PI}$, the mean of ω_{PI} increases by approx. 8% from 1.59 to 1.70-1.74 Hz when feedback is provided (p<0.028, F>6.24). ζ_{PI} shows no differences between conditions (p=0.18, F=1.7).

Fig. 4.11 shows the mean VAFs per subject per condition. VAFs are calculated per repetition, hence each bar graph is an average of four repetitions. Over all repetitions the mean VAF is 95%, with a standard deviation of 1.9%, whereas the minimum VAF for a single repetition is 85%. Such high VAFs indicate that the model accurately describes operator control behavior in both conditions with and without haptic feedback.

The frequency response of the parameterized models of two typical subjects, subject 1 and 9 are shown in Fig. 4.12a and Fig. 4.12b, respectively. Fig. 4.13 shows the measured (dashed line) and modeled (solid line) operator control input of a single repetition of two conditions for subject 1. The high similarity between measured and modeled control input illustrate the VAFs of typically >90%.

Table 4.2: Mean (μ) and standard deviation (σ) of the parameter estimations of the operator control model (n=13).

	μ (σ) for $K_{fb} = 0$	μ (σ) for $K_{fb} = 0.25$	μ (σ) for $K_{fb} = 0.5$	μ (σ) for $K_{fb} = 1$
K_e [-]	1.696 (1.342)	1.662 (1.259)	1.603 (0.945)	1.969 (1.126)
T_{Ie} s	0.604 (0.438)	0.604 (0.431)	0.594 (0.371)	0.787 (0.455)
τ_v s	0.087 (0.066)	0.032 (0.019)	0.026 (0.025)	0.029 (0.023)
K_f [-]	2.22 (1.05)	2.05 (0.82)	2.09 (1.04)	1.70 (0.57)
T_{If} s	0.240 (0.052)	0.220 (0.083)	0.235 (0.034)	0.220 (0.094)
τ_f s	0.527 (0.074)	0.461 (0.061)	0.473 (0.037)	0.475 (0.057)
ω_{PI} Hz	1.59 (0.11)	1.74 (0.19)	1.70 (0.09)	1.70 (0.14)
ζ_{PI} [-]	0.105 (0.051)	0.160 (0.087)	0.159 (0.081)	0.137 (0.050)

4.4. DISCUSSION

For *fast* dynamic systems, haptic feedback of reflected dynamics only marginally affects task execution : performance measured in terms of tracking accuracy is unaffected, while the effects on control effort are limited (~9% reduction for the number of reversals, and a ~0.8 N increase in operator input force). Supposedly, for fast dynamic systems in which the operator's limb dynamics dominate overall system behavior, additional haptic feedback of system dynamics is superfluous.

For *slow* dynamic systems on the other hand, full haptic feedback substantially improves task execution compared to no haptic feedback; the mean tracking error and number of reversals decrease (by ~10% and ~39%, respectively), while the operator's input force increases proportionally with force feedback gain. Interestingly, the same improvements for tracking error and number of reversals occurred for scaled force feedback (i.e., $K_{fb} = 0.25$ and $K_{fb} = 0.5$) as for full haptic feedback, with a substantial reduction of operator input forces. In other words, any of the tested scaled haptic feedback yields the full benefit of unscaled haptic feedback, but with a beneficial decrease in physical control effort. Apparently, feedback of the dynamics of the relatively slow slave device allows operators to adjust their behavior accordingly, such that the closed-loop human-machine characteristics better match the task requirements.

To attain accurate tracking behavior, the operator needs to equalize the *slow* dynamics of the remote slave. These dynamics appear to the human operator as a gain up to the cut-off frequency (~1.5 Hz), and as a critically damped second-order system above this frequency. Thus, the slow dynamic system introduces lag into the human-machine system (approximately 45 degrees at 1 Hz). In previous work [134] we have shown that haptic feedback improves matching of operator control activity to the frequencies of the reference trajectory, especially at higher frequencies (>1 Hz). Putatively, the observed control activity at higher frequencies generates lead to compensate for the lag introduced by the slow dynamic system. Indeed, Frequency-Response Functions (FRFs) of the operators control actions (H_{wc}, see Fig. 4.9) show that any of the tested feedback levels enables operators to generate an increased phase lead, compared to no feedback. This suggests a correlation between increasing phase lead and decreasing tracking error, when haptic feedback is available. By quantifying underlying operator control equalizations, the cybernetic model enables identification of the causal relation between its parameters and

the phase lead.

The parameters of the operator's control model were fitted to the identified FRFs on a per subject basis. The model consists of an operator describing function that modulates the response to a tracking error $H_{o,e}(K_e, T_{Ie}, \tau_v)$, a response to a far viewpoint $H_{o,f}(K_f, T_{If}, \tau_f)$ and a model for the passive physical interaction of human and master device $H_{o,PI}(\omega_{PI}, \zeta_{PI})$. Haptic feedback was observed to affect each of these three transfer functions, specifically the parameters representing the operator's effective time delay τ_v, future viewpoint τ_f and natural frequency ω_{PI}.

For $H_{o,PI}$, damping factor ζ_{PI} is not affected by haptic feedback and the values of 0.06-0.35 [-] are in line with previous work (e.g. 0.1-0.3 [-] for [39], and 0.18-0.67 [-] for [124]). Similarly, with natural frequencies ω_{PI} of 1.4-2.1 Hz, the cutoff frequency of $H_{o,PI}$ is in line with typical values for the open-loop filtering behavior of the neuromuscular system, which is often lumped as a second-order filter with a cutoff frequency around 2 Hz [31] [104]. Haptic feedback does affect the natural frequency: it increases with about 8% for conditions with feedback compared to no haptic feedback. These changes can be attributed to changes in the neuromuscular system, whose settings and contribution cannot be identified in this study, but would require mechanical disturbances and EMG measurements (e.g. [31]).

The lag systems $H_{o,f}$ and $H_{o,e}$ both incorporate an equalization term which can be interpreted as filters on the inputs of the operator's open-loop ($H_{o,f}H_{o,e}$) and feedback error ($H_{o,e}$) response. Interestingly, neither of these filters is affected by haptic feedback gain K_{fb}. This suggests that operators do not change the bandwidth over which they attempt to control the slave system depending on feedback conditions. The absolute values of the gains (K_f and K_e) and time constants (T_{If} and T_{Ie}) are difficult to interpret and compare to previous work as they are heavily affected by, among others, the chosen controlled dynamics, reference trajectory and visualization. Firstly, $K_f > 1$ which means that operators emphasize feedforward over feedback control (i.e.,$K_f K_e > K_e$). This was also found for the gain dynamics in [124]. Also, T_{If} is comparable to the values found in [124]. Furthermore, from a stability perspective, gain and control bandwidth (given by filter cutoff frequency $1/T_I$) have an inverse relation: when the gain increases, the cutoff frequency should decrease. The data shows that the open-loop gain $K_f K_e$ is indeed generally two times larger than the feedback gain K_e, while the corresponding cutoff frequency is lower (~0.22 Hz versus ~0.27 Hz for open-loop response $H_{o,f}H_{o,e}$ and feedback error response $H_{o,e}$, respectively). In the minority of cases where this does not hold, subjects apparently prioritize performance and sacrifice stability.

Besides an equalization term, both $H_{o,f}$ and $H_{o,e}$ incorporate a time constant in the form of a future viewpoint (located τ_f s ahead) and an effective time delay τ_v, respectively. The mean value of 0.087 s for τ_v for the conditions without feedback ($K_{fb} = 0$), is slightly below the typical value of this parameter, which ranges between 0.1-0.2 s for zero order compensatory or pursuit tasks (e.g. [86] [124]). 0.1 s is considered a lower boundary for the human's central nervous system to react, by first processing visual information and subsequently acting through our neuromuscular system. However, the two seconds of trajectory preview are likely to cause operators to anticipate as opposed to react, leading to time delays below 0.1 s. Operators respond to an error ahead in time,

instead of a momentaneous error. Indeed, one cannot compensate for momentaneous errors due to inherent physical limitations. In contrast, such anticipation could not have appeared in previous studies on pursuit tasks, as these studies make use of an (additional) unpredictable perturbation signal to identify the feedback loop [39] [124].

Interestingly, haptic feedback decreases the effective time delay τ_v even further, namely by about a factor 3 to ~0.026-0.032 s, compared to no haptic feedback. Haptic feedback allows operators to not solely control towards a visual reference, but to also apply (haptic) feedback control towards the remote slave. By exploiting their neuromuscular viscoelastic and reflexive capabilities, operators can compensate for errors in the dynamic estimates of the controlled system (i.e., internal models [65] [103]). Such neuromuscular response is much faster than visual or vestibular cues responses. This means that the inclusion of haptic feedback may directly reduce the time to respond to an error, thus reducing effective time delay τ_v by 0.06 s on average and max. 0.03-0.21 s for a single subject, for conditions with feedback compared to no feedback.

Operators use preview to generate phase lead to compensate for their own and slave system time delays [123], by positioning their future viewpoint τ_f s ahead on the previewed target. Therefore, when their own response delays (i.e., τ_v) decrease due to, for example, haptic feedback, operators will use less preview. Indeed, both τ_v and τ_f decreases for all haptic feedback conditions, compared to no haptic feedback. This relation is characterized by the difference between future viewpoint and effective time delay (i.e., τ_f-τ_v), which is constant and resides between 0.42-0.45 s for all conditions.

In summary, the cybernetic model indicates that the observed control benefit of haptic feedback (in terms of reduced tracking error and increased phase lead), is caused by reductions in effective time delay τ_v and a preview τ_f. Changes in these parameters suggest that haptic feedback allows operators to exploit their fast neuromuscular system to compensate for internal model errors which cannot be compensated with their relatively slow visual feedback only.

The estimated model accurately represented the data (i.e., high VAF of typically >90%). Also, coherences of >0.8 indicate that the use of quasi-linear computational models was not substantially complicated during the experiment by large amounts of noise, nonlinearities or time variance (i.e., small remnant r). The repeatability and reproducibility was high for most parameters, with standard deviations of typically 10-20% of the mean (see Tab. 4.2). Gain K_e and time constant T_{Ie}, and to a lesser extent K_f and T_{If}, show an increased variability as gains and time constants mutually affect each others sensitivity: for low gains, the time constant loses sensitivity and vice versa, for high time constants, the gain loses sensitivity.

Although the cybernetic model does not explicitly account for haptic feedback, the model allows to study the meta or high-level control adaptations caused by haptic feedback. Haptic feedback is an implicit yet inherent part of the transfer function from a visual input to a physical control output, as described by the model. The present model can be supplemented or extended with neuromuscular control models (e.g. [125]), if it is desired to expose underlying low-level neuromuscular control control adaptations. Also, the adaptation with respect to the model van der El et al. [124], to omit one of the two future viewpoints as inputs to the operator, seems justified. The single-input model

is well capable of describing the FRFs for each subject for all conditions, with sufficient sensitivity in the frequency as well as the time domain.

Specifically, the cybernetic model showed sensitivity to describe free-space tasks (e.g. tool movement, pick-and-place, visual inspection and metrology tasks) with slave systems that have substantial dynamics (e.g. cranes and robot arms with and without loads) in for example maintenance activities in nuclear (e.g. [15]) or sub-sea (e.g. [77]) environments. The model can describe and predict human control behavior for such tasks, but also for tasks that involve control of vehicles such as cars (e.g. curve negotiation) or aircraft (e.g. pitch and roll angle control [86]); the abstract task - preview tracking of a reference trajectory - is a conceptual representation of a broad variety of control tasks.

Moreover, the cybernetic model can be used as a basis to formalize augmented haptic support design, by serving as the underlying control structure to generate guidance forces in, for example, haptic shared control [6] [98]. While shared control can substantially improve task execution as shown in the automotive domain (e.g. lane changing [7] [104]), and in teleoperation (e.g. obstacle avoidance [8] [68], path guidance [15]), its benefits decrease due to conflicts between individual human operators and intelligent system [35]. The cybernetic model can be used to individualize support trajectories, reducing discomfort and increasing performance.

Hence, in order to fully benefit from the prediction capabilities of (cybernetic) models, and to allow for a priori design of haptic interfaces and haptic support systems, it is required to further develop these computational models for tasks where contact with the environment is made and multiple degrees of freedom, and to verify its applicability in other application domains.

4.5. CONCLUSION

A human factors study was conducted during which subjects used a 1 DoF haptic master device to control a slave system (with either *fast* or *slow* dynamics) in a pursuit task with preview. Subjects received four different levels of haptic feedback from the slave dynamics: full haptic feedback, no haptic feedback and scaled haptic feedback (25% or 50%). For the experimental conditions studied it can be concluded that:

- When controlling *fast* dynamic systems, task execution is only marginally affected by manipulating haptic feedback levels; haptic feedback has no effect on task performance, but improves control effort.
- For *slow* dynamic systems, full haptic feedback substantially improves task execution (in terms of mean tracking error, number of reversals) compared to no haptic feedback, but at the cost of substantially increased operating forces at the master device.
- Interestingly, scaled haptic feedback (25% or 50%) yields identical performance benefits as full haptic feedback, but with a beneficial decrease in physical control effort.

In order to understand underlying operator control behavior for the slow slave, frequency-response functions were estimated on which a linear cybernetic control model incorpo-

rating both feedforward and feedback was fit. The estimated model accurately captured individual operator control behavior in both time and frequency domain (i.e., high VAF), and yielded repeatable and reproducible results. This analysis led to the following conclusions:

- Any of the tested haptic feedback levels enable operators to generate more phase lead compared to no feedback, allowing improved compensation for the lag of the *slow* slave system.
- Haptic feedback enables operators to substantially reduce their effective time delay and, consequently, the amount of preview used, compared to no haptic feedback.

This indicates that the availability of haptic feedback allows operators to adapt their feedback and feedforward responses, such that slow slave systems can be controlled more accurately in free-space, with a higher bandwidth. The parameterized cybernetic model can be used to describe and predict human-in-the-loop telemanipulated control of slave systems (e.g., cranes, robot arms), as well as form a basis to formalize augmented haptic support design, such as haptic shared control or haptic guidance.

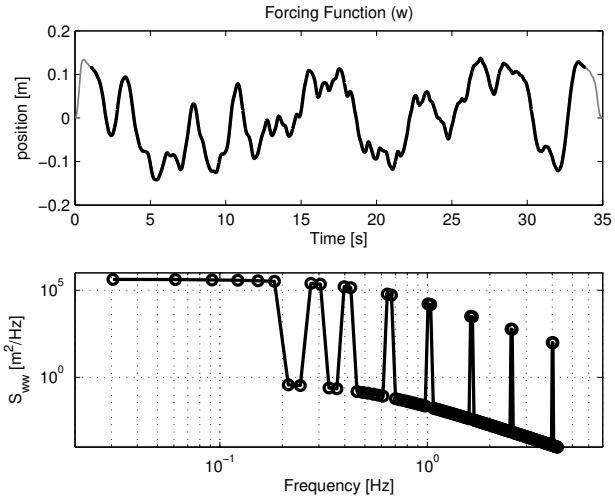

Figure 4.3: One of six realizations of the time trace and the auto spectrum of reference trajectory w. The multisine signal consists of 10 pairs of two log-spaced frequencies ranging from 0.03 to 4 Hz. The signal is filtered with a second-order Butterworth filter with a cutoff frequency of 0.5 Hz.

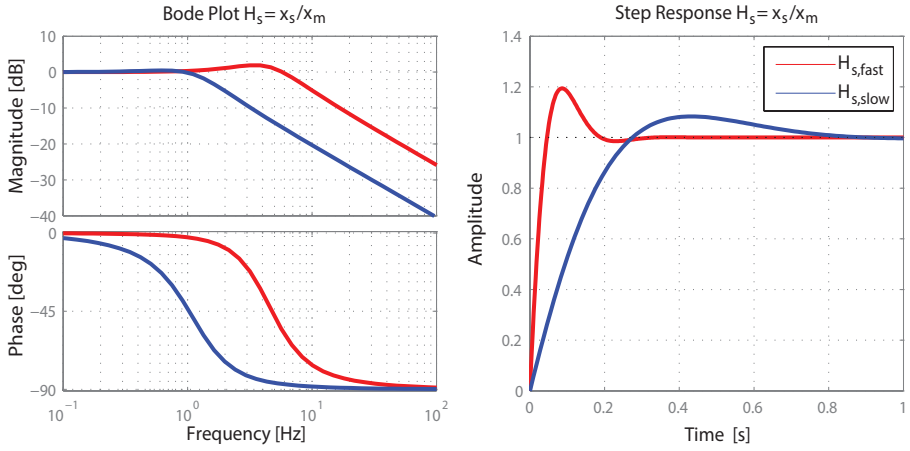

Figure 4.4: Bode plot and step response of the slave system (open-loop). The *slow* slave system ($H_{s,slow}$) has a cutoff frequency of ~1.5 Hz, whereas the *fast* slave system's ($H_{s,fast}$) cutoff frequency is ~8 Hz.

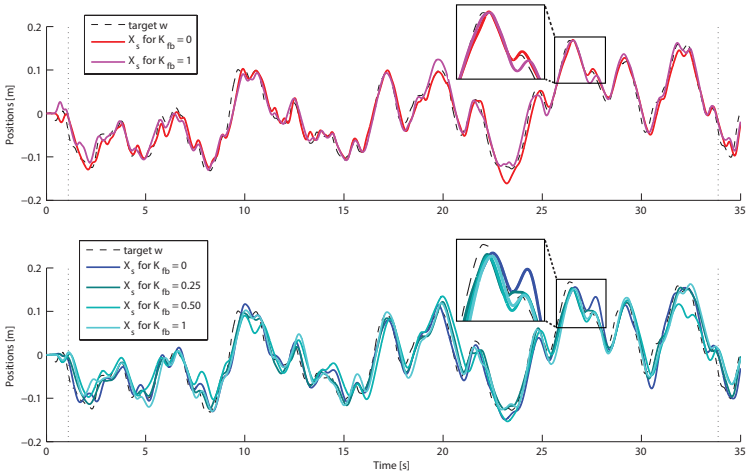

Figure 4.5: Typical example of time traces for each of the five experimental conditions. The red trajectories represent the *fast* dynamic system, whereas the *slow* dynamic system is represented in blue. It appears that in the *slow* dynamic condition operators lag the reference ω more than in the *fast* dynamic condition.

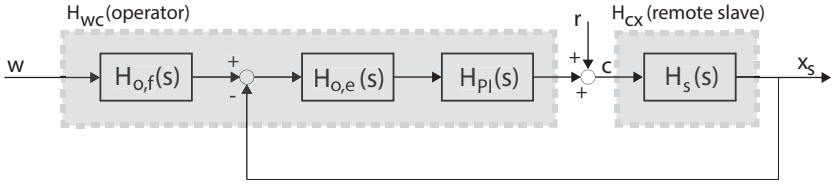

Figure 4.6: Closed-loop control diagram of the human operator (H_{wc}) controlling the remote slave system (H_{cx}), adapted from [124]. The human operator is to minimize the error between slave position x_s and reference trajectory w, by controlling the master position c. $H_{o,f}$ is the transfer function of the far-viewpoint response (Eq. 6), $H_{o,e}$ is the operator describing function (Eq. 5). H_{PI} and H_{cx} describes the transfer function of the physical interaction (Eq. 7) and manipulator dynamics (Eq. 1), respectively. Remnant signal r accounts for non-linearities of the human operator and is a residual that is not modeled by the linear model. The open-loop response ($H_{o,f}H_{o,e}$) can be interpreted as a feedforward controller, and $H_{o,e}$ as a feedback controller. Notice this representation in series (in which the visual reference signal w is processed before being fed to the feedback controller) deviates from typical motor control literature (e.g. [64, 70]) which presents feedforward (H_{ffw}) and feedback (H_{fb}) as a parallel process (the error between reference and target is directly fed to the feedback controller, thus $x_s/w = (H_{fb} + H_{ffw})/(1 + H_{fb})$).

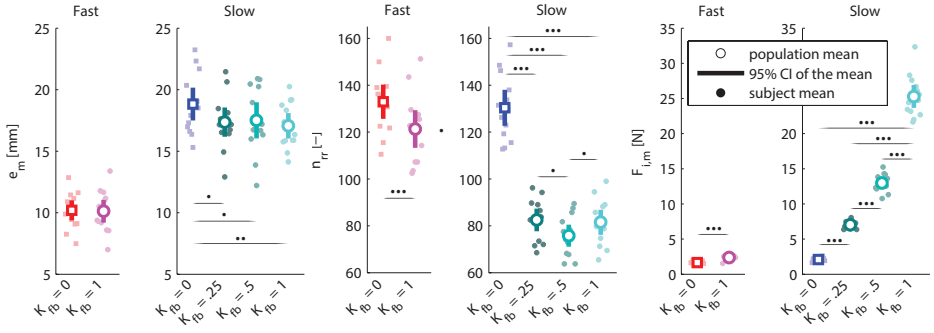

(a) Mean Tracking Error (b) Number of Reversals (c) Mean Interaction Force

Figure 4.7: Time domain metrics for (a) mean tracking error (e_m), (b) number of reversals (n_{rr}) and (c) mean operator interaction force ($F_{i,m}$) for each of the six experimental conditions. Open circles represent population means (n=13), with the error bars representing the 95% confidence interval of the mean. A subject mean is represented by a filled circle. Significance levels of p≤0.05, p≤0.01 and p≤0.001 are denoted by '•', '••' and '•••', respectively. Any force feedback (K_{fb}=0.25, K_{fb}=0.5 or K_{fb}=1) for the *slow* dynamic conditions improves the mean tracking error and number of reversals, at the cost of an increased operator input force.

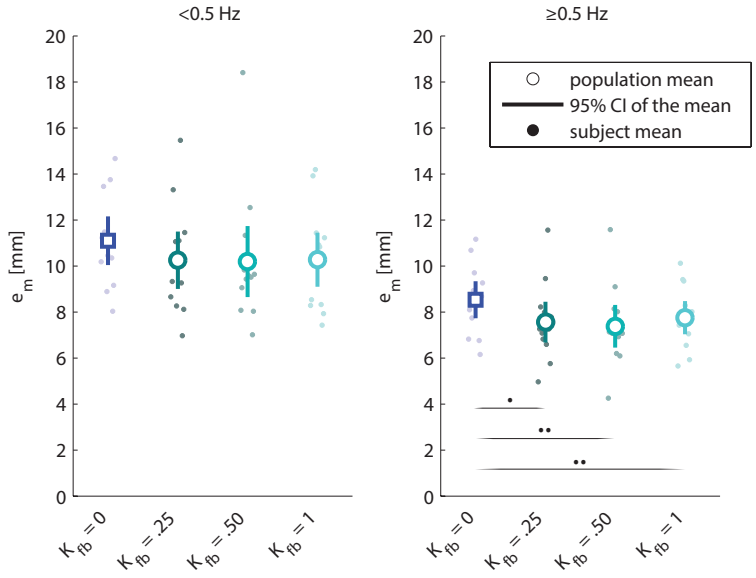

Figure 4.8: Mean tracking error (e_m) calculated for anti-causal filtered signals <0.5 Hz and ≥0.5 Hz, for the *slow* dynamic system. For perturbations below 0.5 Hz, there are no differences between haptic feedback conditions (p=0.25, F=1.41). Above or equal to 0.5 Hz, feedback decreases the tracking error (p<0.030, F>6.1), while haptic feedback conditions K_{fb}=0.25, K_{fb}=0.5 and K_{fb}=1 do not differ from each other (p>0.20, F<1.9).

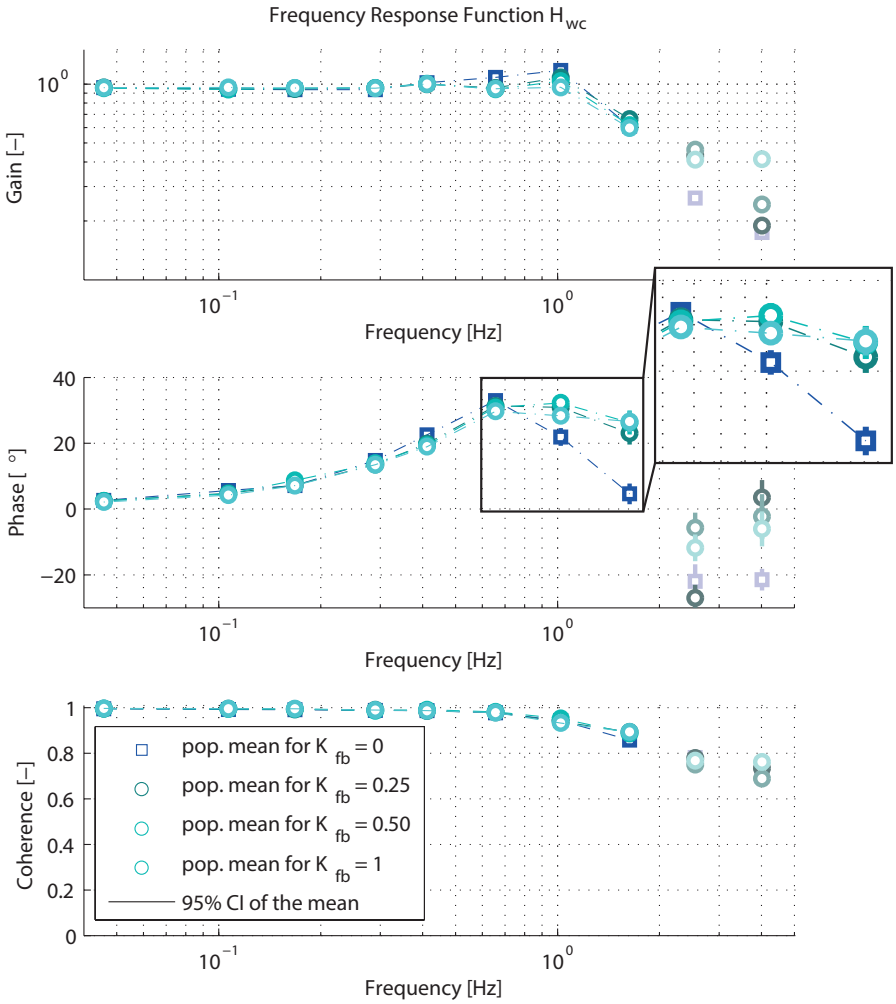

Figure 4.9: Population means of the identified operators' FRFs (H_{wc}). For $K_{fb} = 0$, the phase for the responses at approx. 1.0 and 1.6 Hz is 22 and 5 degrees, respectively. For the conditions with feedback the phase for these two frequency points is about 30 and 25 degrees, respectively. The operator model is fit on the first eight FRFs up to 2 Hz, such that the fitted frequency spectrum is in line with [124].

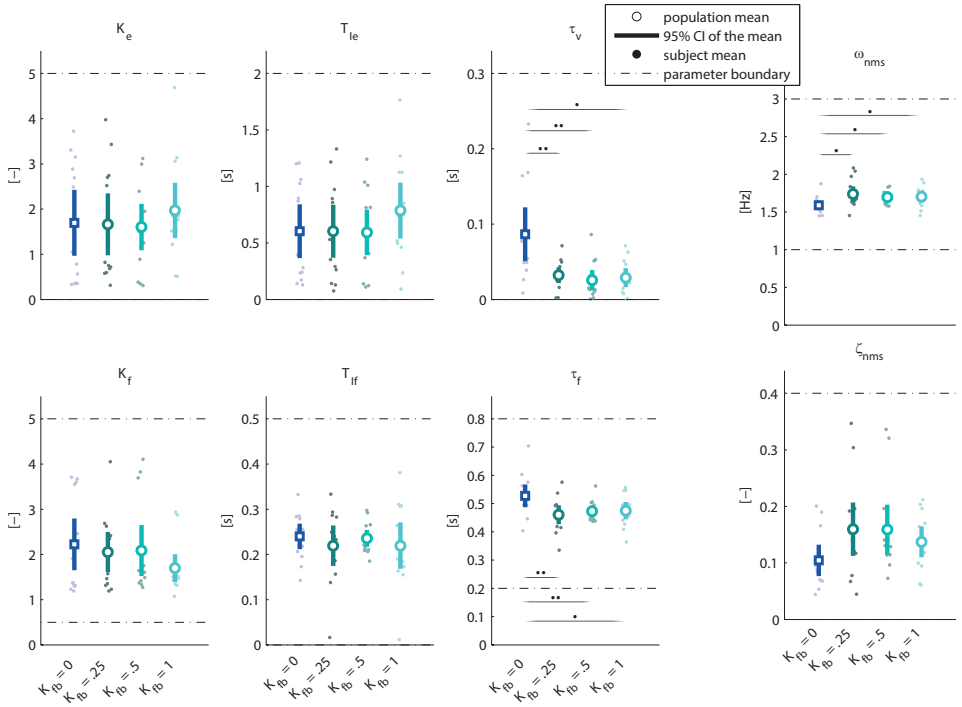

Figure 4.10: Estimated parameters of the operator control model, for for each of the six experimental conditions. Open circles represent population means (n=13), with the error bars representing the 95% confidence interval of the mean. A subject mean is represented by a filled circle. Any force feedback (K_{fb}=0.25, K_{fb}=0.5 and K_{fb}=1) reduces the operator's effective time delay τ_v, whereas scaled force feedback (K_{fb}=0.25 and K_{fb}=0.5) reduces look-a-head time τ_f.

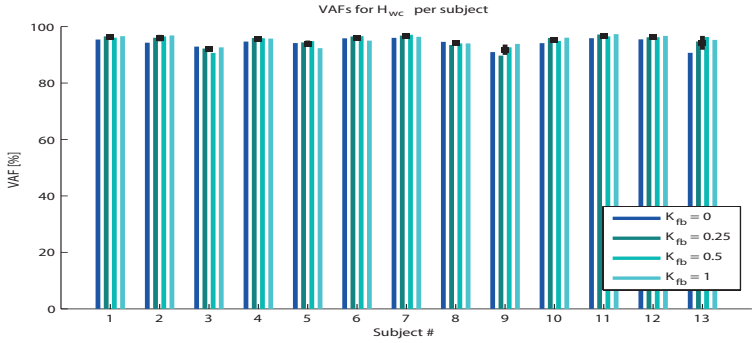

Figure 4.11: Mean VAFs per subject per condition. Each bar graph represents an average of four repetitions. The minimum VAF for a single repetition is 85%. The mean VAF over all repetitions is 95%, with a standard deviation of 1.9%. Such high VAFs indicate that the model accurately describes the data in the time domain.

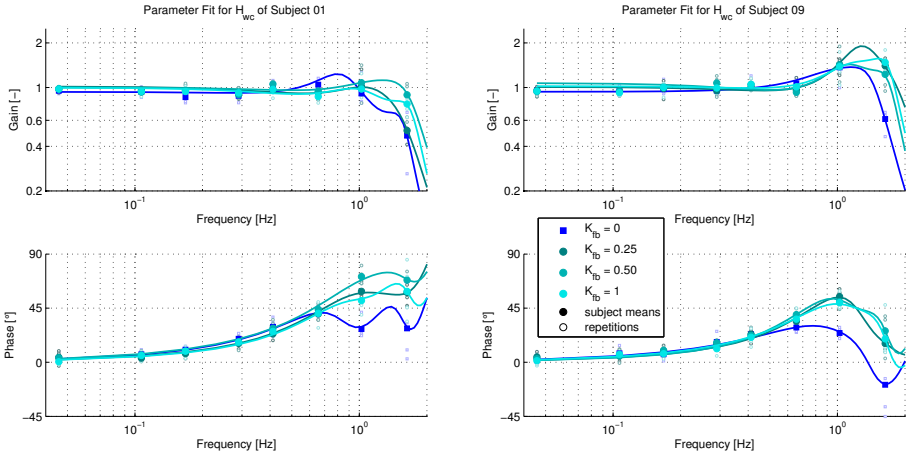

(a) Model fits for subject 1

(b) Model fits for subject 9

Figure 4.12: Model fits for subject 1 (Fig. 4.12a) and 9 (Fig. 4.12b). Circles and squares represent the identified FRFs, which are an average of four repetitions. The lines represent the fitted models. Both subjects show a higher phase lead at high frequencies for conditions with feedback, compared to conditions without. Such phase lead corresponds to decreases in τ_v.

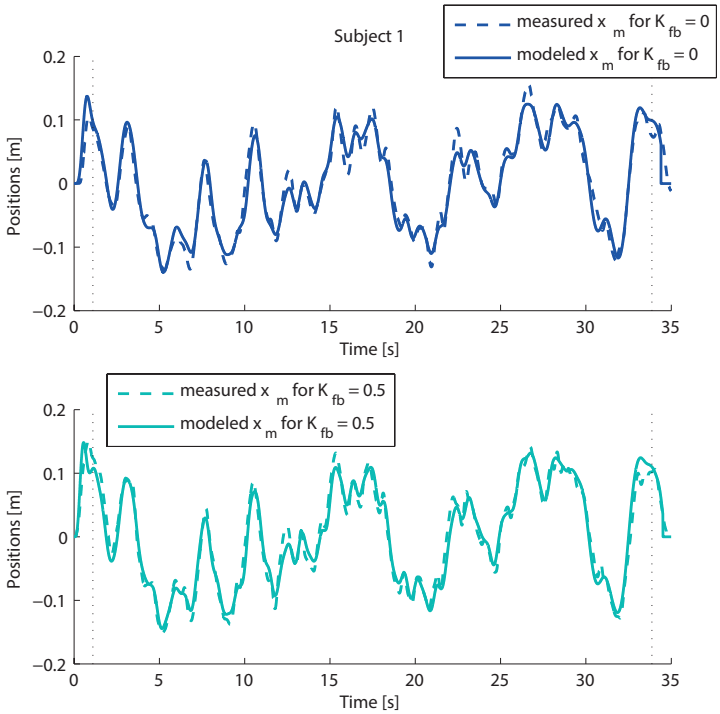

Figure 4.13: Measured (dashed line) and modeled (solid line) operator control input of a single repetition of two conditions for subject 1. Their high similarity illustrate the VAFs of typically >90%.

CHAPTER 5

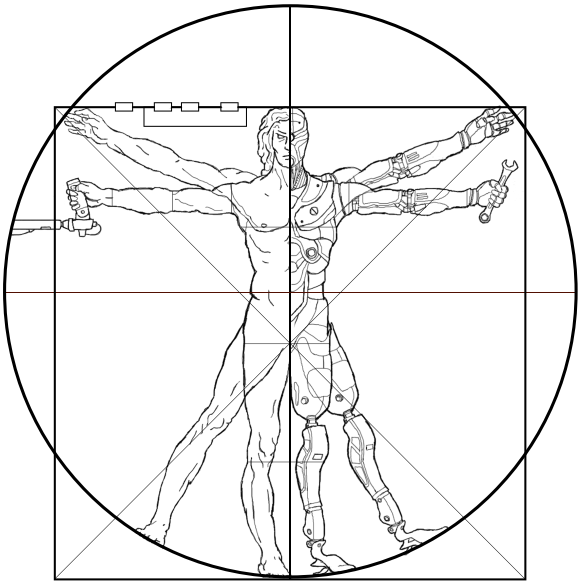

5

Reach Adaptation Applied to Telemanipulation: Does Haptic Feedback Bandwidth Affect Motor Learning?

Motor learning is a fundamental construct in human motor control. Yet, learning the dynamics of task and environment is affected by the dynamics op the telemanipulation system. Within this chapter a key experiment is performed with the goal to quantify the extent to which haptic feedback contributes to motor adaptation in the context of telemanipulation (i.e. generation of internal models). A well-known reach adaptation paradigm was adopted to assess the impact of haptic feedback bandwidth and slave dynamics on task execution. Fig. 5.1 shows a simplified control-theoretic representation of the experimental conditions.

This chapter was submitted for review to IEEE Transactions on Human-Machine Systems

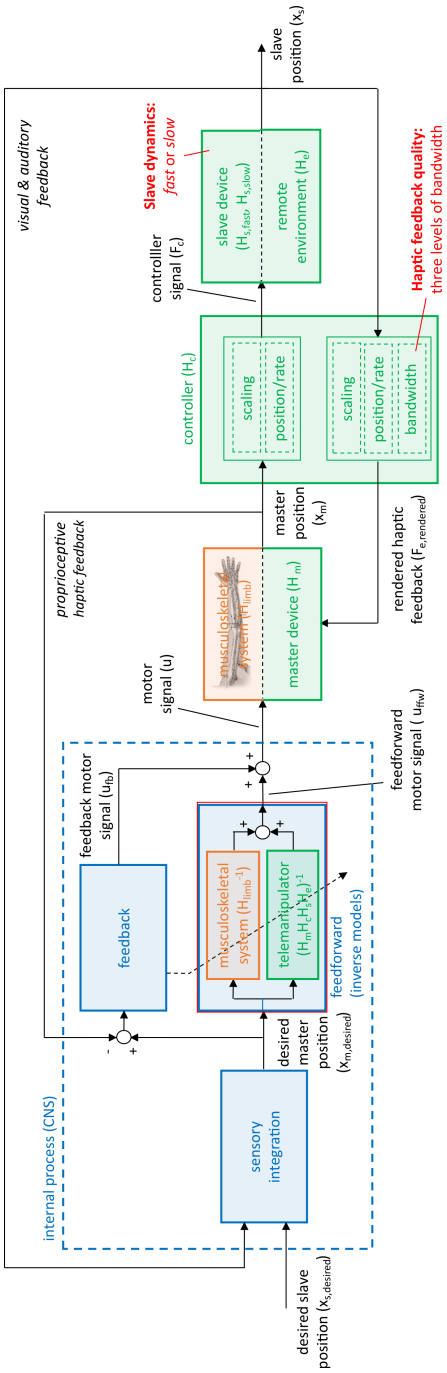

Figure 5.1: Simplified control-theoretic representation of the study as performed in this chapter. We modulated the bandwidth of the haptic feedback signal and the slave dynamics (shown in red) to determine effects on learning rates or learning outcomes. A widely-used reach adaptation experimental paradigm was adopted, in which subjects (implicitly) learn abstract force-curl dynamics, but now through the dynamics of the telemanipulation system.

ABSTRACT

Real-world telemanipulation tasks involve substantial variations in remote environment kinematics and dynamics, which require learning and generalization to handle. Whereas learning and generalization substantially benefit from haptic feedback, the requirements for haptic feedback to be effective are unknown. To determine these requirements, and to determine effects of haptic feedback on learning rates or learning outcomes, we applied a well-known reach adaptation paradigm from motor control literature to a telemanipulation scenario, in which subjects perform 2 DoF movements through a viscous curl force field. However, instead of applying the perturbations directly to the subject's hand, the perturbations were superimposed on the slave's workspace. Thus, subjects were to familiarize themselves with the dynamics of the slave system and, moreover, were to learn the dynamics of the curl field through the feedback dynamics of the telemanipulation device. We then modulated the haptic feedback bandwidth (by filtering the feedback dynamics with a 2 or 10 Hz cutoff 2nd order Butterworth filter, or unfiltered), and slave dynamics (either *fast* or *slow*, 8.5 and 2.1 Hz bandwidth, respectively). We hypothesized that the haptic feedback bandwidth should be at least higher than the bandwidth of the slave system, while feedback above the bandwidth of the human's voluntary control inputs is superfluous. The results show that during learning, motor adaptation to the curl field were similar to those reported in the literature when the field is applied directly to the hand instead of via the slave. Also the learning rate was not affected by slave dynamics or feedback bandwidth. Haptic feedback bandwidth affected generalization: 10 Hz or unfiltered feedback allowed for more accurate compensation of the curl field, but only for the *fast* dynamic system. We conclude that the quality of haptic feedback substantially improves an operator's ability to generalize beyond a set of pre-experienced motions, but only when the feedback bandwidth is higher than the slave system's cutoff frequency. Further increasing the bandwidth is not beneficial.

5.1. INTRODUCTION

Real-world telemanipulation tasks encompass substantial variations in kinematics and dynamics of the slave interacting with the remote environment. To deal with these variations, the human operator needs to learn and generalize the system's kinematics and dynamics. This process of learning a (transferable) mapping between the operator's input and the slave's output is also called sensorimotor learning. Haptic feedback is intrinsic to this process of sensorimotor learning (e.g., [65, 114, 136, 135]), but then the feedback must satisfy certain requirements. And whereas such requirements are instrumental in specifying design requirements of telemanipulation hardware and controllers, it is not well understood what these requirements on haptic feedback quality are.

Haptic feedback quality or 'haptic transparency' describes the fidelity with which force and positional information is sent from the remote environment to the human operator [79] [138]. When haptic feedback is truly transparent, the telemanipulation system reflects the contact forces of the slave with the remote environment one-to-one to the human operator, without any form of (electro-)mechanical distortion from the device and its controllers. High quality haptic feedback is beneficial to telemanipulated

task execution, as has been demonstrated for various tasks and manipulators. For example, feedback of the contact forces with a remote environment improves task execution in terms of task completion time [38] [55] [85], contact force [38] and errors [38] [55]. Furthermore, haptic feedback reduces control effort measured in terms of cognitive workload [129] and operator forces [55], compared to visual feedback alone. Typically, these studies are conducted in scenarios where subjects perform repetitive movements in short time envelopes. In practice however, tele-operated movements have similar but not identical kinematics and dynamics, and are actually learned over long periods of time; even operators with years of training still improve substantially [16].

Besides such task execution benefits measured on the output (i.e. slave or task) side of the telemanipulation system, several studies have argued that haptic feedback may also change the characteristics of the operator's input. For example, when operators were provided with haptic feedback during manual excitation of a sprung mass [62], point-to-point movements with a spanner [133], or visuo-manual control over a system with a priori unknown dynamics [56], their control changed in terms of the absolute amount or the frequency spectrum of the movements. Danion even reported that haptic feedback of the dynamics of the remotely controlled system affected the movement strategy used by subjects, as well as their subsequent performance [33]. These studies suggest that haptic feedback not only affects low-level coordination at an operational level, but also affects neuromuscular planning at the tactical and decision making at the strategical levels; haptic feedback fundamentally affects the way operators control a telemanipulation system.

Fundamental human motor control literature supports these findings; from this literature (e.g., [65] [114] [136] [135]) it is known that haptic feedback enhances the process of building 'mappings' between human input and a system's (i.e., the 'plant') response. For example, when learning to drive a (new) car, *"the magnitude of vehicle movement in response to the amount of wheel turn and accelerator depression varies across vehicles. Thus, the driver must learn the new mapping between his or her actions and the resulting vehicle movements."* [112]. Also, when controlling a one-dimensional mass on a spring, humans learn to control the kinematics of said object by forming an internal model that specifies the forces to be exerted by the hand [37]. Similarly, for telemanipulators, the operator must learn the mapping between his or her movements and the resulting slave response. Moreover, such a mapping should not simply record-and-repeat a movement, but the mapping should be 'transferable' to situations where kinematics and/or dynamics have changed.

In motor control terminology, these mappings of endogenous (e.g., one's musculoskeletal system) or exogenous dynamics (e.g., telemanipulation device or task dynamics) are called 'internal models', and the concept of transferring learning to situations with different kinematics (e.g., a different movements) or dynamics (e.g., a different controller or slave), is called 'generalization'. Hence, internal models describe the causal relations between our central nervous system's command and the plant's response, and include descriptions of the (endogenous) dynamics of our limbs, but also of the (exogenous) dynamics of master, slave and controller, and forces arising from the task that is performed. The internal models are formed and refined over time in a process known as 'sensorimotor adaptation'. This is what allows us to become more skilled at moving our

limbs, tools (e.g. a racket), but also devices that perform tasks like in telemanipulation.

Now in telemanipulation, the process of building the mapping is affected by the feedback dynamics of the slave system, which can, to some extent, be (re)engineered (i.e., the haptic feedback quality). But with respect to which requirements? While the haptic feedback quality may substantially affect gradual or long-term (i.e., days, weeks or even years) task performance, the subject has not been (quantitatively) studied.

The objective of this study is to determine the effects of haptic feedback quality on sensorimotor adaptation rates or outcomes in telemanipulation. We defined the bandwidth of the haptic feedback as the metric for haptic feedback quality, and hypothesize that, in order for the operator to reasonably estimate the system's high-frequency characteristics, the haptic feedback bandwidth should be at least higher than the bandwidth of the slave system, but feedback above the bandwidth of the human's voluntary control inputs would be superfluous. Hence, above this frequency, no differences in motor adaptation characteristics are expected to occur. Specifically, for a slave system with a bandwidth of 8.5 Hz, any haptic feedback bandwidth over 8.5 Hz does not yield any motor adaptation benefits. Similarly, for a slave system with a bandwidth of 2.1 Hz, any haptic feedback bandwidth over approx. 2.1 Hz will yields no differences in motor adaptation.

Motor adaptation is typically studied in well-established reach adaptation paradigms, in which subjects perform straight planar reaching movements, while being perturbed by an a-priori unknown artificial force field (e.g., [65, 112, 114, 136]). Over time subjects learn to adapt to the force field's characteristics, after which subjects are to transfer their learning to a kinematically dissimilar movement (the generalization). In these traditional sensorimotor adaptation experiments the subject's hand grasps a haptic device that directly controls the output and the perturbation or force field is applied directly to the subject's hand. We adopted and modified this approach, instead superimposing the force field on the slave's workspace. Thus, subjects were to familiarize themselves with the dynamics of the slave system and were to learn the dynamics of the force field, both through the feedback dynamics of the telemanipulation device.

We previously applied this sensorimotor adaptation paradigm to a telemanipulation task [134], and found that an operator's ability to learn and generalize beyond a set of pre-experienced motions increased when the quality of the haptic information was (close to) natural. Quantitative conclusions on the effect of haptic feedback could not be drawn, and specific requirements for haptic feedback could not be defined, as the number of subjects was limited and inhomogeneous device dynamics resulted in a high variance of the experimental data. For the current study we decided to work with a virtual slave system, such that homogeneity of device dynamics and experimental conditions (i.e. haptic feedback quality and slave dynamics) could more easily be controlled.

5.2. MATERIALS & METHODS

We adapted a well-known reach adaptation paradigm (e.g., [47] [60]) from the motor control literature to a telemanipulated reaching task: subjects performed 2 DoF reaching movements with a simulated slave (with either *slow* or *fast* dynamics) in a viscous curl force field under three haptic feedback bandwidths (for which we filtered the master's feedback dynamics). In Stage I of the experiment, subjects familiarized themselves with

the dynamics of the task and manipulator, in Stage II and III subjects were required to adapt to a viscous curl force field, and finally, in Stage IV subjects were to generalize their movement to a different direction.

5.2.1. SUBJECTS

Seventy-eight healthy, aged between 21 and 43 years, all affiliated with the Delft University of Technology were recruited. Subjects required to be right-handed, and between 1m70 and 1m90 of length, to minimize joint angle variations. The participants had no or limited experience with robotic systems. All subjects gave informed consent and the study was approved by the Delft Human Research Ethics Committee.

5.2.2. APPARATUS

The experiments were performed on the 3 degree-of-freedom admittance-controlled FCS Moog HapticMASTER with a simulated slave device. The device has a position resolution of <12e-6 m, a stiffness of >10000 N/m and a force sensitivity of 0.01 N [82]. It was constrained to only enable movements in a horizontal plane (Fig. 5.2). The virtual inertia, damping and Coulomb friction of the device were set at J_m = 2 kg, B_m = 0 Ns/m and $F_{Coulomb}$ = 0.001 N, respectively. The device was controlled with a VxWorks RT operating system running at 2048 Hz. Servo-gains were hand tuned to provide unity frequency response functions, which resulted in proportional, derivative and acceleration gains of [400, 2, 0.003] and [400, 2, 0.005] for the r- (arm in/out) and ϕ-axis (base rotation), respectively.

The slave system, designed in Matlab Simulink, was simulated on an additional real-time controller by Bachmann GmbH. This industrial controller runs at 1000 Hz and logs position and force at the same frequency. The visualization was updated at a rate of 30 Hz.

5.2.3. EXPERIMENTAL DESIGN

TASK DESCRIPTION

Subjects performed 10 cm long reach adaptation tasks with a virtual slave system by controlling a 2 DoF mechanical master device. Subjects either moved from starting point A to target box B, or from starting point C to target box D. The movement A-B was performed in the sagittal plane, i.e. straight ahead right in front of the subject, whereas the movement C-D has a 45 degree angle with respect to the sagittal plane. A, B, C and D were respectively located at (x, y) = (0, 0cm), (0, 10cm), (2.59, -0.69cm) and (7.59cm, 7.97cm). A marker on the floor positioned the subjects, who were standing. As such, the elbow angle approximated 90 degrees for both A-B and C-B movements, whereas for the shoulder there was a difference of approximately 45 degrees in the transverse plane between the two movements. To minimize passive and active dynamic effects from the FCS Moog HapticMASTER, we mirrored movements A-B and C-D around the r-axis of the device (arm in/out). The slave cursor as controlled by the subjects was displayed as a 1 mm diameter blue open circle. Atarting points (A & C) were displayed as 2 mm diameter black open circles, whereas targets (B & D) were described by boxes with 5mm ribs (in red). The scene was shown from the top view perspective on a monitor located right in front of the subject (see Fig. 5.2). Thus subjects were to (implicitly) make the

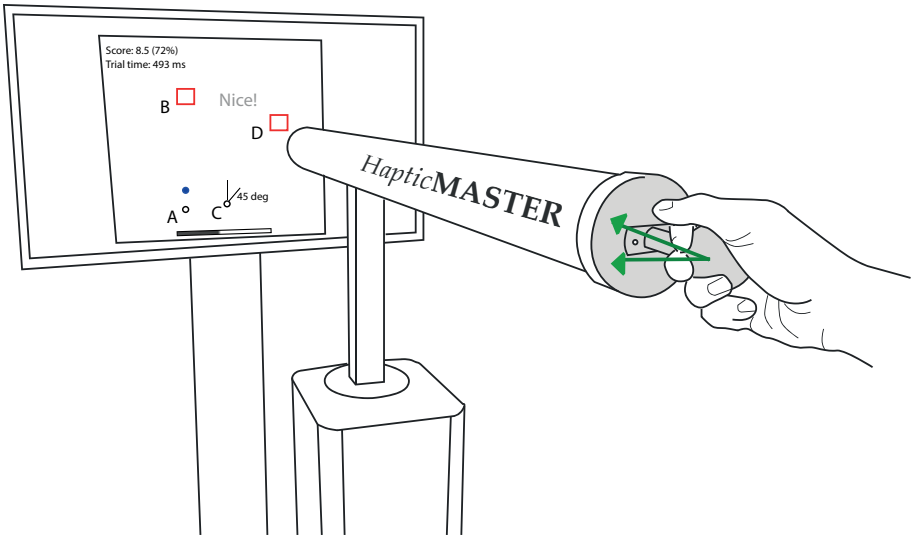

Figure 5.2: Experimental setup showing the (physical) master device and virtual slave system (the blue open circle on the screen). Subjects made reaching movements in 500±50 ms from A to B, or from C to D, by moving the master device in the horizontal plane (in green). Only a single trajectory was shown at a time. After each trial, feedback of the performance was provided ('Nice!', 'Too fast',...), and the subject was guided back to the starting point. Additionally, trial time and a performance indication were shown in the top left, and a progress bar on the bottom.

transformation between manual and visual workspaces.

Subjects were exposed to an artificial viscous curl force field (F_{curl})on the slave side. This field produces forces of which the amplitude is proportional to the velocity, while its orientation is perpendicular to the movement. This can be expressed mathematically by $F_{curl} = Bx'$:

$$\begin{bmatrix} F_{curl,x} \\ F_{curl,y} \end{bmatrix} = \begin{bmatrix} 0 & -26 \\ 26 & 0 \end{bmatrix} \begin{bmatrix} x'_x \\ x'_y \end{bmatrix} \tag{5.1}$$

TASK INSTRUCTION

Subjects were instructed to move the cursor after a visual prompting signal ("Go" and color coding of the screen) from the blue starting points to the red targets in 500±50 ms. It was advised to move from start to end in one smooth movement, explaining that moving too fast may lead to overshoot, and correcting for this overshoot is time-costly. After reaching the target, subjects were given feedback on their performance. The task-completion-time was shown, and additionally, for reaching movements between 450 and 550 ms, subjects were given the visual feedback "Nice!". For movements between <450, "Too fast." was shown, for movements >600 ms "It took too long.". After finishing the task, the device's controller automatically moved the handle to the next starting point.

EXPERIMENTAL CONDITIONS

The two independent variables were *haptic feedback bandwidth* (master feedback bandwidth $H_{m,F}$ filtered with a 2 or 10 Hz cutoff second-order Butterworth filter H_{FBfilt}, or unfiltered) and simulated *slave dynamics* H_s (either fast or slow). Each subject performed the experiment with a single haptic feedback bandwidth and a single slave dynamics (i.e., between-group design).

The *slave dynamics* H_s were emulated by a simulated second-order mass-damper, of which is characteristics were chosen with respect to the frequency range of the operator's voluntary control inputs. The human's neuromuscular system only allows for precision movements up to approximately 1 Hz, with voluntary inputs up to several Hertz (up to 6-8 Hz for skilled professionals like pilots [130]). As such, the dynamics of the *fast* and *slow* dynamic systems were chosen to have a cutoff frequency - the point at which the output of the system drops -3 dB relative to the nominal value - of f_c = ~8.5 Hz and f_c = ~2.1 Hz, respectively. Hence the *fast* dynamic system predominantly appears to the human operator as a gain, whereas the *slow* dynamic system appears as a second-order system (a mass-damper) above its cutoff frequency, substantially affecting closed-loop human-machine performance. The transfer function of the second-order slave system together with its position servo actuator is given by:

$$H_s(s) = \frac{x_s(s)}{x_m(s)} = \frac{k_{d,s}s + k_{p,s}}{J_s s^2 + (B_s + k_{d,s})s + k_{p,s}} \tag{5.2}$$

Here x_m and x_s represent master and (virtual) slave position, respectively. Slave inertia J_s and damping B_s were set at 1 kg and 1 Ns/m for both the *fast* and the *slow* system. The systems were tuned to be critically damped. As such, proportional gain $k_{p,s}$ and derivative gain $k_{d,s}$ were set at 490 [-] and 43 [-], respectively, for the *fast* and 37 [-] and 11 [-] for the *slow* dynamic system. Fig. 5.3 shows a bode plot and step response for the two different slave dynamics.

Independent variable *haptic feedback bandwidth* was chosen relative to the two slave systems and the human operator dynamics:

- 2 Hz, as it is around the bandwidth of the *slow* slave system and below the human operator cutoff frequency,
- 10 Hz, as it is above the bandwidth of the *slow* slave system, around the bandwidth of the *fast* slave system and above the bandwidth of the human operator dynamics,
- unfiltered, which approximates 20 Hz due to device limitations, as it is above the bandwidth of the *fast* slave system.

These haptic feedback bandwidths were operationalized by filtering the outputs of both the slave-to-master feedback controller $F_{fb,sm}$ and the curl field F_{curl} with second-order Butterworth filters with cutoff frequencies of 2 Hz, 10 Hz and no filtering (H_{FBfilt}, see Fig. 5.4A). Hence, as the two forces are superimposed, the total force presented to the operator equals:

$$f_{fb}(s) = H_{FBfilt}\big(f_{fb,sm}(s) + f_{curl}(s)\big) \tag{5.3}$$

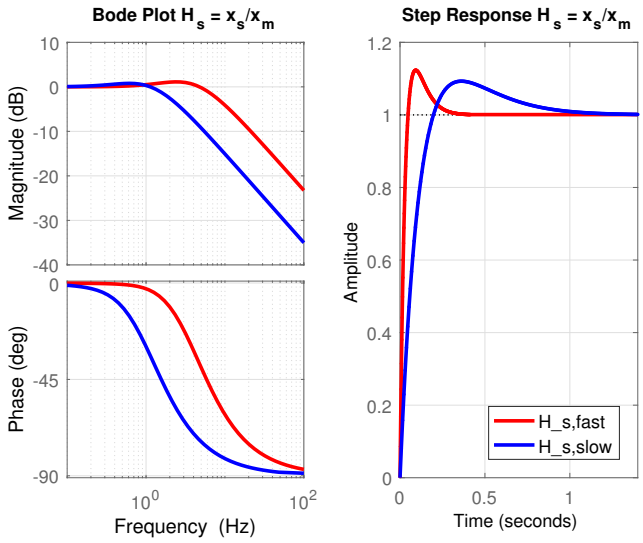

Figure 5.3: Bode plot and step response of the slave system and its controller (open-loop), modeled as mass-spring-damper. The *slow* slave system ($H_{s,slow}$) has a bandwidth of ~2.1 Hz, whereas the *fast* slave system's ($H_{s,fast}$) bandwidth is ~8.5 Hz.

A position servo was applied as a slave-to-master feedback controller to feedback the dynamics of the slave:

$$F_{fb,sm}(t) = \big(x_s(t) - x_m(t)\big)k_{p,m} + \big(\dot{x}_s(t) - \dot{x}_m(t)\big)k_{d,m} \tag{5.4}$$

Proportional $k_{p,m}$ and derivative $k_{d,m}$ gains were chosen such that the magnitude of the forces generated by the serve $F_{fb,sm}$ approximated the forces generated by the curl field F_{curl} (which is approx. 7-11 N). Hence, $k_{p,m}$ and $k_{d,m}$ were chosen at 1400 [-] and 140 [-] for the *fast* system, respectively, and 270 [-] and 27 [-] for the *slow* system, respectively. Theoretically, working with a virtual master inertia of 2 kg and no damping, this gives a bandwidth for $F_{fb,sm}$ of approximately 81 Hz. However, in practice, this bandwidth is limited by (electro-)mechanical limitations and dynamics of the HapticMASTER (hence the choice for $k_{p,m}$ and $k_{d,m}$ is rather arbitrary). The same holds for the bandwidth of the forces generated by F_{curl}: it is the master dynamics and not the Nyquist frequency (i.e., 500 Hz) that describes the achievable bandwidth. Therefore, we estimated the master's force frequency response function ($H_{m,F}$, see Fig. 5.4B): in both the r- and ϕ-axis of the HapticMaster the bandwidth of the frequency response approximates 20 Hz. The net result or effective haptic feedback frequency response function H_{FB} ($= H_{FBfilt}H_{m,F}$), is shown in Fig. 5.4C. Notice that instead of an ideal linear second-order system (i.e., as depicted in Fig. 5.4A) the estimated and effective frequency responses ($H_{m,F}$ and H_{FB}) show non-linear effects, as the responses dip below 0 dB before the filter cutoff frequency, while simultaneously showing underdamped behavior near the cutoff frequency.

EXPERIMENTAL PROTOCOL

Before commencing the experiment, each subject was quasi-randomly assigned to a haptic feedback and slave dynamics condition. Subjects were presented with written instruction, as annexed to the informed consent form. After this, subjects were given a couple of minutes to explore the setup by moving the device as they wished. The actual experiment was was divided into four stages. In Stage I, the 'familiarization' stage, subjects performed thirty-six reaching movements in randomized order to both targets, without the curl field. This allowed subjects to get familiar with the manipulator dynamics, the camera view and the experimental protocol. In Phase II and III, the 'learning' stages, subjects performed two times 72 movements from starting point A to target B, but now under the effect of a viscous curl force field. Finally, in Phase IV, the 'generalization' stage, subjects moved ten times from C to D. In between the stages the subjects had a one-minute break to relax their arms. From introduction to debriefing, the experiment lasted about 15 to 20 min.

Table 5.1: Experimental protocol. Each subject was quasi-randomly assigned to a haptic feedback and slave dynamics condition, and presented with written instruction. Subsequently, each subject was lead through four stages, in which subjects familiarized themselves with manipulator and task (Stage I), learned the dynamic of the force-curl field (Stages II and III), and generalized their learning (Stage IV). In order to measure how accurate subjects performed their movements, quasi-randomized force-clamp trials were performed.

	Stage I: Familiarization	***Stage II: Learning***	***Stage III: Learning***	***Stage IV: Generalization***
# repetitions	36	72	72	10
movement	A-B & C-D	A-B	A-B	C-D
force-curl field	disabled	enabled	enabled	disabled
# error-clamp trials	4	8	8	10

At set trial numbers in each of the Stages, the robot produced a channel that artificially eliminated movement errors. These so-called 'error-clamp' trials, enabled the measurement of the forces subjects produced perpendicular to the direction of movement, which are indicative of changes in the subjects' motor output. For Stage I, these trials were number 20, 26, 30 and 35. For Stages II and III, these were trials 4, 16, 28, 39, 50, 58, 65 and 70. For Stage IV, all trials were error-clamp trials. Subjects were not informed of these error-clamps. Tab. 5.1 provides an overview of the settings per stage.

5.2.4. METRICS & DATA ANALYSIS

The quality of generalization is expressed by the forces during error-clamp trials (Stage IV, trial 1); higher error-clamp forces indicate a more accurate representation of the force-curl dynamics by the internal model. Error-clamp forces are normalized by the peak ideal force needed to compensate for the full strength curl field during late adaptation, in accordance to [60], as such reducing inter-subject variability. Hence, we multiplied the slave velocity during Stage III trials 65 and 70 (i.e., 'late adaptation') with the force-curl field (Eq. 5.1), and used the max. to normalize the error-clamp forces. In addition, to illustrate the learning behavior, the lateral deviation from the ideal path (i.e. a straight line from starting point to target) is measured.

The experiment had a between-group design; each subject performed the experiment with a single force feeedback bandwidth and a single slave dynamics. Hence six groups of thirteen subjects (n=13). Comparison of experimental conditions was made on the basis of populations, assuming a normal distribution and variance homoscedasticity. A one-way analysis of variance (ANOVA) was performed on the data. p-values of 0.05 or below are deemed significant (α = 0.05). Results for the *fast* and *slow* dynamic system are presented independently.

Table 5.2: Mean (μ) and standard deviation (σ) of the normalized error-clamp forces in the generalisation stage (Force [% perturbation]), for each of the experimental conditions. The metrics are calculated from a population of 13 subjects per condition (n=13), totaling 78 subjects.

	μ (σ) **for 2 Hz FFB**	μ (σ) **for 10 Hz FFB**	μ (σ) **for no FFB filter**
Fast: F [% pert.]	39.8 (7.1)	64.5 (11.9)	59.1 (15.4)
Slow: F [% pert.]	55.3 (14.2)	54.8 (14.5)	49.8 (8.2)

5.3. RESULTS

Fig. 5.5 and Fig. 5.6 show the across subject mean of the lateral deviation (top figures) and the forces during error-clamp trials (bottom figures) for the *fast* and the *slow* system, respectively.

In Stage I, the lateral deviation decreases over trials as subjects familiarize themselves with task and device for both the *fast* and the *slow* system. Also, the lateral deviation in Stage I shows a relatively high variation, illustrating the exploratory behavior. The force during error-clamp trials is around 30% of the peak ideal force to compensate for the full strength force field (no force-curl is present during Stage I). This force is caused by motor noise, as well as subject-specific preferences to slightly deviate from a straight line between start- and endpoint. Obviously, during error-clamp trials the lateral deviation is negligible, as the clamp restrains lateral movement.

In Stage II, the force-curl is introduced. This initially results in lateral errors of several centimeters for both the *fast* and the *slow* slave system. Over trials this error decreases to several millimeters. A similar pattern is seen for the error-clamp forces. At first the clamp forces are between 40 and 80%, while during late Stage II, the forces are between 80 and 120%. This task execution continues in Stage III; during Stage III, both the lateral deviation and error-clamp force are relatively stable, sitting between approx. 3-8 millimeters and 80-120%, respectively.

Finally, in Stage IV, subjects only perform error-clamp trials in a kinematically dissimilar scenario compared to Stage I-III, to measure their ability to generalized the force-curl dynamics. Initially, this results in error-clamp forces of 40 to 70%, while error-clamp forces slowly return to baseline (Stage I). This pattern is seen for both the *fast* (Fig. 5.5) and the *slow* (Fig. 5.6) slave system.

The mean (μ) and standard deviation (σ) of the main metric, the normalized error-clamp forces, are shown in Tab. 5.2. Fig. 5.7 shows the population and subject means of these

error-clamp forces expressed as a percentage of the perturbation forces during late adaptation (i.e. final clamp trials of Stage III).

For the *fast* slave system, the mean error-clamp force was 39.8, 64.5 and 59.1% for haptic feedback with 2 Hz, 10 Hz or unfiltered haptic feedback bandwidth, respectively. The error-clamp force is affected by haptic feedback bandwidth for the *fast* dynamic system (p=0.017, F=4.5): 10 Hz filtered or unfiltered feedback yield approximately 50% higher error-clamp forces compared to 2 Hz filtered feedback (p=0.002, F=12.2 and p=0.034, F=5.0, respectively. There is no difference between 10 Hz filtered and unfiltered feedback (p=0.60, F=0.3).

The *slow* slave system yielded mean error-clamp forces of 55.3, 54.8 and 49.9% for haptic feedback with 2 Hz, 10 Hz or unfiltered haptic feedback bandwidth, respectively. No differences between haptic feedback conditions were observed (p=0.8, F=0.2).

5.4. DISCUSSION

Real-world telemanipulated tasks encompass substantial variations in kinematics and dynamics. Effective learning and generalization of these variations implies certain requirements on the haptic feedback, and therefore affects design requirements of telemanipulation hardware and controllers. In this study we quantified the effect of haptic feedback bandwidth on an operator's ability to learn and generalize kinematics and dynamics in a telemanipulation scenario. We expected that the required minimal haptic feedback bandwidth to allow optimal generalization of learning would be dependent on the bandwidth of the slave system. Therefore, we manipulated the haptic feedback bandwidth (three cutoff frequencies: 2 Hz, 10 Hz, no filter) for a system with *fast* and a *slow* dynamics (i.e., bandwidths of approx. 8,5 and 2.1 Hz, respectively). Specifically, we hypothesized that when the haptic feedback bandwidth is at least higher than the bandwidth of the slave system, no differences in motor adaptation characteristics occur.

For the *slow* dynamic system, haptic feedback bandwidth did not impact generalization of learning: the forces in the error clamp trials during generalization showed no differences between the three haptic feedback bandwidths (with mean error clamp forces of approximately 55%, 55% and 50% for the 2 or 10 Hz filtered, and unfiltered haptic feedback condition, respectively). Apparently, for the *slow* system, a bandwidth of approx. 2 Hz or higher suffices for operators to accurately adapt to the perturbation forces.

On the other hand, the *fast* dynamic system showed significant differences between haptic feedback conditions; the error clamp forces during generalization in the 2 Hz filtered haptic feedback conditions were approximately 40% of the forces during late adaptation, which was significantly lower than the error clamp forces generated during the 10 Hz filtered and unfiltered haptic feedback (64% and 59%, respectively). Apparently, a low haptic feedback bandwidth substantially reduces the operator's ability to generalize their learning compared to higher bandwidth feedback conditions, at least for fast dynamic systems. Furthermore, error clamp forces during the 10 Hz filtered haptic feedback and the unfiltered feedback were not significantly different. This suggest that the haptic feedback bandwidth should be at least higher than the cutoff frequency of the slave system (8.5 Hz), as hypothesized.

REACH ADAPTATION IN TELEMANIPULATION

To the best of our knowledge this is the first study to apply the widely used reach adaptation paradigm from neuroscience to bilateral telemanipulation. The specific variation of the paradigm we applied was derived from the paradigm of Haswell et al. [60] and Izawa et al. [66]. It is similar to the first description of reach adaptation studies that date from 1994 by Shadmehr and Mussa-Ivaldi [114]. Here, subjects made movements in a viscous curl force field, starting from the center of a circle to eight targets which were homogeneously distributed around the starting point. Variations on the original paradigm include movements to a multitude of targets (e.g. [97]) and different amplitudes or proportions of the components of the force field (e.g. [91]). In essence however, all reach adaptation paradigms follow the same principle: subjects familiarize themselves with setup and task, learn to adapt to the force field and then generalize their learning to another part of the workspace. The Haswell paradigm constitutes a relatively simpler learning stage, as learning is performed in a single direction instead of multiple. This was deemed sufficient to validate our experimental hypothesis.

The general results of the learning paradigm applied to limb movements show a high level of similarity for each of the learning stages with our observed results during telemanipulated reaching tasks. During familiarization, subjects get acquainted with the dynamics of task and manipulator, the type of visual and haptic feedback and the experimental procedure. Typically, the behavior converges over the first 20 trials, after which moderate exploratory behavior is observed, just as in this study. In the learning stage, subjects initially show a high lateral deviation due to the sudden introduction of the force-curl. This deviation converges quickly over approx. 10 trials, and then gradually decreases to a steady-state deviation of approximately 5 mm in the studies of Haswell et al. [60] and Izawa et al. [66]. In our telemanipulated learning scenario we see similar behavior, with rapid convergence over the first 10 trials and a steady-state lateral error (measured at the slave side) of approx. 5 mm. Finally, for the generalization stage, the magnitude observed error clamp forces lie in the range of those reported by Haswell and Izawa (35% and 43%, respectively). Compensation forces during generalization in our study are slightly larger, with 40 and 60% for the *fast* slave and 50 and 55% *slow* slave, compared to the compensation forces during learning. This relative increase can be accounted to the the design of our curl field forces; these were substantially higher with an absolute value of 26 Ns/m in our study, compared to 10-13 Ns/m as typically used (e.g. [47] [66] [97] [114]).

IMPLICATIONS

The error-clamp forces are a measure for the representation of the force-curl dynamics by the internal model; higher error-clamp forces indicate a more accurate representation. In fact, if an operator would have perfectly learned the curl field and manipulator dynamics, the error-clamp trials in Phase II and III would show an exact inverse of these dynamics (given the subject moves feedforward without sensorimotor noise). Phase IV shows how well the learning is 'transferable' or 'generalizable' to a kinematically dissimilar movement, and, as such, describes the quality of the internal model learned by the human operator, which, in this case, constitutes of models of slave manipulator and curl field. Such internal models lie at the basis of well executed tasks; high quality internal

models are essential for accurate feedforward (i.e. predictive) control, a characteristic of skilled (tele)manipulation [65] [135]. Over the course of the experimental trials the operator develops the internal model, thereby increasing the contribution of feedforward control while simultaneously reducing the feedback contribution [97]. Eventually, the operator can generate sensorimotor commands which predict exogenous dynamics, like those from a curl field or a telemanipulator.

This study shows that the quality of the internal model is affected by the haptic feedback quality, but only for haptic feedback bandwidths up to several Hz higher than the slave system's dynamics. This finding, that haptic feedback impacts motor adaptation tasks, is different from findings from other studies, which generally state that haptic feedback does not affect tasks without contact. For example, Hannaford et al. [55] report no difference in task execution time for feedback and no-feedback conditions. Other studies for tasks without environmental contact even suggest that haptic feedback may negatively affect task performance (e.g. [61] [133]). Essentially, the motor adaptation paradigm we used in the current study magnifies the effects that occur when an operator controls an object with new dynamics, both when operators first internalize the new dynamics, and more importantly, when movements are made that require a high quality representation of the dynamics by means of the internal model. This is in contrast to studies that measure task performance with subjects performing repetitive movements in short time envelopes, effectively taking place in the saturation part of the learning curve. Besides magnification of learning effects, using an abstraction of dynamics rather than real world dynamics allows for an unprecedented interaction for the subject. Hence, sensorimotor learning behaviour can be studied cleanly, with minimal influences from confounding factors like individual training or experience.

Apparently, haptic feedback quality has an important, previously overlooked effect on motor adaptation. How this, in turn, quantitatively impacts task performance should be further investigated. Perhaps haptic feedback of sufficient quality can speed up the typically long learning curves encountered in telemanipulation. For example, an operator with 2 months of experience shows a 50% increase in task execution times compared to operators with 12 or 33 months of experience [16]. Also, crane drivers (who do not receive haptic feedback from the crane or manipulated load) typically require hundreds of hours of training before being considered 'experts' [67]. Could training with the right haptic feedback bandwidth speed this up?

LIMITATIONS

There is more to sensorimotor learning than solely motor adaptation - the topic of this study. Learning skilled behavior also includes gathering task-relevant sensory information, decision making and selection of strategies [135]. How haptic feedback affects such processes is only marginally understood. Interesting in this context is the work of Danion et al. [33], who found that movement strategy and subsequent performance during training of an under-actuated object is affected by haptic feedback. With haptic feedback, subjects adopted a strategy involving control of the object's degrees of freedom and fast hand movements. In contrast, without haptic feedback subjects locked the degrees of freedom and never attempted another, more efficient strategy.

Although the reach adaptation paradigm is widely used and well-established, initially we found difficulty to reproduce basic learning and generalization patterns with our own equipment and limited experience in motor learning experiments. During replication, we found that whilst some experimental variables are well described (e.g., movements, force field parameters), other experimental design choices were not well motivated (e.g., passive device dynamics, force clamp design, precise instruction on task execution). This complicated finding the right combination of experimental design choices for our experimental setup, which has different advantages and limitations in hardware and software compared to literature. In particular, the polar kinematic configuration of the Haptic Master we used suffered from parasitic dynamics, which affected the subject's movement. To create more homogeneous dynamics, we mirrored the learning and generalization movement around the radial axis of the device. This substantially reduced the effect of parasitic dynamics, and therefore variation unrelated to the experimental conditions. Still, our results show relatively more variation when compared to similar studies (e.g. [60]). This may partly be explained by less strict constraints in limb positioning (i.e., arm angles) and unrestrained wrist movement (which a cuff could have avoided [97]).

We defined haptic feedback bandwidth as a single parameter with linear properties. In practice, the effective realized bandwidth is affected by, among others: friction, play, dynamic coupling, structural dynamics, and dynamic behavior of actuators and controllers. This results in non-linear behavior, also present in the frequency response function of the haptic feedback as shown in Fig. 5.4C. Instead of an ideal second-order system (5.4A) the realized transfer function dips below 0 dB before the filter cutoff frequency, while simultaneously showing underdamped behavior near the cutoff frequency. Hence, the absolute values of the experimental conditions should be viewed in approximation. Also, it is important to realize that the absolute value of the optimal feedback bandwidth depends not only on the mechanical slave dynamics of the slave, but also on the master dynamics and controller properties, as these all substantially have an impact on the effective realized frequency response.

CATERING TOWARDS THE HUMAN OPERATOR

Despite many decades of research, real-world telemanipulated task execution is characterized by long task completion times, errors and a high mental workload, compared to hands-on task execution. In the literature two avenues of research aim to improve this. First, high-quality haptic feedback is being pursued, which requires high-bandwidth ripple-free actuators, high-stiffness low-inertia mechanics, joints and transmissions with negligible play and friction, high-bandwidth low-delay controllers and high-resolution low-noise sensors (e.g., [21] [33] [52]).

An alternative approach to improve task execution is by the addition of virtual feedback information, either visually (e.g., augmented reality [11]) or haptically (e.g., event-based haptic feedback [76], virtual fixtures [107], or haptic shared control [15]). Regardless which approach is adopted, engineering haptic feedback quality beyond human sensorimotor capabilities is superfluous and will not lead to task execution improvements [28] [133].

We therefore argue to base design guidelines for haptic feedback quality on quanti-

fied human operator characteristics. Previously, Daniel and McAree [32] observed that a natural partitioning exists between information and energy in haptics: information is conveyed at frequencies above roughly 30 Hz, while the energetic interaction between the slave and the environment takes place below roughly 30 Hz. Our study suggests that even for free-air task components, where the slave does not touch a remote environment, critical information about slave dynamics is conveyed at frequencies well below 30 Hz (2 and 8 Hz in this study, dependent on cutoff frequency of the slave system). For tasks components where the slave is in contact with a real environment, we agree with researchers like Kuchenbecker and Pacchierotti (e.g., [76, 99]) that the *notion* of contact is important, rather than the absolute dynamics of the interaction. Notable exceptions for this guideline include expert tasks like tissue palpation, where absolute perception of stiffness is critical [92].

Hence, we would suggest to design the telemanipulation system such that relatively low-frequent bilateral haptic feedback suffices the motor learning requirements, whilst this feedback is enriched with high-frequent vibrations (e.g., event-based haptic feedback [76] [99]) to emulate high-frequency forces like contact (up hundreds of Hz), or slip (~30 Hz) [21].

As such, we hope that our findings contribute to establishing design guidelines for haptic feedback in telemanipulation; the desired haptic feedback bandwidth does not only depend on the dynamics of the physical interaction with the remote environment, but also on the dynamics during unconstrained (i.e. free-space) motions. These motor learning requirements influence low-frequent device bandwidth requirements, and when combined with high-frequent information, we believe that this creates a design philosophy for haptic feedback that is truly catered towards human operator characteristics.

5.5. CONCLUSION

To determine requirements of haptic feedback bandwidth for motor learning, we applied a well-known reach adaptation paradigm from motor control literature to a telemanipulation scenario; human subjects used a 2 DoF haptic master device to control a simulated slave system perturbed by a viscous curl force field. This allowed us to quantify the extent to which haptic feedback bandwidth affects motor learning and generalization for different slave dynamics, namely either *fast* or *slow*. We provided subjects with three different levels of haptic feedback from the slave dynamics: 2 Hz filtered haptic feedback, 10 Hz filtered feedback and unfiltered haptic feedback. For the experimental conditions studied we conclude that:

- Subjects learned to adapt to the curl force field acting on the simulated slave similarly as to literature describing motor adaptations with perturbations directly to the subject's hand, and independently of slave dynamics or haptic feedback bandwidth.
- When generalizing with a *fast* dynamic systems, high-quality haptic feedback allows for more accurate compensation of the perturbation forces; 10 Hz filtered haptic feedback or unfiltered haptic feedback improves the mean generalization forces over 2 Hz filtered feedback.

- When generalizing with a *slow* dynamic system, low-frequent, 2 Hz filtered haptic feedback suffices to accurately control the slave system, as we observed no differences between haptic feedback conditions.

We conclude that the quality of haptic feedback, operationalized as its bandwidth, substantially improves an operator's ability to generalize beyond a set of pre-experienced motions (i.e. generalization). The haptic feedback bandwidth should be at least higher than the slave system's cutoff frequency, but further increasing the bandwidth does not benefit generalization. These findings contribute to design guidelines for telemanipulators; the desired haptic feedback bandwidth may not only depend on the dynamics of this slave, but also on the task dynamics during unconstrained motions. And depending on the task at hand, motor learning requirements may be more stringent that requirements derived from the task, and may, as such, drive overall device bandwidth requirements.

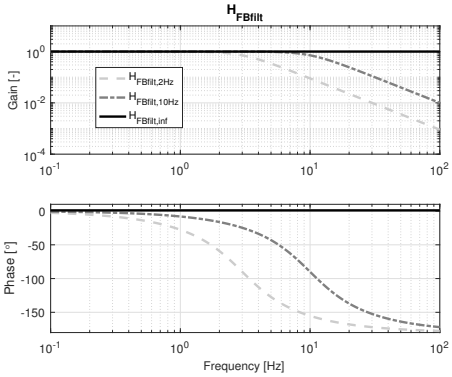

A. Haptic feedback filters

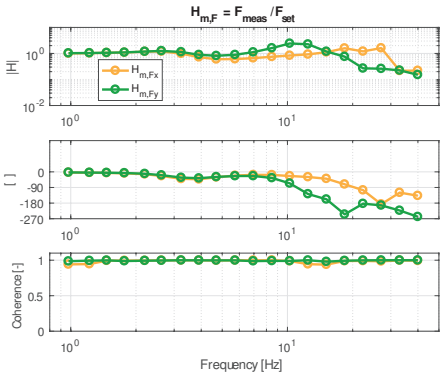

B. Estimated master force frequency response function

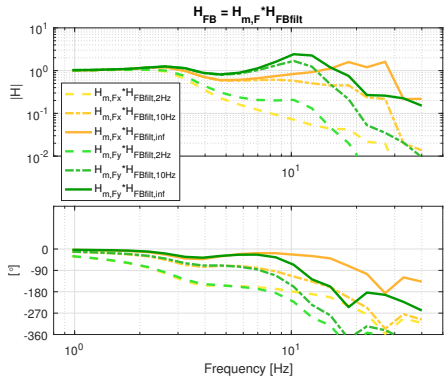

C. Effective haptic feedback frequency response function

Figure 5.4: A. Bode plots of the filters used to realize different bandwidths of haptic feedback (H_{FBfilt}). B. Estimated Haptic master force frequency response functions ($H_{m,F}$, n=4). C. The effective haptic feedback frequency response functions as displayed to the human operator ($H_{FB} = H_{FBfilt} H_{m,F}$). The effective or realized frequency response function is affected by non-linear effects such as structural dynamics and dynamic behavior of actuators and controllers. Instead of an ideal second-order system (5.4A) the realized transfer function dips below 0 dB before the filter cutoff frequency, while simultaneously showing underdamped behavior near the cutoff frequency. Therefore, the absolute values of the experimental conditions should be viewed in approximation.

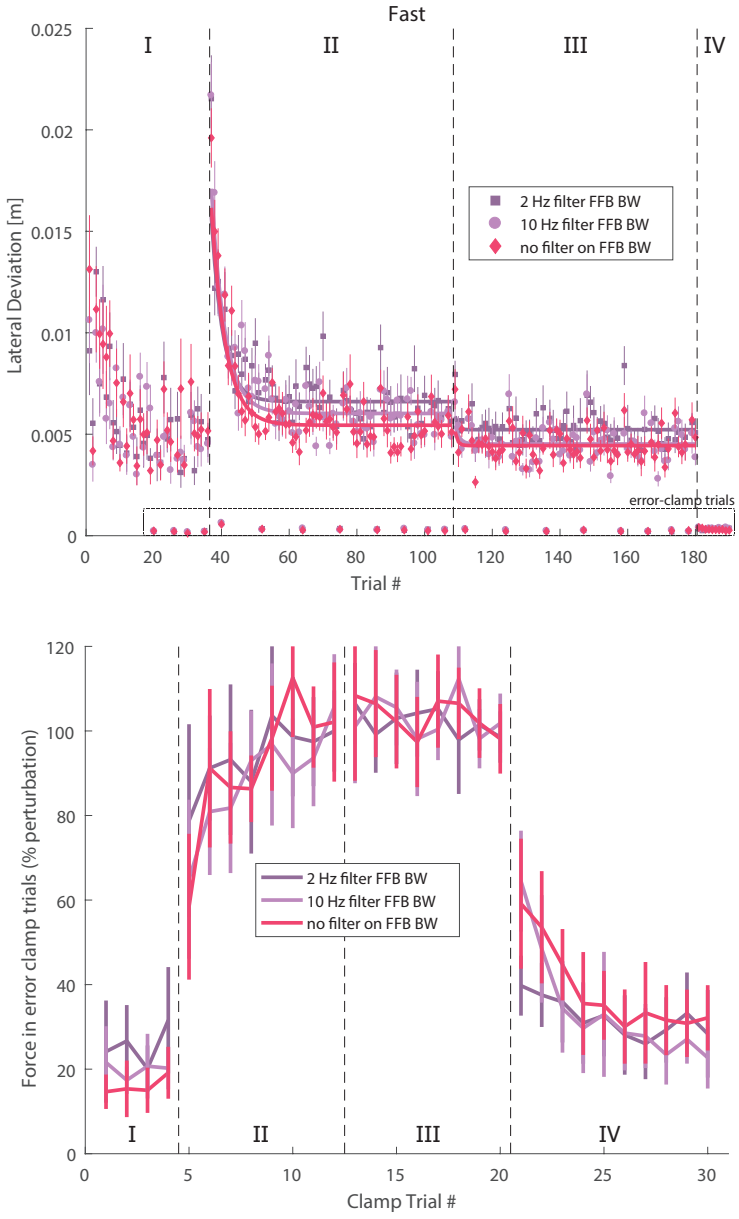

Figure 5.5: Across subject mean lateral deviation (top) and maximum clamp force in error-clamp trials (bottom) during Stages I to IV, for the *fast* dynamic system. Error bars represent the 95% confidence interval of the mean. The movement error was quantified by measuring the maximum lateral deviation during the reaching movement. In error-clamp trials, the robot nullified any lateral movements by means of a spring-damper. We measured the force subjects produced against this spring-damper, and normalized it against the peak ideal force to compensate for the full strength force field during late adaptation.

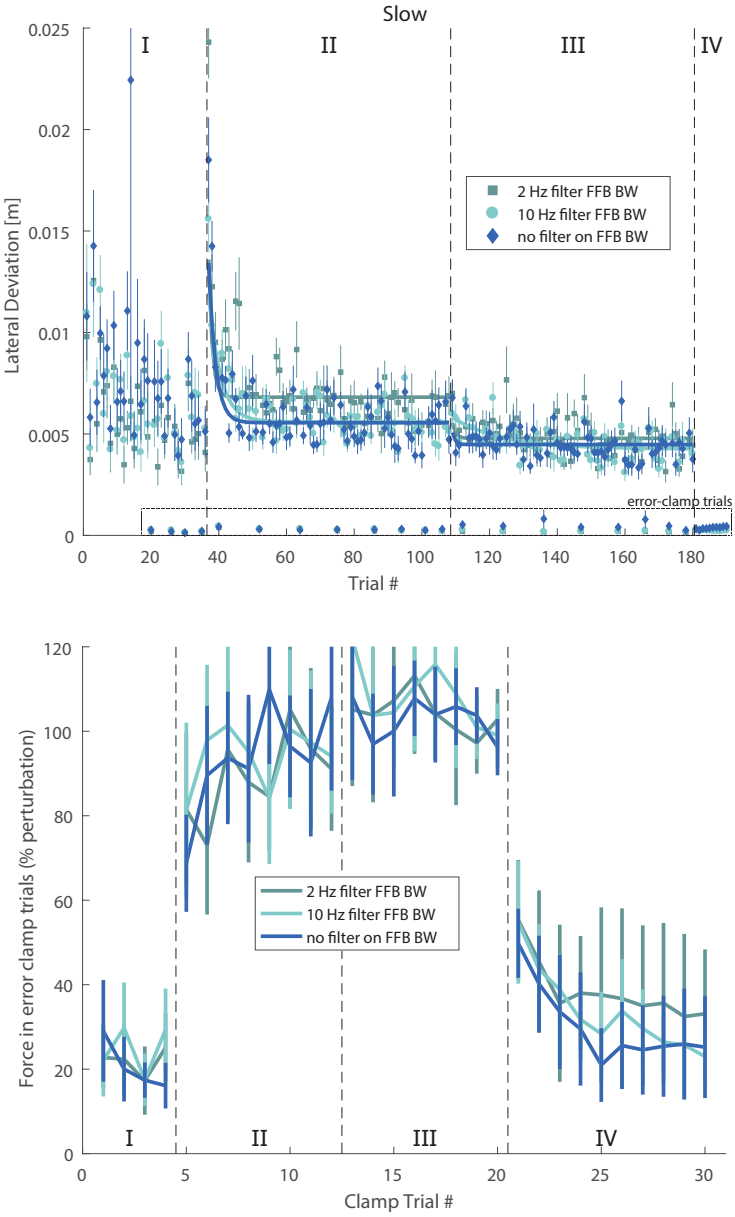

Figure 5.6: Across subject mean lateral deviation (top) and maximum clamp force in error-clamp trials (bottom) during Stages I to IV, for the *slow* dynamic system. Error bars represent the 95% confidence interval of the mean.

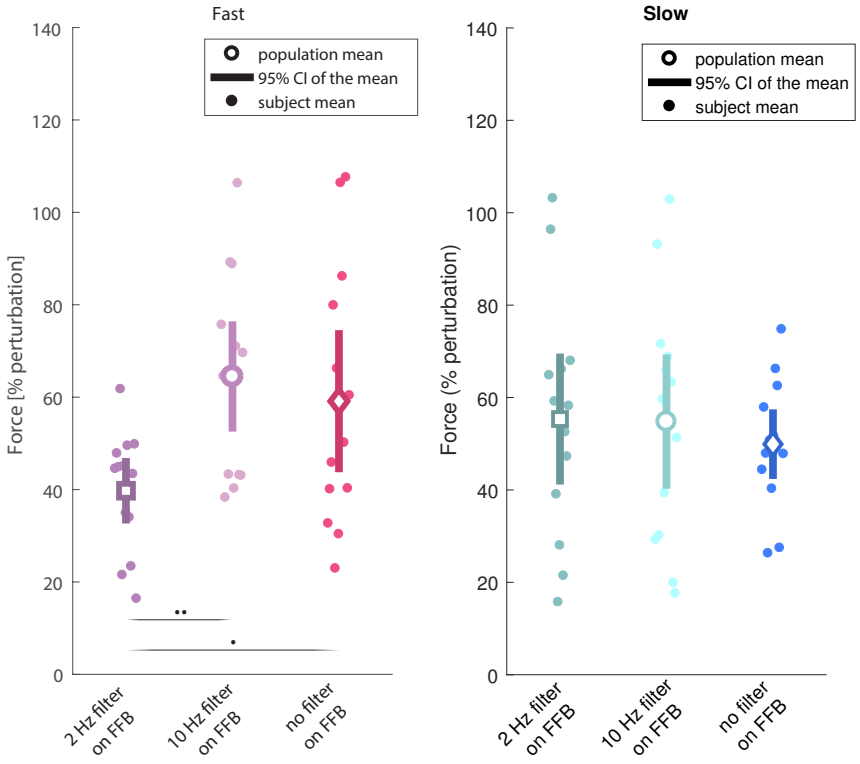

Figure 5.7: Mean normalized error-clamp forces in the generalization stage (stage IV) for the *fast* (left) and *slow* (right) slave systems, for each of the experimental conditions. The force is expressed as a percentage of the perturbation forces during late adaptation (i.e., final clamp trials of Stage III). Open circles represent population means (n=11), with the error bars representing the 95% confidence interval of the mean. Closed circles represent subject means. Significance levels of $p \leq 0.05$ and $p \leq 0.01$ are denoted by '•' and '••', respectively. For the *fast* dynamic system, 10 Hz filtered haptic feedback or unfiltered haptic feedback improves the mean generalization forces over 2 Hz filtered feedback. For the *slow* dynamic system, no differences are observed.

Chapter 6

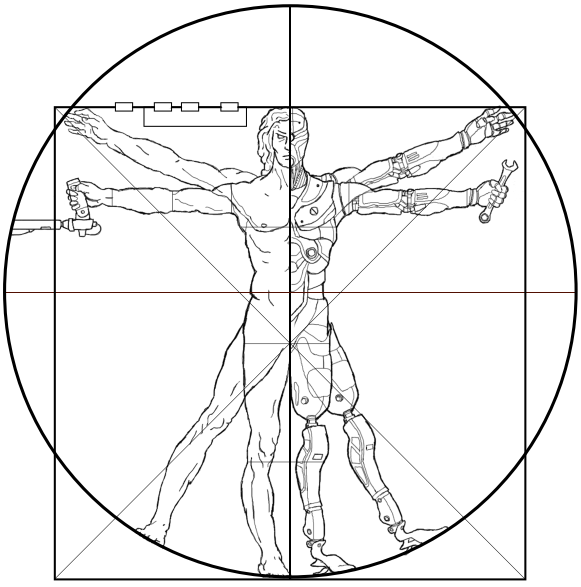

6

DISCUSSION

6.1. INTRODUCTION

Effectively, telemanipulation systems function as an extension to a human's motor apparatus such that tasks can be performed in environments with, for example, limitations with respect to distance (e.g., space), scale (e.g., surgery or microassembly) or unfavourable environments (e.g,. subsea, nuclear). However, in extending the operator's motor apparatus, the mapping between telemanipulation system and the human's motor control system is, inevitably, distorted. Haptic feedback - both proprioceptive and tactile or cutaneous feedback - is key in restoring such mapping and can be re-engineered; how to design haptic feedback (i.e. what quality of feedback is good enough) to best enable humans to perform practical tasks? As no theory or integrated view for human-in-the-loop design and evaluation of haptic feedback is available, finding an answer to this question is pestered by trial-and-error or heuristics, and moreover, findings cannot be transferred from one task or application domain to the other. Such generalization over devices, tasks, or even applications can only be realized by adapting a uniform approach, consisting of experimental frameworks and/or paradigms, guidelines and (cybernetic) models.

In this thesis an integrated view on human-centered design and evaluation of haptic feedback is presented, and fundamental understanding of the effect of haptic feedback on (closed-loop) operator neuromuscular control mechanisms is developed. More specifically, this thesis addressed the following:

- It is well-known *that* haptic feedback is useful for telemanipulation tasks, but the question of *how much* it helps, is often answered with "it depends". Favored design of haptic feedback depends on factors like operator talent, training, the type of task or application, the quality of the visual feedback, and task instruction. Chapter 2 presents a uniform framework that enables the assessment and validation of haptic feedback design for position control (Aim I-a, §1.4). Chapter 3 presents a similar framework for rate control (Aim I-b).

- Generalized models of the operator not only contribute to the understanding of operator control behaviour, but, moreover, enable the prediction of outcomes when task constraints change, such that informed *a priori* design considerations of haptic interfaces (and haptic support systems) can be made. Cybernetic models (Ch. 4) and motor control paradigms (Ch. 5) were adapted to quantify the effect of haptic feedback on fundamental neuromuscular control mechanisms (Aim II-a and II-b), namely feedback and feedforward control.

The outcomes of the studies will be discussed in the upcoming paragraphs. Results with respect to design requirements of haptic feedback for a given task are discussed in §6.2, whereas the effects of haptic feedback on the human operator's (neuromuscular) control mechanisms are discussed in §6.3. Finally, §6.4 presents guidelines for generalized haptic feedback design.

6.2. HAPTIC FEEDBACK IN TELEMANIPULATION SCENARIOS

THE FAVOURED HAPTIC FEEDBACK DESIGN TO PERFORM A GIVEN TELEMANIPULATED TASK PREDOMINANTLY DEPENDS ON THE REQUIRED TASK WORKSPACE AND TASK ACCURACY, AND THE NEED TO REFLECT BACK CONTACT TRANSITIONS

Whereas it is widely established *that* haptic feedback benefits the execution of telemanipulation tasks, the *extent* of its effects are governed by external factors. Important factors that the benefit of haptic feedback depends on are i) design choices in haptic feedback (amplitude and frequency content) and ii) the type of task, and iii) dynamics of the slave and environment. In this thesis two key human factors studies were performed with the goal of quantifying the benefit of haptic feedback on task execution for said conditions within an abstract task taxonomy. The first experiment focused on the benefit of haptic feedback in *position controlled* telemanipulation scenarios (Chapter 2), and the impact of *task instruction* and *availability of visual feedback* for free-space tasks, contact transition task and constrained in-contact tasks. In the second experiment the efficacy of four different haptic interface designs for rate control was determined for free-space, contact transition and force-level tasks (Chapter 3).

It is concluded that:

- An increase in telemanipulator quality is not always correlated to an increase in human-in-the-loop task performance; engineering haptic feedback beyond the (bilateral) motor capabilities of the human involves redundancies and will not lead to (instantaneous) task execution improvements (Chapter 2), or long-term improvements resulting from motor learning (Chapter 5).
  - For a generalizable abstract telemanipulation task, providing low-frequency haptic feedback provided task performance benefits over not providing any haptic feedback, while further increasing the haptic feedback bandwidth yielded only marginal improvements, even if a full natural spectrum of haptic feedback is provided (Chapter 2). This illustrates i) that haptic feedback quality

does not need to be perfect, and ii) that the required bandwidth can be determined by human-in-the-loop experiments, within a uniform, generalizable framework described by sets of (sub)tasks, conditions and metrics.

  - Improvements due to low-frequency haptic feedback occur specifically in tasks which involve contact with the environment, such as Constrained Translation (a reduction in task-completion-time, maximum input force and reversal rate) and Constrained Rotation subtasks (a reduction in task-completion time and reversal rate), and tasks which contain transitions from free-space to contact (Chapter 2). In many scenarios the notion of contact interaction suffices, as the absolute amplitude can be adjusted by the human operator.
  - When learning the dynamics of a slave manipulator and a force curl field, the haptic feedback bandwidth should be at least higher than the slave system's cut-off frequency, while further increasing the bandwidth does not benefit generalization (Chapter 5).

- For slaves with large workspaces (i.e. an order of magnitude larger than the human's workspace, typically large hydraulic manipulators), and system bandwidths 0.1 Hz or smaller (i.e. an order of magnitude slower than the human), rate control is favourable over position control, as it offers lower workload for such tasks (Chapter 3). Rate controlled systems usually do not provide haptic feedback [78], yet haptic feedback may be beneficial for task execution; depending on the task at hand, different feedback design approaches are favoured: a passive spring design is sufficient for rate-controlled tasks in which free-space subtasks dominate and basic in-contact tasks, whilst for advanced in-contact tasks a spring design with clear zero velocity (e.g., by a 'notch'), or feedback of the environment force as additional stiffness may further improve task performance and reduce control effort. In both cases, making system behaviour tangible to the human operator by means of haptic feedback is what underlies the performance and control effort benefits.

- Even in free-space tasks, one still wants haptic feedback in case the slave has substantial dynamics with respect to the human's dynamics; here, haptic feedback is beneficial for the operator in learning the slave dynamics or the dynamics of an held (rigid or non-rigid) object (Chapter 5).

Hence, controller choice (i.e. position or rate control) and haptic feedback design requirements are driven by the task to be performed in the remote environment, specifically its workspace and required accuracy. Large workspaces are more easily covered using rate control (e.g. characterized by a low workload), whereas positional accuracy is higher when using position control. Hybrid controllers (with rate in an outer control ring, and position in an inner ring) may fulfill a niche in which large workspaces and high positional accuracy is required. Also, nonlinear dynamics (as in the case of large hydraulic manipulators) favour the bang-bang control style of rate control, as feedforward control by means of proprioceptive mapping of master and slave workspaces in position control is difficult due to non-linearities.

Furthermore, these findings imply that haptic feedback should be designed using an

integrated view of the telemanipulation system with the human *in-the-loop*, as is performed within these studies. This implies that a human-centered evaluation approach should be adopted, both assessing the problem and validating the solution with the human *in-the-loop*. For such an integrated view of controller and haptic feedback design one should construct an evaluation framework which incorporates (at least): an abstract task taxonomy, a baseline to compare against, task instruction, speed-accuracy trade-offs (i.e. what metric to look at), performance-control effort trade-off, operator training and quality of visual feedback. Also, haptic feedback design requirements regarding instantaneous task performance should be weighted versus requirements regarding long-term effects (i.e., weeks, months, or even years) resulting from motor learning, as, depending on the task at hand, either set may drive overall bandwidth requirements.

THE AMPLITUDE OF HAPTIC FEEDBACK CAN BE SCALED DOWN WITHOUT HARMING TASK PERFORMANCE

Excessive haptic feedback leads to muscle fatigue, and the interaction forces in some telemanipulation scenarios (e.g. cranes, nuclear maintenance) are simply too large to directly feedback to the human operator. So how to scale down haptic feedback? This thesis describes two human factors studies in which the haptic feedback was scaled, namely i) for position controlled (Chapter 4) and ii) for rate controlled telemanipulation (Chapter 3).

- In free-air position controlled telemanipulation, haptic feedback of which the amplitude was scaled down (e.g., 25% or 50% of the forces at the slave side) yielded identical performance benefits as full haptic feedback, but with a beneficial decrease in physical control effort (Chapter 4).
  - When controlling fast dynamic slave systems, scaling haptic feedback has no effect on task performance, but improves control effort.
  - For slow dynamic systems, full haptic feedback substantially improves task execution (in terms of mean tracking error, number of reversals) compared to no haptic feedback, but at the cost of substantially increased operating forces at the master device.
- For rate control (Chapter 3):
  - Scaling is irrelevant when feeding back the velocity error between master and slave either as force-based or additional stiffness, as such feedback does not improve task performance nor increase control effort.
  - Feeding back scaled information about the physical interaction is beneficial for in-contact tasks and force level tasks, where stiffness feedback results in benefits over feeding back the derivative of the environment interaction force. The absolute amplitude is irrelevant as it has no physical representation (Chapter 3).

These results suggest that human operators are capable of adjusting their (neuromuscular) control parameters independently of the absolute magnitude (i.e. gain) of the haptic

feedback controller. Such adaptive behaviour is more commonly observed for example when scaling movements [86], or when (re)producing forces (e.g. [1, 6, 26]). However, when scaling, one should account for reasonable lower boundaries, that putatively may be given by Just Noticeable Differences (JNDs, e.g. [1, 137]), such that cues stay distinguishable. Similarly, upper boundaries may be given by comfort levels. Such comfort levels will vary from person to person.

Cybernetic models have been shown to be suitable tools to quantify the effects of scaling on task execution and an underlying operator control behaviour adaptations. The adapted approach can be extended to telemanipulation scenarios that include contact forces, or similarly, scenarios that require upscaling of the feedback forces such as those encountered in, for example, surgery or micro-assembly.

6.3. THE HUMAN AS A CONTROLLER

HAPTIC FEEDBACK SUBSTANTIALLY AFFECTS AN OPERATOR'S UNDERLYING MOTOR CONTROL MECHANISMS (I.E. FEEDBACK AND FEEDFORWARD CONTROL) WHEN CONTROLLING A SLAVE SYSTEM

The extent to which haptic feedback affects operator control behaviour is only partially understood. This thesis describes two key experiments aimed at quantifying the role of haptic feedback during free-air telemanipulation tasks. The first human factors experiment focused on the role of haptic feedback in *trained movements* (Chapter 4), and the impact of *slave dynamics* and *scaling* of presented haptic feedback. The second experiment focused on the role of haptic feedback when *learning movements* (Chapter 5), and the impact of *slave dynamics* and *bandwidth* of the presented haptic feedback.

The first experiment quantified the extent to which operators are able to control slow slave systems (i.e., cutoff frequency lower than 2 Hz, similar to a human arm) in a tracking task with preview, with and without haptic feedback. Here, the presence of haptic feedback allows operators to control slow slave systems more accurately and at a higher control bandwidth than without feedback (Chapter 4). This performance benefit persists even when amplitude is scaled down.

- Cybernetic system identification shows that operators generate more phase lead (up to 25 deg at 1-1.5 Hz) with haptic feedback than without. This extra phase lead allows improved compensation for the lag of the slow slave in the telemanipulation system, explaining the increase in control bandwidth and performance.

- State-of-the-art cybernetic modeling [123] was used for the first time to disentangle the contributions of visual and neuromuscular feedback, in order to show the underlying control-theoretic reason for the observed increased in phase lead, control bandwidth and performance. Operators substantially reduce their effective time delay when haptic feedback is present compared to no haptic feedback (a reduction from approximately 90 to 30 ms in estimated effective time delay τ_v). The presence of haptic feedback allows operators to exploit neuromuscular feedback, which is considerably faster compared to visual feedback (30-40 ms for reflexive

haptic feedback [125] versus 200 ms for visual feedback control [86]. Additionally, the amount of preview that operators require to compensate for the system lag, can be reduced when the effective time delay reduces. Indeed, the estimated future viewpoint (τ_f) reduced from approximately 530 to 470 ms when haptic feedback was present.

- In short, haptic feedback allows adaptation of both feedback and feedforward responses, such that slave systems can be controlled more accurately with a higher bandwidth.

Improving haptic feedback bandwidth substantially improves an operator's ability to generalize beyond a set of pre-experienced motions (i.e. generalization), but only up to the slave's cutoff frequency (Chapter 5).

- When generalizing to fast dynamic systems, high quality haptic feedback allows for more accurate compensation of the perturbation forces; 10 Hz filtered haptic feedback or unfiltered haptic feedback improves the mean generalization forces over 2 Hz filtered feedback.

- When generalizing with a slow dynamic system, low frequent, 2 Hz filtered haptic feedback suffices to accurately control the slave system, as we observed no differences between haptic feedback conditions.

Haptic feedback is the predominant information source next to visual feedback to restore the mapping between operator and remote environment. Its effects are observed in both instantaneous improvements of task execution due to feedback of environmental forces or device dynamics (i.e. trained movements), as well as task execution improvements over longer periods of time due to improved internal models (i.e. learning). Fundamental human motor control literature supports these findings related to motor learning; from this literature it is known that haptic feedback enhances the process of building 'mappings' between human input and a system's response (e.g., [65] [114] [136] [135]).

Interestingly, real-world telemanipulation is characterized by relatively low-fidelity haptic feedback [50] or even no haptic feedback at all (e.g. the Da Vinci or Zeus systems for teleoperated surgery [94], or the robots commissioned after the Fukushima-Daiichi accident [71]). For these applications, long training periods of months or even years are not uncommon as illustrated by detailed task analysis studies of the operators at the Joint European Torus (JET) [15], or more generically for systems with distinctive kinematics and dynamics, either superhuman (e.g. cranes [67]) or subhuman (e.g. robot-assisted surgery [41]). Would improved quality of the haptic feedback improve learning rates (i.e. efficacy), and improve motor control responses (i.e. efficiency)? The results of this thesis suggest *that* learning rates and responses will be improved. However, how haptic feedback quantitatively affects motor learning, and the time-scales at which this occurs should be further investigated.

CYBERNETIC MODELS AND REACH ADAPTATION: EXPERIMENTAL PARADIGMS OFFER GENERALIZABLE INSIGHTS ON THE IMPACT OF HAPTIC FEEDBACK ON HUMAN OPERATOR CONTROL BEHAVIOR DURING TELEMANIPULATION

Computational models for telemanipulator control and hardware are widely used (e.g. [52, 40]). However, computational models that capture the connected telemanipulator - describing the operator, linked by the telemanipulator to a remote environment [27] - are much less well-developed. As a result, the telemanipulation design and evaluation process is often based on heuristics.

In this thesis two models were applied as a tool to describe and predict operator control behaviour in key telemanipulation scenarios. Firstly, the well-established "Crossover" cybernetic modelling framework (as proposed by McRuer et al., e.g. [86, 130]) was applied to free-space telemanipulation tasks, aimed at quantifying the role of haptic feedback in *trained movements* (Chapter 4). Secondly, a widely-applied reach adaptation paradigm (e.g. [65, 114, 136, 112]) was adapted to quantify the role of haptic feedback when *learning movements* (Chapter 5).

- Quasi-linear cybernetic control models extending the "Crossover model" [86] with both feedforward and feedback components (e.g. [123]) accurately describe human operators performing telemanipulated pursuit tasks. These pursuit tasks are an abstract representation of a free-space movement task (e.g. tool movement, pick-and-place, visual inspection and metrology tasks), as in, for example, maintenance activities in nuclear (e.g., [87, 15]) or subsea (e.g. [115, 78]) environments (Chapter 4). The models consistently described changes in operator control parameters when experimental conditions (*slave dynamics* and *scaling* of presented haptic feedback) varied.
- Reach adaptation paradigms from the literature can be adopted to describe and study operator behaviour when *learning* or *adapting to* dynamics in a telemanipulation task (Chapter 5). Operators learned to adapt to the viscous curl force field acting on the simulated slave (and therefore fed back to the operator through the feedback dynamics of the telemanipulation system) similarly to literature describing motor adaptations with such perturbations applied directly to the subject's hand (e.g. [60, 66, 47, 97, 114]), independently of slave dynamics or haptic feedback bandwidth.

These two studies illustrate that computational models and paradigms from the motor control literature can be adopted to provide generalizable descriptions of human operator behaviour in (free-space) telemanipulation tasks for systems like cranes and robot arms, and are representative for activities in domestic, nuclear or subsea environments. The cybernetic models allow for an exclusive understanding of the underlying operator control mechanisms (i.e. feedback and feedforward control) by looking in the frequency domain, thus complementing and enhancing the insights gained from the time-domain data. The reach adaptation paradigm enables the determination of the extent to which haptic feedback bandwidth affects motor learning and generalization for different slave dynamics, and more fundamentally, to study the role of haptic feedback in motor learning (for telemanipulation). Moreover, both models enable inter- and extrapolation of

findings and predict outcomes when task constraints change, such that informed *a priori* design considerations of haptic interfaces (and haptic support systems) can be made.

In this thesis limited topics have been studied (among others, slave dynamics, feedback scaling, feedback quality) and models have been adapted. However, the framework and model-analytic approach can be applied to other design variables or telemanipulation scenarios, not necessarily related to haptic feedback. Also, the results should be interpreted as intra- and extrapolatable for the conditions studied and not truly predictive for a generic telemanipulation task. The latter would require, for example, bootstrapping and (robustness) assessment in a wider condition set (e.g. tasks with contact, more degrees-of-freedom, other application subdomains).

Hence, to avoid a design process based on heuristics and trial-and-error, and to avoid outcomes with fundamental disclaimers with respect to task and/or device, it is required to adopt a common language in the form of an integral approach using uniform models and paradigms. Only by developing such a uniform basis can a knowledge base be created that gradually can be extended on.

6.4. GUIDELINES

GUIDELINES FOR THE DESIGN OF HAPTIC FEEDBACK

Based on this thesis the following guidelines for the design of haptic feedback can be formulated:

- Haptic feedback should be designed using an integrated view of the telemanipulation system with the human in-the-loop, using human factors studies in an evaluation framework which incorporates (at least): an abstract task taxonomy, a baseline to compare against, task instruction, speed-accuracy trade-offs (i.e. what metric to look at), performance-control effort trade-off, operator training and quality of visual feedback.

- Such design and evaluation should be performed within a uniform framework of (cybernetic) models and paradigms. Only by adopting such an integral approach and developing a uniform basis, a knowledge base can be created that can be gradually extended on.

- There is an upper limit to performance gains from haptic feedback, which holds individually for each element of the telemanipulation system (master, slave, controller). Haptic feedback should be designed accordingly.

- Haptic feedback can be scaled without sacrificing task execution or adapting the operator's control behaviour, as long as reasonable upper and lower boundaries are respected.

- Haptic feedback quality is deemed sufficient when (short-term) task execution improvements are no longer observed. For example, when the environmental forces or device dynamics are reflected sufficiently to identify contact or estimate forces

or stiffness. However, depending on the task at hand, requirements for adequate motor learning (i.e. building internal models) may be more stringent than requirements derived from the task, and may, as such, drive overall device bandwidth requirements (Chapter 5). Improvements in task performance due to improved internal models are far more gradual and long-term (weeks or years), as opposed to the instantaneous improvements due to haptic feedback of environment or device dynamics (minutes or hours).

GUIDELINES FOR THE DESIGN OF SYSTEMS WITH AUGMENTED HAPTIC FEEDBACK

Substantial performance improvements may be attained by providing augmented haptic feedback to the human operator in the form of, for example, shared control [3] or virtual fixtures [107]. Based on this thesis, the following guidelines for the design of augmented haptic feedback for telemanipulation systems can be formulated:

- Augmented haptic feedback (e.g. [14, 105]) should be considered when determining scope for task execution improvements - for certain telemanipulation tasks (e.g. hard-hard assembly) limited task performance improvements may be expected when improving haptic feedback quality (Chapter 2).
- Long-term effects (e.g. weeks, months, or even years) due to motor learning, and effects relating to trust [81] or situation awareness [43] (and subsequently off-nominal task execution, e.g. [127]) should be evaluated next to the instantaneous task execution improvements of augmented haptic feedback.
- Augmented haptic feedback should be designed and evaluated by extending upon the uniform framework of (cybernetic) models and paradigms for natural haptic feedback, therefore ensuring an integrated view of the augmented controller, telemanipulation system and human operator. Cybernetic models may even be used to generate or individualize support trajectories, reducing discomfort and increasing performance [35].

Moore's Law is merciless and multidimensional, and there is no denying that autonomous agents will gain momentum in the telemanipulation domain (e.g. [6, 98, 7, 104, 8, 68, 15]). As there will be human in-the-loop involvement (at least for the next few upcoming decades) [100] due to the unpredictable, dynamic and complex nature of telemanipulation tasks, it is merely essential to adopt a uniform, model based approach which provides thorough insight in human control behaviour. Only then can automation-issues such as trust, loss of skills, situation awareness and over-reliance (e.g., [44, 43, 81, 117, 118, 100]) be coped with.

BIBLIOGRAPHY

[1] L. A Jones. Matching forces: Constant errors and differential thresholds. *Perception*, 18:681–7, 02 1989.

[2] M. A. Srinivasan and R. Lamotte. Tactual discrimination of softness. *Journal of neurophysiology*, 73:88–101, 02 1995.

[3] D. Abbink, T. Carlson, M. Mulder, J. C. F. de Winter, F. Aminravan, T. L. Gibo, and E. R. Boer. A topology of shared control systems—finding common ground in diversity. *IEEE Transactions on Human-Machine Systems*, 48(5):509–525, Oct 2018.

[4] D. Abbink and M. Mulder. Exploring the dimensions of haptic feedback support in manual control. *Journal of Computing and Information Science in Engineering*, 9:1–9, 03 2009.

[5] D. A. Abbink. *Neuromuscular Analysis of Haptic Gas Pedal Feedback during Car Following*. PhD thesis, Department of Biomechanical Engineering, Delft University of Technology, Delft, The Netherlands, 2006.

[6] D. A. Abbink et al. Measuring neuromuscular control dynamics during car following with continuous haptic feedback. *IEEE Transactions on Systems, Man, and Cybernetics - Part B: Cybernetics*, 41, 2011.

[7] D. A. Abbink and M. Mulder. *Neuromuscular Analysis as a Guideline in designing Shared Control*, chapter 27, pages 499–516. IntechOpen, 2010.

[8] S. Alaimo, L. Pollini, J. Bresciani, and H. Bülthoff. Evaluation of direct and indirect haptic aiding in an obstacle avoidance task for tele-operated systems. In *Proceedings of the 18th IFAC World Congress*, page 6472–6477, 2011.

[9] I. Aliaga, A. Rubio, and E. Sanchez. Experimental quantitative comparison of different control architectures for master-slave teleoperation. *IEEE Transactions on Control System Technology*, 2004.

[10] R. O. Ambrose et al. Robonaut: Nasa's space humanoid. *IEEE Intelligent Systems Journal*, 15(4):57–63, 2000.

[11] R. T. Azuma. A survey of augmented reality. *Presence: Teleoperators and Virtual Environments 6*, 1997.

[12] A. Bejczy and B. Hannaford. Man-machine interaction in space telerobotics. In *International Symposium on Teleoperation and Control*, 1988.

[13] E. Bizzi, N. Accornero, W. Chapple, and N. Hogan. Posture control and trajectory formation during arm movement. *Journal of Neuroscience*, 4(11):2738–2744, 1984.

[14] H. Boessenkool, D. A. Abbink, C. J. Heemskerk, F. C. van der Helm, and J. G. Wildenbeest. A task-specific analysis of the benefit of haptic shared control during telemanipulation. *IEEE Transactions on Haptics*, pages 1–1, 2013.

[15] H. Boessenkool, J. Thomas, C. Heemskerk, M. de Baar, M. Steinbuch, and D. Abbink. Task analysis of human-in-the-loop tele-operated maintenance: What can be learned from jet? *Fusion Engineering and Design*, 89(9-10):2283–2288, Oct. 2014.

[16] H. Boessenkool, J. Thomas, J. G. Wildenbeest, C. J. Heemskerk, M. R. de Baar, M. Steinbuch, and D. A. Abbink. Where to improve in human-in-the-loop teleoperated maintenance? a phased task analysis based on video data of maintenance at jet. *Fusion Engineering and Design*, 2017.

[17] H. Boessenkool, J. G. Wildenbeest, C. J. Heemskerk, M. R. de Baar, M. Steinbuch, and Abbink. A task analysis approach to quantify bottlenecks in task completion time of telemanipulated maintenance. *Fusion Engineering and Design*, 129:300–308, 2018.

[18] A. Bolopion and S. Regnier. A review of haptic feedback teleoperation systems for micromanipulation and microassembly. *IEEE Transactions on Automation Science and Engineering*, 10(3), 2013.

[19] S. A. Bowyer, B. L. Davies, and F. R. y Baena. Active constraints/virtual fixtures: A survey. *IEEE Transactions on Robotics*, 30(1):138–157, Feb 2014.

[20] J. M. Bradshaw, R. R. Hoffman, D. D. Woods, and M. Johnson. The seven deadly myths of "autonomous systems". *IEEE Intelligent Systems*, 28(3):54–61, May 2013.

[21] T. Brooks. Telerobotic response requirements. In *IEEE International Conference on Systems, Man, and Cybernetics Conference Proceedings*, pages 113–120, Nov 1990.

[22] T. Brooks and A. K. Bejczy. Hand controllers for teleoperation. Technical report, Jet Propulsion Laboratory, Pasadena, CA, 1981.

[23] E. Burdet, R. Osu, D. W. Franklin, T. E. Milner, and M. Kawato. The central nervous system stabilizes unstable dynamics by learning optimal impedance. *Nature*, 414, 2001.

[24] G. C. Pettinaro. Behaviour-based peg-in-hole. *Robotica*, 17:189–201, 03 1999.

[25] L. Cardinali, F. Frassinetti, C. Brozzoli, C. Urquizar, A. C Roy, and A. Farnè. Tool-use induces morphological updating of the body schema. *Current Biology*, 19:R478–479, 06 2009.

[26] B. Christiansson. *Is the force with you? On the accuracy of human force perception.* PhD thesis, Delft University of Technology, 2016.

[27] G. A. V. Christiansson. *Hard Master Soft Slave Haptic Teleoperation*. PhD thesis, Delft University of Technology, 2007.

[28] G. A. V. Christiansson. An experimental study of haptic feedback in a teleoperated assembly task. *Journal of Computing and Information Science in Engineering*, 8, 2008.

[29] G. A. V. Christiansson and F. C. T. van der Helm. The low-stiffness teleoperator slave - a trade-off between stability and performance. *International Journal of Robotics Research*, 26(3):287–299, 2007.

[30] J. D. Van Der Laan, A. Heino, and D. Waard. A simple procedure for the assessment of acceptance of advance transport telematics. *Transportation Research Part C: Emerging Technologies*, 5:1–10, 02 1997.

[31] H. Damveld, D. Abbink, M. Mulder, M. Mulder, M. van Paassen, F. van der Helm, and R. Hosman. Measuring the contribution of the neuromuscular system during a pitch control task. In *Proceedings of the AIAA Modeling and Simulation Technologies Conference*, 2009.

[32] R. W. Daniel and P. R. McAree. Fundamental limits of performance for force reflecting teleoperation. *The International Journal of Robotics Research*, 17(8), 1998.

[33] F. Danion, J. S Diamond, and J. Flanagan. The role of haptic feedback when manipulating nonrigid objects. *Journal of neurophysiology*, 107:433–41, 01 2012.

[34] G. De Gersem, H. Van Brussel, and F. Tendick. Reliable and enhanced stiffness perception in soft-tissue telemanipulation. *The International Journal of Robotics Research*, 25(10), 2005.

[35] A. W. de Jonge, J. G. W. Wildenbeest, H. Boessenkool, and D. A. Abbink. The effect of trial-by-trial adaptation on conflicts in haptic shared control for free-air teleoperation tasks. *IEEE Transactions on Haptics*, 9(1):111–120, Jan 2016.

[36] E. de Vlugt, A. Schouten, and F. van der Helm. Quantification of intrinsic and reflexive properties during multijoint arm posture. *Journal of neuroscience methods*, 155:328–49, 10 2006.

[37] J. Dingwell, C. Mah, and F. Mussa-Ivaldi. Manipulating objects with internal degrees of freedom: Evidence for model-based control. *Journal of Neurophysiology*, 88:222–235, 07 2002.

[38] J. V. Draper et al. Effects of force reflection on servomanipulator task performance. In *Proceedings of the International Topical Meeting on Remote Systems and Robots in Hostile Environments*, 1986.

[39] F. M. Drop, D. M. Pool, H. J. Damveld, M. M. van Paassen, and M. Mulder. Identification of the feedforward component in manual control with predictable target signals. *IEEE Transactions on Cybernetics*, 43(6):1936–1949, 2013.

[40] J. Dudragne et al. A generalized bilateral control applied to master slave manipulators. In *Proceedings of the 20th ISIR*, 1989.

[41] G. Dulan, R. Rege, D. Hogg, K. Gilberg-Fisher, N. Arain, S. Tesfay, and D. Scott. Developing a comprehensive, proficiency-based training program for robotic surgery. *Surgery*, 152(3), 2012.

[42] M. Elton, R. Winck, and W. Book. Command feedback for position control of hydraulic machines. In *ASME/BATH 2013 Symposium on Fluid Power and Motion Control, FPMC 2013*, 10 2013.

[43] M. Endsley and D. Kaber. Level of automation effects on performance, situation awareness and workload in a dynamic control task. *Ergonomics*, 42:462–492, 1999.

[44] M. Endsley and E. Kiris. The out-of-the-loop performance problem and level of control in automation. *Human Factors: The Journal of the Human Factors and Ergonomics Society*, 37(2):381–394, 1995.

[45] M. J. et al. Team ihmc's lessons learned from the darpa robotics challenge trials. *Journal of Field Robotics*, 32(2), 2015.

[46] P. Fitts. Human engineering for an effective air navigation and traffic control system. Technical report, National Research Council, Washington, DC, USA, 1981.

[47] D. W. Franklin, R. Osu, E. Burdet, M. Kawato, , and T. E. Milner. Adaptation to stable and unstable dynamics achieved by combined impedance control and inverse dynamics model. *Journal of Neurophysiology*, 90(5):3270–3282, 2003.

[48] R. G. D. Steel and T. JH. Principles and procedures of statistics. a biometric approach. *Biometrics*, 2, 12 1981.

[49] S. G. Hart and L. E. Stavenland. Development of nasa-tlx (task load index): Results of empirical and theoretical research. *Adv. Psychol*, 52:139–, 12 1988.

[50] L. Galbiati, T. Raimondi, P. Garetti, and G. Costi. Control and operational aspects of the mascot 4 force feedback servomanipulator of jet. In *Fusion Engineering. Proceedings., 14th IEEE/NPSS Symposium on*, pages 563–566, 1991.

[51] M. A. Goodrich and A. C. Schultz. Human-robot interaction: A survey. *Found. Trends Hum.-Comput. Interact.*, 1(3):203–275, jan 2007.

[52] B. Hannaford. A design framework for teleoperators with kinesthetic feedback. *IEEE Transactions on Robotics and Automation*, 5(4), 1989.

[53] B. Hannaford. Stability and performance tradeoffs in bi-lateral teleoperation. In *IEEE International Conference on Robotics and Automation*, 1989.

[54] B. Hannaford and J.-H. Ryu. Time-domain passivity control of haptic interfaces. *Robotics and Automation, IEEE Transactions on*, 18:1 – 10, 03 2002.

[55] B. Hannaford, L. Wood, D. A. McAffee, and H. Zak. Performance evaluation of a six-axis generalized force-reflecting teleoperator. *IEEE Transactions on Systems, Man and Cybernetics*, 21(3), 1991.

[56] S. Hanneton, A. Berthoz, J. Droulez, and J. Slotine. Does the brain use sliding variables for the control of movements? *Biological Cybernetics*, 77, 1997.

[57] C. M. Harris and D. M. Wolpert. Signal-dependent noise determines motor planning. *Nature*, 394, 1998.

[58] K. Hashtrudi-Zaad and S. E. Salcudean. Transparency in time-delayed systems and the effect of local force feedback for transparent teleoperation. *Robotics and Automation, IEEE Transactions on*, 18:108 – 114, 03 2002.

[59] K. Hashtrudi-Zaad and S. Salcudean. On the use of local force feedback for transparent teleoperation. In *Proceedings 1999 IEEE International Conference on Robotics and Automation*, volume 3, pages 1863–1869. IEEE, 1999.

[60] C. C. Haswell, J. Izawa, L. R. Dowell, S. H. Mostofsky, and R. Shadmehr. Representation of internal models of action in the autistic brain. *Nature Neuroscience*, 12(8):970–2, 2009.

[61] F. Huang, R. Gillespie, and A. Kuo. Haptic feedback and human performance in a dynamic task. In *Proceedings 10th Symposium on Haptic Interfaces for Virtual Environment and Teleoperator Systems*, 2002.

[62] F. Huang, R. Gillespie, and A. Kuo. Haptic feedback improves manual excitation of a sprung mass. In *12th International Symposium on Haptic Interfaces for Virtual Environment and Teleoperator Systems*, 2004.

[63] I. W. Hunter et al. A teleoperated microsurgical robot and associated virtual environment for eye surgery. *Presence*, 2(4):265–280, 1993.

[64] M. Ito. Mechanisms of motor learning in the cerebellum. *Brain Research*, 886(1–2):237 – 245, 2000.

[65] M. Ito. Bases and implications of learning in the cerebellum–adaptive control and internal model mechanism. *Progress in brain research*, 148:95–109, jan 2005.

[66] J. Izawa, S. Pekny, M. Marko, C. Haswell, R. Shadmehr, and S. Mostofsky. Motor learning relies on integrated sensory inputs on adhd, but over-selectively on proprioception in autism spectrum conditions. *Autism Research*, 5(2):124–136, 2012.

[67] D. E. M. J. W. Hill and A. J. Sword. Study to design and develop remote manipulator system. Technical report, Stanford Research Institute, 1974.

[68] F. Janabi-Sharifi and I. Hassanzadeh. Experimental Analysis of Mobile-Robot Teleoperation via Shared Impedance Control. *IEEE Transactions on Systems, Man and Cybernetics-Part B: Systems and Humans*, 41(2):591–606, 2011.

[69] L. A. Jones, , and H. Z. Tan. Application of psychophysical techniques to haptic research. *IEEE Transactions on Haptics*, 6(3), 2013.

[70] M. Kawato, K. Furukawa, and R. Suzuki. A hierarchical neural-network model for control and learning of voluntary movement. *Biological Cybernetics*, 57(3):169–185, 1987.

[71] S. Kawatsuma, M. Fukushima, and T. Okada. Emergency response by robots to fukushima-daiichi accident: summary and lessons learned. *Industrial Robot*, 39(5):428–435, 2012.

[72] W. S. Kim, F. Tendick, S. R. Ellis, and L. W. Stark. A comparison of position and rate control for telemanipulations with consideration of manipulator system dynamics. *IEEE Journal on Robotics and Automation*, 3(5), 1987.

[73] R. Klatzky, S. J. Lederman, and C. Reed. There's more to touch than meets the eye: The salience of object attributes for haptics with and without vision. *Journal of Experimental Psychology: General*, 116:356, 12 1987.

[74] R. Klein. Attention and visual dominance: A chronometric analysis. *Journal of experimental psychology. Human perception and performance*, 3:365–78, 09 1977.

[75] E. S. Krendel and D. T. McRuer. A servomechanisms approach to skill development. *Journal of the Franklin Institute*, 269(1):24—-42, 1960.

[76] K. J. Kuchenbecker, J. Fiene, and G. Niemeyer. Improving contact realism through event-based haptic feedback. *IEEE Transactions on Visualization and Computer Graphics*, 12(2):219–230, March 2006.

[77] R. J. Kuiper, J. C. L. Frumau, F. C. T. van der Helm, and D. A. Abbink. Haptic support for bi-manual control of a suspended grab for deep-sea excavation. In *IEEE International Conference on Systems, Man, and Cybernetics, Manchester*, 2013.

[78] R. J. Kuiper, D. J. F. Heck, I. A. Kuling, and D. A. Abbink. Evaluation of haptic and visual cues for repulsive or attractive guidance in nonholonomic steering tasks. *IEEE Transactions on Human-Machine Systems*, PP(99), 2016.

[79] D. A. Lawrence. Stability and transparency in bilateral teleoperation. *Proceedings of the 31st Conference on Position and Control*, 1993.

[80] P. D. Lawrence, S. E. Salcudean, N. Sepehri, D. Chan, S. Bachmann, N. Parker, M. Zhu, and R. Frenette. Coordinated and force-feedback control of hydraulic excavators. In O. Khatib and J. K. Salisbury, editors, *Experimental Robotics IV*, pages 181–194, Berlin, Heidelberg, 1997. Springer Berlin Heidelberg.

[81] J. D. Lee and K. A. See. Trust in automation: Designing for appropriate reliance. *J. Hum. Factors Ergon. Soc.*, 46(1):50–80, 2004.

[82] R. v. d. Linde, P. Lammertse, E. Frederiksen, and B. The hapticmaster, a new high-performance haptic interface. In *Proceedings of EuroHaptics*, 2002.

[83] W. A. MacDonald and E. R. Hoffmann. Review of relationship between steering wheel reversal rate and driving task demand. *Human Factors*, 22, 1980.

[84] M. J. Massimino and T. B. Sheridan. Variable force and visual feedback effects on teleoperator man/machine performance. In *Proceedings of the NASA Conference on Space Robotics*, volume 1, pages 89–98, 1989.

[85] M. J. Massimino and T. B. Sheridan. Teleoperator performance with varying force and visual feedback. *Human Factors: The Journal of the Human Factors and Ergonomics Society*, 36(145), 1994.

[86] D. T. McRuer and H. R. Rex. A review of quasi-linear pilot models. *IEEE Transactions on Human Factors in Electronics*, 8(3), 1967.

[87] S. Mills et al. Remote handling of jet in-torus components - a practical experience. In *Proceedings of the Symposium on Fusion Engineering*, 2000.

[88] F. Mobasser and K. Hashtrudi-Zaad. Transparent rate mode bilateral teleoperation control. *I. J. Robotic Res.*, 27:57–72, 01 2008.

[89] W. Mugge, J. Schuurmans, A. Schouten, and F. van der Helm. Sensory weighting of force and position feedback in human motor control tasks. *The Journal of neuroscience : the official journal of the Society for Neuroscience*, 29:5476–82, 05 2009.

[90] M. Mulder, D. Abbink, and E. Boer. Sharing control with haptics. *Human factors*, 54:786–98, 10 2012.

[91] F. Mussa-Ivaldi and E.Bizzi. Motor learning through the combination of primitives. *Philosophical transactions of the Royal Society of London. Series B, Biological sciences*, 355:1755–69, 01 2001.

[92] I. Nisky, F. Mussa-Ivaldi, and A. Karniel. A regression and boundary-crossing-based model for the perception of delayed stiffness. *IEEE Transactions on Haptics*, 1(2):73–82, July 2008.

[93] D. Norman. The 'problem' with automation: inappropriate feedback and interaction, not 'over-automation'. *Philosophical Transactions of the Royal Society of London. B, Biological Sciences*, 327(1241):585–593, 1990.

[94] A. Okamura. Methods for haptic feedback in teleoperated robot-assisted surgery. *The Industrial robot*, 31(6):499–508, 2004.

[95] M. O'Malley and M. Goldfarb. The effect of virtual surface stiffness on the haptic perception of detail. *Mechatronics, IEEE/ASME Transactions on*, 9:448 – 454, 07 2004.

[96] M. Ostoja-Starzewski and M. Skibniewski. A master-slave manipulator for excavation and construction tasks. *Robotics and Autonomous Systems*, 4:333–337, 04 1989.

[97] R. Osu, M. Dimitriou, D. W. Franklin, D. M. Wolpert, H. Kato, H. Gomi, K. Domen, T. Hunter, P. Sacco, M. A. Nitsche, and D. L. Turner. Short- and long-term changes in joint co-contraction associated with motor learning as revealed from surface emg. *Science And Technology*, pages 991–1004, 2002.

[98] M. K. O'Malley, A. Gupta, M. Gen, and Y. Li. Shared Control in Haptic Systems for Performance Enhancement and Training. *Journal of Dynamic Systems, Measurement, and Control*, 128(1):75, 2006.

[99] C. Pacchierotti, A. Tirmizi, and D. Prattichizzo. Improving transparency in teleoperation by means of cutaneous tactile force feedback. *ACM Transactions on Applied Perception*, 11(1):4:1–4:16, apr 2014.

[100] R. Parasuraman and C. Wickens. Humans: Still vital after all these years of automation. *Human Factors, J. Human Factors Ergonom. Soc.*, 50(3):511–520, June 2008.

[101] S. Park, C. Seo, J.-P. Kim, and J. Ryu. Robustly stable rate-mode bilateral teleoperation using an energy-bounding approach. *Mechatronics*, 21:176–184, 02 2011.

[102] N. Parker, S. Salcudean, and P. Lawrence. Application of force feedback to heavy duty hydraulic machines. In *Proceedings - IEEE International Conference on Robotics and Automation*, volume 1, pages 375 – 381 vol.1, 06 1993.

[103] J.-B. Passot, N. R. Luque, and A. Arleo. Internal models in the cerebellum: A coupling scheme for online and offline learning in procedural tasks. In *SAB*, 2010.

[104] A. J. Pick and D. J. Cole. A mathematical model of driver steering control including neuromuscular dynamics. *Journal of Dynamic Systems, Measurement, and Control*, 130(3), 2008.

[105] R. Reilink, S. Stramigioli, A. Kappers, and S. Misra. Evaluation of flexible endoscope steering using haptic guidance. *International Journal of Medical Robotics and Computer Assisted Surgery*, 7(2):178–186, 2011. 10.1002/rcs.386.

[106] A. Rolfe. A perspective on fusion relevant remote handling techniques. *Fusion Engineering and Design*, 82:1917–1923, 10 2007.

[107] L. B. Rosenberg. Virtual fixtures: Perceptual tools for telerobotic manipulation. In *Proceedings of IEEE Virtual Reality Annual International Symposium*, pages 76–82, Sept 1993.

[108] S. S. Haykin. *Active Network Theory*. Addison-Wesley, 01 1970.

[109] S. Salcudean, S. Tafazoli, K. Hashtrudi-Zaad, P. Lawrence, and C. Reboulet. Evaluation of impedance and teleoperation control of a hydraulic mini-excavator. *Lecture Notes in Control and Information Sciences*, 232, 09 1999.

[110] S. E. Salcudean, M. Zhu, W.-H. Zhu, and K. Hashtrudi-Zaad. Transparent bilateral teleoperation under position and rate control. *The International Journal of Robotics Research*, 19(12):1185–1202, 2000.

[111] G. Schulein and A. Ehrensperger. Multi-axle manual control unit, 2012.

[112] B. J. . A. J. A. Seidler, R. D. Wneurocognitive contributions to motor skill learning: the role of working memory. *Journal of Motor Behavior*, 6(44), 2012.

[113] N. Sepehri, P. D. Lawrence, F. Sassani, and R. Frenette. Resolved-Mode Teleoperated Control of Heavy-Duty Hydraulic Machines. *Journal of Dynamic Systems, Measurement, and Control*, 116(2):232–240, 06 1994.

[114] R. Shadmehr and F. A. Mussa-ivaldi. Adaptive representation of dynamics during learning of a motor task. *The Journal of Neuroscience*, 14(5), 1994.

[115] T. Sheridan and W. Verplank. Human and computer control of undersea teleoperators. man-machine systems laboratory, department of mechanical engineering, 1978.

[116] T. B. Sheridan. Telerobotics. *Automatica*, 25(4), 1989.

[117] T. B. Sheridan. *Humans and Automation: System Design and Research Issues*. John Wiley & Sons, Inc., New York, NY, USA, 2002.

[118] T. B. Sheridan and R. Parasuraman. Human-automation interaction. *Reviews of Human Factors and Ergonomics*, 1(1):89–129, 2005.

[119] K. Shimoga. Finger force and touch feedback issues in dexterous telemanipulation. In *Fourth Annual Conference on Intelligent Robotic Systems for Space Exploration*, pages 159 – 178, 01 1992.

[120] M. Steele and B. Gillespie. Shared control between human and machine: Using a haptic steering wheel to aid in land vehicle guidance. *Proceedings of the Human Factors and Ergonomics Society Annual Meeting*, 45:1671–1675, 10 2001.

[121] M. S. R. Uno, Y.and Kawato. Formation and control of optimal trajectory in human multijoint arm movement. *Biological Cybernetics*, 61(2):89–101, Jun 1989.

[122] J. Uzawa, S. Pekny, M. Marko, C. Haswell, R. Shadmehr, and S. Mostofsky. Motor learning relies on integrated sensory inputs on adhd, but over-selectively on proprioception in autism spectrum conditions. *Autism Research*, 5(2):124–136, 2012.

[123] K. van der El, D. M. Pool, , M. R. M. van Paassen, and M. Mulder. Effects of preview on human control behavior in tracking tasks with various controlled elements. *IEEE Transactions on Cybernetics*, 48(4), 2018.

[124] K. van der El, D. M. Pool, H. J. Damveld, M. R. M. van Paassen, and M. Mulder. An empirical human controller model for preview tracking tasks. *IEEE Transactions on Cybernetics*, 46(11):2609–2621, 2015.

[125] F. C. van der Helm, A. C. Schouten, E. de Vlugt, and G. Brouwn. Identification of intrinsic and reflexive components of human arm dynamics during postural control. *Journal of Neuroscience Methods*, 119(1):1–14, 2002.

[126] R. van der Linde and P. Lammertse. Hapticmaster - a generic force controlled robot for human interaction. *Industrial Robot: An International Journal*, 30:515–524, 12 2003.

[127] J. van Oosterhout, J. Wildenbeest, H. Boessenkool, C. Heemskerk, M. de Baar, F. van der Helm, and D. Abbink. Haptic shared control in tele-manipulation: Effects of inaccuracies in guidance on task execution. *Haptics, IEEE Transactions on*, 8(2):164–175, April 2015.

[128] J. Vertut. Robot technology, teleoperation and robotics. *Applications and Technology*, 3, 1984.

[129] H. Vitense. Multimodal feedback: An assessment of performance and mental workload. *Ergonomics*, 46:68–87, 2003.

[130] R. J. Wasicko, D. T. McRuer, and R. E. Magdaleno. Human pilot dynamic response in single-loop systems with compensatory and pursuit displays. Technical report, Air Force Flight Dynamics Laboratory, Wright-Patterson Air Force Base, OH, USA, 1966.

[131] N. Wiener. *The Human Use of Human Beings*. London, U.K.: Eyre and Spottiswoode, 1950.

[132] J. Wildenbeest. Improving the quality of haptic feedback yields only marginal improvements in teleoperated task performance. Master's thesis, Delft University of Technology, 2010.

[133] J. G. W. Wildenbeest, D. A. Abbink, C. J. M. Heemskerk, F. C. T. van der Helm, and H. Boessenkool. The impact of haptic feedback quality on the performance of teleoperated assembly tasks. *IEEE Transactions on Haptics*, 6(2), 2013.

[134] J. G. W. Wildenbeest, R. J. Kuiper, F. C. T. van der Helm, and D. A. Abbink. Position control for slow dynamic systems: Haptic feedback makes system constraints tangible. In *2014 IEEE International Conference on Systems, Man, and Cybernetics (SMC)*, pages 3990–3995, Oct 2014.

[135] D. M. Wolpert, J. Diedrichsen, and J. R. Flanagan. Principles of sensorimotor learning. *Nature reviews. Neuroscience*, 12(12):739–51, Dec. 2011.

[136] D. M. Wolpert, Z. Ghahramani, and M. I. Jordan. An internal model for sensorimotor integration. *Science (New York, N.Y.)*, 269(5232), Sep 1995.

[137] B. Wu, R. Klatzky, and R. Hollis. Force, torque, and stiffness: Interactions in perceptual discrimination. *IEEE Transactions on Haptics*, 4(3):221–228, 2011.

[138] Y. Yokokohji and T. Yoshikawa. Bilateral control of mater-slave manipulators for ideal kinesthetic coupling-formulation and experiment. *IEEE Transactions on Robotics and Automation: a Publication of the IEEE Robotics and Automation Society*, 10(5):605–620, 1994.

[139] M. Zhu and S. E. Salcudean. Achieving transparency for teleoperator systems under position and rate control. In *Proceedings 1995 IEEE/RSJ International Conference on Intelligent Robots and Systems. Human Robot Interaction and Cooperative Robots*, volume 2, pages 7–12 vol.2, Aug 1995.

ACKNOWLEDGEMENTS
DANKWOORD

Lieve allemaal,

Aan alles komt een einde, zo ook aan mijn periode als promovendus. Gelukkig :) In een periode van een klein decennium zijn daar een hoop mensen die een dankwoord verdienen, vanwege een directe dan wel indirecte bijdrage aan de totstandkoming dit proefschrift. Hierbij een poging daartoe.

Om bij het begin te beginnen: Cock, je hebt me als master student onder je vleugels genomen en mij laten proeven aan de geneugten van de wetenschap. Na mijn afstuderen heb je me aangesteld bij HIT, waar ik heb kunnen ondervinden waar mijn hart echt sneller van gaat kloppen, om mij vervolgens partieel (parallel aan mijn promotietraject mocht ik voor je blijven werken) en later geheel (was ik eindelijk klaar, startte ik voor mijzelf) te laten gaan. Wat ben ik je ongelofelijk dankbaar voor alle kansen, vrijgevigheid, inzichten, wijsheden, en alles wat daar niet onder valt.

Dan de volgende grootheid: David. Mentor, vriend, promotor, multimiljonair in talenten. Wat heb ik een hoop van je geleerd en wat heb ik dankzij jou een hoop kunnen leren over zowel de wetenschap als over het leven. En altijd alles met veel humor en een overvolle dosis aan energie. Misschien is dat wel waar ik je het meest dankbaar voor ben: je hebt me laten zien wat het waard is de “happy" in “happy puppy" te etaleren.

Zei ik grootheid? Monument! Frans, dank voor het zijn van de vaderfiguur. Op de achtergrond het vertrouwen geven zelf te wandelen, en altijd beschikbaar indien nodig (o.a. om mij op gezette tijden met beide benen op de grond te zetten). En natuurlijk het fietsen en de mooie weekenden Cyclosportive d’Epaule. Het ga je goed.

Maarten, je complementeert een prachtig trio aan promotoren. Dank voor de scherpe terugkoppeling vanuit een niet-Delftse invalshoek. Dank ook voor het inzicht in het proportionele aspect hiervan, om immer spijkers met koppen te willen slaan.

Aan mijn paranimfen Bram en Teun: dank om schouder aan schouder met jullie dit traject te mogen doorlopen (althans voor het grootste gedeelte ervan). Dank voor de vriendschap, de inspiratie, de inhoudelijke en niet-inhoudelijke discussies, of simpelweg de gezelligheid. Dat dat huis van jullie staande is gebleven onder al die nuchterheid en standvastigheid.

Aan mijn oud-collega’s van het Delft Haptics Lab: Henri, Roel, Tricia, Jack, en Patrice, dank voor het bieden van een werkomgeving die ik altijd als een voorbeeld zal blijven zien. Wat een fijne, veilige, inspirerende, productieve, gezellige (en eigenwijze!) omgeving om in te werken en in te leren.

Aan mijn collega's van H-Haptics: dank voor het bieden van context voor mijn werk, en voor het aanhoren van mijn ad hoc presentaties. Jan, dank voor de heerlijke speur- en ontdekkings-tochten door Japan en Zuid-Korea.

Aan de talloze collega's van de TU: Eline, Bastiaan, Marta, Paul, Ewout, Elise, Frederique, Annetje, Mona, Peter, Ingrid, Awaz, Nadia, Milton, Nick, en anderen, dank voor het vele lachen, de gesprekken, lunches en borrels. En borrels. Nergens smaakt de negroni zo goed als op de First-Friday-of-the-Month-borrel. En dat komt niet door de negroni.

Aan Luuk en mijn collega's van DigiNova: dank voor het bieden van de ruimte en de motiverende woorden om dit hoofdstuk een einde te geven.

Aan mijn vrienden van de universiteit, de heerlijke mannen (en dames!) van de Andere Trein, de Roedel, LSVV '70 2 a.k.a. Jong LSVV, en andere vrienden met wie ik het leven (be)leef: dank voor de ongekende waarde die de avonden/dagen/weekenden/weken Friesland, Londen, Lowlands, Senegal, burenborrels, spelletjes, Copenhagen, vakantieparken, Canada, wintersport, New York, (kerst)diners, San Francisco, Ijsland, donkere techno bunkers (...en nog veel meer) hebben. De energie die uit deze vriendschappen komt is een belangrijke basis voor dit werk.

Over een belangrijke basis gesproken: pa, ma & zuster, dank voor bieden van een veilige thuishaven om mijn vleugels vanuit uit te slaan. Juist omdat jullie er zijn, en juist vanwege hetgeen ik van jullie heb meegekregen, durf ik keuzes te maken - ik weet wat ik heb om op terug te vallen. Uiteindelijk is dat het echte begin van mijn promotie avontuur. Tom, je hebt het (net) niet meegemaakt, maar ik heb daadwerkelijk ook op de universiteit aan mijn onderzoeken gewerkt. Aan Theo, Ellie, Daan, Ilse, Roel, dank voor het bieden van een plek die vanaf moment een als (een tweede) thuis aanvoelde, en steun te beiden als dat nodig is.

En aan Eef. Lieve Eef, wat maak jij het leven mooi. Om samen met jou, inmiddels ruim 15 jaar, het leven te mogen ontdekken is een geschenk op zich. Je moet op momenten gek worden van mijn ondernemingen, en wat dat ook voor ons betekent. Maar (bijna) het enige wat ik daarvan terugzie is ruimte en liefde. Dank daarvoor. Ik kan mij alleen maar verheugen op de jaren die komen gaan.

Allen veel dank, gran tangi, en tot mooie momenten op andere plaatsen & tijden,

Jeroen Wildenbeest
17 mei 2020

Curriculum Vitæ

Jeroen Gerrit Willem Wildenbeest

Born: 18 September 1986, Lisse, The Netherlands

Education

2011–2020	Doctoral Candidate at the Delft Haptics Lab Department of BioMechanical Engineering, Faculty of 3mE Delft University of Technology, The Netherlands
2008–2010	MSc in Mechanical Engineering track BioMechanical System Design Delft University of Technology, The Netherlands
2004–2008	BSc in Mechanical Engineering Delft University of Technology, The Netherlands

Professional Experience

2017–current	CTO at DigiNova B.V., Delft
2010–2017	Consultant at Heemskerk Innovative Technology B.V., Delft
2008–2010	Junior Consultant at Heemskerk Innovative Technology B.V., Noordwijk
2008–2009	Internship at FOM DIFFER, Nieuwegein

LIST OF PUBLICATIONS

JOURNAL ARTICLES

9. **Jeroen G.W. Wildenbeest**, Franc C.T. van der Helm, David A. Abbink, *Reach Adaptation Applied to Telemanipulation: Does Haptic Feedback Bandwidth Affect Motor Learning?* submitted for review to IEEE Transactions on Haptics

8. **Jeroen G.W. Wildenbeest** and Roel I.J. Kuiper, Frans C.T. van der Helm, David A. Abbink, *A Cybernetic Approach to Quantify the Effect of Haptic Feedback on Operator Control Behavior in Free-Space Telemanipulation,* submitted for review to IEEE Transactions on Cybernetics

7. Roel I.J. Kuiper **and Jeroen G.W. Wildenbeest**, Franc C.T. van der Helm, David A. Abbink, *Exploring Haptic Feedback Designs for Rate Controlled Systems,* submitted for review to IEEE Transactions on Haptics

6. **J.G.W. Wildenbeest**, D.A. Abbink, C.J.M. Heemskerk, F.C.T. van der Helm and H. Boessenkool, *The Impact of Haptic Feedback Quality on the Performance of Teleoperated Assembly Tasks,* IEEE Transactions on Haptics, Vol. 6, Issue 2, pp. 242-252, 2013

5. J. van Oosterhout, **J.G.W. Wildenbeest**, H. Boessenkool, C.J.M. Heemskerk, M.R. de Baar, F.C.T. van der Helm, D.A. Abbink, *Haptic Shared Control in Tele-manipulation: Effects of Inaccurate Support on Task Execution,* IEEE Transactions on Haptics, preprints 2015, doi: 10.1109/TOH.2015.2406708

4. Henri Boessenkool, **Jeroen G.W. Wildenbeest**, Cock J.M. Heemskerk, Marco R. de Baar, Maarten Steinbuch, David A. Abbink, *What to improve in Human-in-the-loop Tele-operated Maintenance? Analysis of executed Remote Maintenance at JET,* submitted for review to IEEE Transactions on Human Machine Systems

3. Henri Boessenkool, **Jeroen G.W. Wildenbeest**, Cock J.M. Heemskerk, Marco R. de Baar, Maarten Steinbuch, David A. Abbink, *How to quantify what is so difficult in tele-manipulated maintenance using task analysis – A case study,* submitted for review to Ergonomics

2. Arnold W. de Jonge, **Jeroen G.W. Wildenbeest**, Henri Boessenkool, Frans C.T. van der Helm, David A. Abbink, *The Effect of Trial-by-trial Adaptation on Conflicts in Haptic Shared Control for Free-Air Teleoperation Tasks,* IEEE Transmission on Haptics, 2015

1. H. Boessenkool, D.A. Abbink, C.J.M. Heemskerk, F.C.T. van der Helm and **J.G.W. Wildenbeest**, *A task-specific analysis of the benefit of haptic shared control during tele-manipulation,* IEEE Transactions on Haptics, Vol. 6, Issue 1, pp. 2-12, 2013

PEER REVIEWED CONFERENCE PROCEEDINGS

5. **J.G.W. Wildenbeest**, R.J. Kuiper, F.C.T. van der Helm, D.A. Abbink, *Position Control for Slow Dynamic Systems: Haptic Feedback Makes System Constraints Tangible,* IEEE International Conference on Systems, Man and Cybernetics (SMC) 2014, pp. 3990-3995, 5-8 Oct. 2014, doi: 10.1109/SMC.2014.6974555

4. **J.G.W. Wildenbeest**, D.A. Abbink, J.F. Schorsch, *Haptic transparency increases the generalizability of motor learning during telemanipulation,* World Haptics Conference (WHC) 2013, pp. 707–712, 2013

3. **J.G.W. Wildenbeest**, D.A. Abbink, H. Boessenkool, C.J.M. Heemskerk, J.F. Koning, *How operator admittance affects the response of a teleoperation system to assistive forces – A model analytic study and simulation,* Fusion Engineering and Design, Vol. 88, Issue 9, pp. 2001-2005, 2013

2. J. van Oosterhout, D.A. Abbink, J.F. Koning, H. Boessenkool, **J.G.W. Wildenbeest**, C.J.M. Heemskerk, *Haptic shared control improves hot cell remote handling despite controller inaccuracies,* Fusion Engineering and Design, Vol. 88, Issue 9, pp. 2119–2122, 2013.

1. H. Boessenkool, D.A. Abbink, C.J.M. Heemskerk, M. Steinbuch, M.R. de Baar, **J.G.W. Wildenbeest**, D. Ronden, J.F. Koning, *Analysis of human-in-the-loop tele-operated maintenance inspection tasks using VR,* Fusion Engineering and Design, Vol. 88, Issue 9, pp. 2164-2167, 2013

OTHER SCIENTIFIC CONTRIBUTIONS

- Demonstration "Novel HMI for Needle Insertion" at the IEEE World Haptics Conference 2015 in Chicago on June 22, 2015.

- Co-organiser and speater at tutorial "Human-Centered Design and Evaluation of Haptic Shared Control across different Applications" at the IEEE WorldHaptics Conference 2015 in Chicago on June 22, 2015.

- Gemini HMI - The Gemini was developed initially in collaboration with the Bachelor students Leroy Boerefijn en Ward Heij to demonstrate the basic working of a single degree of master slave setup with a Capstan drive.

(CO-)SUPERVISED MASTER'S THESIS

10. Jelle Hofland, *Evaluating trading and sharing control for constraint motion tasks in a domestic environment using a remote controlled semi-autonomous robot,* MSc Thesis, TU Delft, 2018

9. Karel Sirks, *Which position do I pick, if I don't know how to do the task?: A model to predict advantageous base poses for semi-autonomous robots,* MSc Thesis, TU Delft, 2018

8. Roel van der Klauw, *A Design method for Variable Rotational Workspace Extension applied to Telemanipulation Tasks,* MSc Thesis, TU Delft, 2017

7. Guido van het Hart, *Robust control architecture for domestic telemanipulation*, MSc Thesis reports, TU Delft, 2016

6. Frank Hoeckx, *Machine learning for haptic shared control in telerobotics,* MSc Thesis, TU Delft, 2016

5. Nienke van Driel, *Influence of steering wheel stiffness and road width on drivers' neuromuscular stiffness,* MSc Thesis, TU Delft, 2015 (co-supervision with Tricia Gibo)

4. Graham Nixon, *Haptic Manipulation with an UAV,* MSc Thesis, TU Delft, 2015

3. Marjon Voskuijl, *A hybrid design combining position and rate control allows for intuitive workspace extensions in teleoperation,* MSc Thesis, TU Delft, 2015 (co-supervision with Roel Kuiper)

2. Arnold de Jonge, *The Effect of Online Adaptation on Conflicts in Haptic Shared Control for Free-Air Teleoperation Tasks,* MSc Thesis, TU Delft, 2012 (co-supervision with Henri Boessenkool)

1. Jeroen van Oosterhout, *Robustness of haptic shared control against model inaccuracies during telemanipulation,* MSc Thesis, TU Delft, 2012 (co-supervision with Henri Boessenkool)